

AIRCRAFT TAKEOFF
PERFORMANCE MONITORING
IN FAR-NORTHERN REGIONS:
AN APPLICATION OF THE
GLOBAL POSITIONING SYSTEM

A Thesis Submitted to the College of
Graduate Studies and Research
in Partial Fulfilment of the Requirements
for the Degree of Doctor of Philosophy
in the Department of Mechanical Engineering
University of Saskatchewan
Saskatoon

By

Shane Donald Pinder

April 2003

© Copyright Shane Donald Pinder, 2003. All rights reserved.

PERMISSION TO USE

In presenting this thesis in partial fulfilment of the requirements for a postgraduate degree from the University of Saskatchewan, I agree that the Libraries of this University may make it freely available for inspection. I further agree that permission for copying of this thesis in any manner, in whole or in part, for scholarly purposes may be granted by the professor or professors who supervised my thesis work or, in their absence, by the Head of the Department or the Dean of the College in which my thesis work was done. It is understood that any copying or publication or use of this thesis or parts thereof for financial gain shall not be allowed without my written permission. It is also understood that due recognition shall be given to me and to the University of Saskatchewan in any scholarly use which may be made of any material in my thesis.

Requests for permission to copy or to make other use of material in this thesis in whole or part should be addressed to:

Head of the Department of Mechanical Engineering
University of Saskatchewan
Saskatoon, Saskatchewan S7N 5A9

ABSTRACT

A design approach for an aircraft takeoff performance monitoring system (TOPMS) is described. In this approach, it is proposed that the Global Positioning System (GPS) in conjunction with a discrete Kalman Filter be used to determine aircraft acceleration, ground speed, and position relative to the end of the runway. A practical evaluation of the feasibility of this proposal showed clear superiority of a GPS-derived acceleration over a more traditional method employing accelerometers. This study found that, when compared to observations from carefully mounted accelerometers, the GPS-derived observation agreed to within 0.10 metres per second squared ninety percent of the time. Advantages of the GPS-derived observation included a modest noise level, insusceptibility to gravity and temperature-influenced variations, and far simplified mounting criteria.

A theoretical dynamic model of an aircraft in contact with the ground was developed in consideration of factors pertaining to runways at far-northern Canadian airports. In the model, factors such as runway slope, wind velocity, wheel friction coefficient, and aircraft control settings were considered constant. While variability in any parameter considered constant by the model could influence the performance of a TOPMS, such variability was deemed beyond the scope of this preliminary investigation of a TOPMS designed specifically for the far-northern environment. A device containing a GPS receiver and data acquisition system was designed and certified, then installed in an aircraft operated by an airline servicing far-northern Canadian airports. The data collected in this manner were used to validate the theoretical model. It was concluded that a projection of displacement can be determined to within an uncertainty of fifteen metres in sufficient time to alert the pilot of an unsafe situation.

ACKNOWLEDGEMENTS

I will begin by acknowledging the corporate sponsorship of Transwest Air. Their willingness to provide space aboard a passenger aircraft for a prototype device enabled the research conducted during this project to be much more relevant than would have been the case with an economical alternative. Partners such as Transwest are rare and invaluable.

My supervisors, Trever Crowe and Peter Nikiforuk, are two of the most genuinely professional and insightful people I know. Their willingness to allow generous latitude and flexibility in my research was inspiring. While I am sure they would both underestimate their impact on the last few years of my life, I can truly say that I have learned immeasurably from their example and guidance. This went far beyond the technical guidance one might expect of professors of engineering. They have been role models of integrity and professionalism.

Dan Aspel and Glenn Wright are friends who have served as my personal navigation system over the past few years. As with any occupation, or preoccupation, that consumes so much of one's time, friends are often consulted for reassurance regarding the usefulness of the undertaking. I sincerely appreciated the patience of those who acted as my sounding board, as well as the advice that was constantly available.

I would like to thank my family for their support and understanding. While I credit my parents with teaching me to question everything that is generally considered to be factual, an approach which has served me very well in technical matters, they know too well that this particular trait often has a downside. I would like to express my sincere appreciation to my entire family for their patience.

Finally, I would like to acknowledge the support of Claire over the last several years. She has had to endure the conflicting obligations of my teaching, research, and involvement with the Graduate Students' Association which I am sure, at times, must have seemed outrageous when compared to the responsibilities of preparing for our wedding and, more recently, the arrival of our first child. I hope that I have the opportunity someday to make similar sacrifices for her.

Aeronautical charts are based on information taken from Canada Flight Supplement.
© 2002 Her Majesty the Queen in Right of Canada with permission of Natural Resources Canada.

DEDICATION

I have been told that the one common desire of people the world over is to leave the world a slightly better place for the next generation.

For Nathan.

TABLE OF CONTENTS

	Page
PERMISSION TO USE	i
ABSTRACT	ii
ACKNOWLEDGEMENTS	iii
DEDICATION	iv
TABLE OF CONTENTS	v
LIST OF FIGURES	viii
NOMENCLATURE	x
CONVENTIONS USED	xiv
Chapter 1 - Introduction	1
1.1 Aircraft Landing and Takeoff Performance Monitoring	1
1.2 The Far-Northern Environment	5
Chapter 2 - Literature Review	6
2.1 Background - Aircraft Landing and Takeoff Safety	6
2.1.1 Early Research in Takeoff Performance Monitoring	6
2.1.2 Regulatory Issues	8
2.2 The Global Positioning System	9
2.2.1 GPS Signal Structure	12
2.2.2 GPS Signal Tracking	14
2.3 State Observers	17
2.4 The Discrete Kalman Filter	17
2.5 Applied Kalman Filtering, an Example	23
Chapter 3 - Objectives	27
3.1 Introduction	27
3.2 Project Objectives	28
3.3 Methodology	28
3.4 Scope	29
Chapter 4 - Theoretical Prototype System	30
4.1 Background	30
4.2 Parametric Model of an Aircraft During Takeoff	30

4.3	Projection of Displacement	33
4.4	Signal Processing Technique	35
	4.4.1 Standard Treatment of the Discrete Kalman Filter	35
	4.4.2 Non-linear Manipulation of the Discrete Kalman Filter	36
4.5	Required Accuracy	37
4.6	Uncertainty Analysis	38
4.7	Takeoff Rejection Simulation using a Theoretical Model	46
Chapter 5 - Sensor Selection		50
5.1	Background	50
5.2	Acceleration From GPS	51
5.3	Required Accuracy	54
5.4	Experimental Investigation	56
5.5	Results and Discussion	59
Chapter 6 - Model Validation through Experimental Investigation		65
6.1	Introduction	65
6.2	Materials and Methods	66
	6.2.1 Certification	68
	6.2.2 Mechanical Considerations	69
	6.2.3 Electrical Considerations	71
	6.2.4 Installation	73
	6.2.5 System Summary	74
	6.2.6 Data Collection Software	75
6.3	Results and Discussion	78
Chapter 7 - Major Conclusions and Recommendations		88
7.1	Major Findings	88
7.2	Takeoff Performance Monitoring - Future Work	89
	7.2.1 Modular Device Development	89
	7.2.2 Target Environment Testing	89
7.3	Device Development - Future Work	90
	7.3.1 GPS/INS Sensor Integration	90
	7.3.2 Actuator Integration - Automatic Deceleration Systems	92
7.4	Other Applications - Unmanned Aerial Vehicles (UAVs)	92
REFERENCES		95
Appendix I - CD-ROM		98
Appendix II - Limited Supplemental Type Certificate Application		99
Compliance Program - Rev. 1, 23 Aug 00		109
	Purpose and Scope	109
	Mechanical Considerations	110

Electrical Considerations	110
Substantiation Report - Rev. 1, 23 Aug 00	111
Subpart D, Design and Construction	111
Subpart F, Equipment	111
Test Plan - Rev. 1, 23 Aug 00	114
Subpart C, Structure	114
Test C1:	114
Test C2:	114
Subpart F, Equipment	115
Test F1:	115
Test F3:	115
Installation Instructions - Global Positioning Data Recorder - Rev. 1, 12 Jul 00	116
Detailed Test Plan - Rev. 1, 23 Aug 00	117
Test C1	117
Test C2	117
Test F1	117
Test F3	121
Appendix III - Antenna Splitter Evaluation	125
Appendix IV - Takeoffs from Runway 15, Saskatoon Airport	132

LIST OF FIGURES

P_2 and P_3

	Page
Figure 1.1 Speed and Acceleration vs Displacement in a Theoretical Rejected Takeoff . . .	3
Figure 1.2 Aftermath of Canadian Airlines International Flight 17 Takeoff Rejection . . .	4
Figure 2.1 The Boeing B-777, a Massive Commercial Airliner	7
Figure 2.2 PRN Code: a Repeating Series, Characteristic of the Transmitter Satellite . .	13
Figure 2.3 Phase Locked Loop Block Diagram	16
Figure 2.4 Delay Locked Loop Block Diagram	16
Figure 2.5 Recursive Kalman Filter Algorithm	23
Figure 4.1 Error in Projection of Displacement as a Function of Error in \hat{v} and \hat{a}	45
Figure 4.2 Error in Projected Displacement as a Function of Speed	46
Figure 4.3 Simulation Results: Projected Displacement and Margin of Safety	48
Figure 4.4 Margin of Safety during the Response to a Simulated Takeoff Rejection . .	49
Figure 5.1 Unknown Sensor Inclination Results in “Accelerometer Gravity Error” . . .	53
Figure 5.2 Accelerometer and GPS-derived Acceleration Observation Processing	59
Figure 5.3 Speed and Acceleration of the Test Vehicle vs Time	60
Figure 5.4 GPS-derived Acceleration Data Agree with Accelerometer Data	62
Figure 5.5 Difference between GPS-derived Acceleration and Accelerometer Data . . .	63
Figure 6.1 Wollaston Lake Airport: an Unmonitored and Uncontrolled Airport	65
Figure 6.2 Left Side View of Aircraft	70
Figure 6.3 GPDR Installed in the Tray belonging to the Removed TCAS Processor . .	71
Figure 6.4 Antenna Splitter used to Share the Signal of the Existing GPS Antenna . . .	72

Figure 6.5 Global Positioning Data Recorder - System Electrical Schematic	76
Figure 6.6 Internal Configuration of Global Positioning Data Recorder	77
Figure 6.7 The projection of displacement in a typical takeoff converged to within ten metres of the actual future displacement a few seconds after control settings were fixed.	79
Figure 6.8 Parameter Estimation in a Typical Takeoff	81
Figure 6.9 Parameter Estimation in a Typical Takeoff - Model Validation	83
Figure 6.10 Parameter Estimation in a Typical Takeoff - Acceleration Noise	84
Figure 6.11 Scatter Plot of All Projections of Displacement over 175 Takeoffs	85
Figure 6.12 The number of takeoffs in which the error in projection of displacement was less than fifteen metres increased to 175 by a speed of forty-one metres per second.	86
Figure 7.1 Phase Locked Loop with Inertial Aiding	92
Figure 7.2 Altus II: an Operational Unmanned Aerial Vehicle	93
Figure 7.3 Boeing X-45A UCAV: the Next Generation of Unmanned Air Vehicle	94
Figure II.1 Splitter Evaluation Experimental Apparatus	126
Figure II.2 The carrier to noise ratio for satellite PRN 23 was unaffected by the presence of a signal splitter	129
Figure II.3 The carrier to noise ratio for satellite PRN 17 was unaffected by the presence of a signal splitter	130
Figure II.4 The carrier to noise ratio for satellite PRN 26 was unaffected by the presence of a signal splitter	131

NOMENCLATURE

Lowercase Variables and Vectors

a	the component of acceleration in the tangential or subscripted direction
a^*	the observation from an accelerometer
c	the speed of light
\bar{e}	a vector of state estimate errors
g	the gravitational constant
j	the tangential jerk, where jerk is the first time derivative of acceleration
m	the mass of an object
q	a zero-mean random variable describing process noise
r	a zero-mean random variable describing sensor noise
s	one-dimensional displacement
t	the time elapsed since a reference event
v	the tangential speed
v_a	the component of wind velocity in the direction of vehicle motion
$v_{/a}$	the speed with reference to a moving mass of air
\bar{w}_1	the process noise in a state space representation
\bar{w}_2	the sensor noise in a state space representation
x	the displacement in the x-direction of a coordinate system
\bar{x}	a vector of state variables in a state space representation
\hat{x}	a vector of state estimates
y	the displacement in the y-direction of a coordinate system
\bar{y}	a vector of measurement variables in a state space representation
\hat{y}	a vector of measurement estimates
z	the displacement in the z-direction of a coordinate system

Matrices

A	the state transition matrix in a state space representation
C	a matrix relating measurements to states in a state space representation
I	the identity matrix
K	the observer gain matrix
Q	the state covariance matrix in a state space representation
R	the measurement covariance matrix in a state space representation

Uppercase Variables

A	frontal area
D	the force due to aerodynamic drag
D_n	constants in a function modelling aerodynamic drag
D_1	component of aerodynamic drag at rest
D_2	component of aerodynamic drag proportional to speed
D_3	component of aerodynamic drag proportional to speed squared
$E\{ \}$	the expected value of an expression containing random variables
F	the force due to friction
F_n	constants in a function modelling friction
F_2	component of frictional force proportional to speed
L_1	the primary GPS carrier frequency
L_2	the secondary GPS carrier frequency
P_n	constant parameters modelling vehicle dynamics
P_1	component of vehicle acceleration at rest
P_2	component of vehicle acceleration proportional to speed
P_3	component of vehicle acceleration proportional to speed squared
T	the force due to engine thrust
T_n	constants in a function modelling engine thrust
T_0	component of engine thrust at zero airspeed
T_1	component of engine thrust at rest

T_2	component of engine thrust proportional to speed
T_3	component of engine thrust proportional to speed squared
V_1	critical engine failure recognition speed
W	the force due to weight
W_1	the sine of the angle describing the inclination of a surface

Greek Variables

ρ_{air}	the density of air
λ	the wavelength of a signal

Superscripts

–	superscript indicating a value estimated in the prior time step
T	superscript indicating the transpose of the superscripted matrix

Subscripts

k	subscript identifying the “current” time step in a discrete filter
$k + 1$	subscript identifying the “next” time step in a discrete filter
x	subscript identifying the component of a quantity in the x-direction

Acronyms and Abbreviations

ASDR	Accelerate-Stop Distance Required
ATR	Air Transport Radio
C/A-Code	Coarse/Acquisition-Code
CD-ROM	Compact Disk - Read Only Memory
DGPS	Differential GPS
DLL	Delay Locked Loop
FLL	Frequency Locked Loop
GPDR	Global Positioning Data Recorder
GPS	Global Positioning System
IMU	Inertial Measurement Unit
INS	Inertial Navigation System
LDR	Landing Distance Required
Mcps	Megachips per Second
MCU	Modular Component Unit

MHz	Megahertz
NASA	National Aeronautics and Space Administration
NCO	Numerically Controlled Oscillator
P-Code	Precise-Code
PLL	Phase Locked Loop
PRN	Pseudorandom Noise
SA	Selective Availability
SV	Space Vehicle
TCAS	Traffic/Collision Avoidance System
TNC	Threaded Niell-Concelman
TOPMS	Takeoff Performance Monitoring System
UAV	Unmanned Aerial Vehicle
UCAV	Unmanned Combat Air Vehicle
VDC	Volts, Direct Current

CONVENTIONS USED

In the presentation of equations within this document, two conventions have been used to incorporate equations within the narrative. When a variable is first defined, the first convention applies. In subsequent uses, the second convention applies. The following examples illustrate the two conventions.

EXAMPLE OF FIRST CONVENTION

The force on an object,

$$F = ma ,$$

where: m is the mass of the object, and;
 a is the acceleration of the object.

Read as:

The force on an object, F , is equal to m multiplied by a , where: m is the mass of the object, and; a is the acceleration of the object.

EXAMPLE OF SECOND CONVENTION

In the instance where only gravity acts on an object,

$$F = mg ,$$

where: g is the gravitational constant.

Read as:

In the instance where only gravity acts on an object, F is equal to m multiplied by g , where: g is the gravitational constant.

Chapter 1 - Introduction

1.1 Aircraft Landing and Takeoff Performance Monitoring

Aircraft landing and takeoff performance monitoring is an area of research aimed at improving the information available to the pilot for decision making during takeoff or landing. A system capable of instantaneously determining the stopping distance of an aircraft could form an integral component of a monitoring system. Particularly difficult to quantify is the frictional coefficient between the runway and the aircraft tires, should such a measurement be necessary. In secluded far-northern regions, where a monitoring system would be particularly useful given extreme weather conditions, few airports are equipped to attempt frictional measurements. In such instances, a monitoring system would need to be totally self-contained and able to determine aircraft ground speed, acceleration, and position relative to the end of the runway with reference to a theoretical dynamic model relating these parameters. Prediction of the aircraft's location at rest would then be possible.

Landing and takeoff performance monitoring systems are aimed at averting runway overrun when an aircraft is in contact with the ground. Typical causes of runway overrun include engine failure on takeoff and reduced braking resulting from runway contamination. In Canada in the 1990s, engine failures occurred during one in every 76,000 jet takeoffs¹.

The “critical engine failure recognition speed” (V_1) is defined as the speed above which takeoff could continue safely if the most critical engine failed,² assuming the runway length is sufficient. V_1 is often calculated prior to startup based on aircraft parameters and estimation of runway and weather conditions. Choosing a throttle setting to reach V_1 is a more complicated matter. With a low throttle setting, takeoff rejection initiated at a speed slightly below V_1 may result in runway overrun, while a high power setting increases the likelihood of an engine failure on takeoff. As well, engine service life depends largely on its peak power setting.

In a theoretical rejected takeoff, the aircraft accelerates gradually until the rejection is initiated. Drag increases with airspeed, giving rise to lower accelerations at higher airspeed. Once the rejection is initiated, the aircraft decelerates gradually to rest. In practicality, there would be a measurable reaction time delaying the application of braking and reverse thrust.

Operators often use the so called “balanced field concept” to calculate the lowest possible power setting for use during takeoff. Then, at speeds below V_1 , there is mathematically enough runway remaining to abort the takeoff. Once V_1 is reached, the aircraft could safely takeoff even in the event of the failure of one engine. With this in mind, V_1 becomes a “decision” speed. Figure 1.1 shows this scenario with a takeoff rejection initiated at a decision speed of eighty metres per second on a 2400-metre runway. In reality, pilots refer to performance charts to determine power settings and decision speeds. The degree of uncertainty present in this method is substantial. Consequently, some pilots

have little confidence in the utility of such charts at times when decisions must be made quickly.³

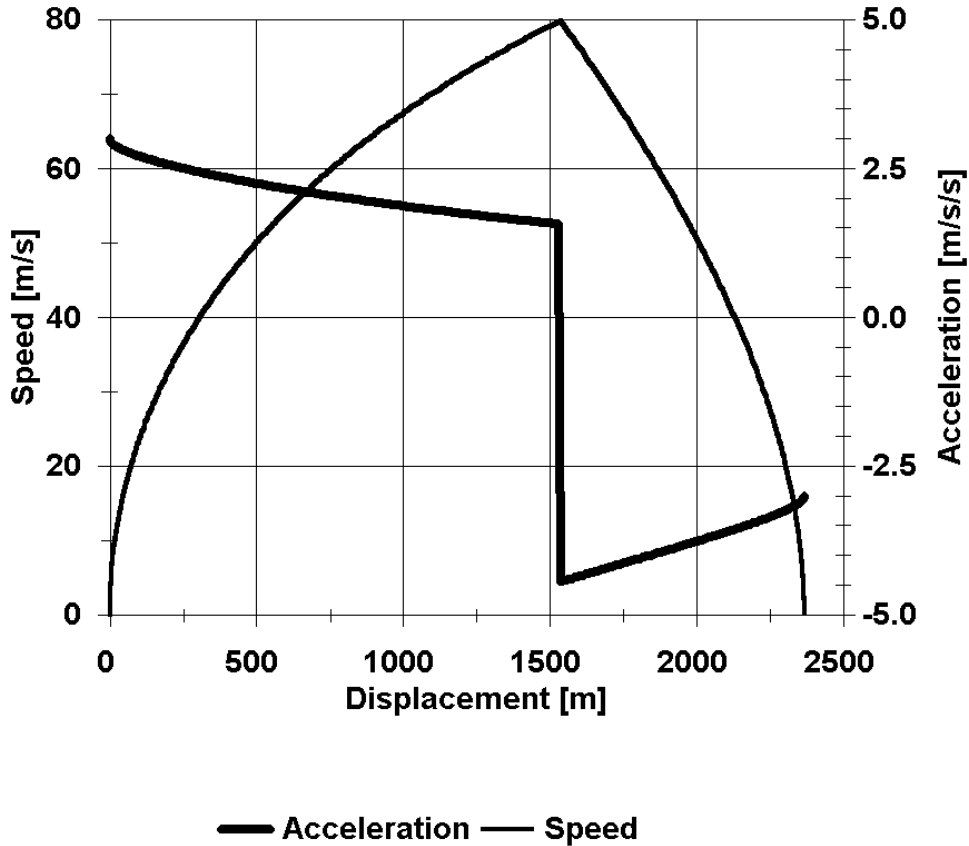


Figure 1.1 Speed and Acceleration vs Displacement in a Theoretical Rejected Takeoff

Figure 1.2 shows the results of a takeoff rejected less than a second after reaching V_1 . The full report regarding this accident appears in Appendix 1.01 (CD-ROM) under the “CAI Flight 17” directory. Performance monitoring systems⁴ that could provide to the pilot information pertaining to the level of safety with which a takeoff is proceeding are currently in existence, but have yet to be adopted by manufacturers. In such prototype

systems, the pilot is required to provide overall runway length information as well as runway frictional coefficient data based on observations from ground-based vehicle-mounted measurement systems. The level of error in such data can be substantial.



Transport Canada

Figure 1.2 Aftermath of Canadian Airlines International Flight 17 Takeoff Rejection

A similar system for use during approach and landing is currently unavailable because of the inability for the pilot to provide remaining runway length. The Global Positioning System (GPS) could be used in conjunction with a database of runway information to determine remaining runway length. The same observer system could then be used for both takeoff and landing.

1.2 The Far-Northern Environment

The runway overrun problem is further aggravated in inclement weather, where runway surfaces are contaminated by water or ice. Far-northern regions experience this sort of climate over six months of the year. Further, as such regions are relatively less populated, facilities may receive infrequent maintenance. Accounting for these factors in the landing or takeoff decision-making process represents a considerable challenge for pilots.

Many airport runways in far-northern regions are gravel surfaced. The behaviour of a gravel runway may be unpredictable, especially when temperatures are near the freezing point. Measurements of runway friction attempted in such conditions would be relatively unreliable.

The availability of radio navigation systems in far-northern regions is also an issue. While such facilities exist, they are sparsely distributed and tend to service the airports of major population centres. Air carriers that service airports in support of mining and forestry are less likely to have reliable access to radio navigation facilities. Navigational information provided by GPS receivers is now available in these areas and has enhanced or, in some cases, replaced existing facilities. Appendix 1.02 (CD-ROM) contains data regarding a few airports in northern regions in the “airports” directory.

Chapter 2 - Literature Review

2.1 Background - Aircraft Landing and Takeoff Safety

One of the most common aviation accident events continues to be runway overrun during takeoff or landing.⁵ In the case of takeoff runway overrun, the problem is often associated with engine power loss. This problem is further aggravated in inclement weather where runway surfaces are contaminated by water or ice. Pilots of multi-engine aircraft must evaluate a complex set of variables in situations involving varying winds, limited control of ground traction, and necessary application of reverse thrust.

2.1.1 Early Research in Takeoff Performance Monitoring

In 1984, the Society of Automotive Engineers began drafting a specification⁶ to govern the design standards for takeoff performance monitors. In 1985, Raghavachari Srivatsan authored a doctoral thesis⁷ at the University of Kansas regarding the design of a Takeoff Performance Monitoring System (TOPMS). He continued work on this project and, by 1987, such a system was developed at NASA's Langley Research Centre for potential implementation in Boeing's B-777 shown in Figure 2.1. The B-777 is a massive and complicated aircraft. Devices installed in such aircraft must withstand considerable scrutiny prior to acceptance. Simulator evaluations⁸ were completed in 1992, and flight testing⁹ was performed in 1994. The proposal to include the instrument in the B-777 was inevitably rejected due to practical shortcomings.¹⁰ Specifically, there was concern over

the non-predictability and variability of wind and runway conditions and the manner in which the device would compensate for this lack of information. Manufacturers feared that the device may do more harm than good, possibly distracting the pilot unnecessarily.



™ & © Boeing. Used under license.

Figure 2.1 The Boeing B-777, a Massive Commercial Airliner

Concern over unpredictable conditions is understandable. On dry, paved runways, the primary means of deceleration for a large jet aircraft is the application of wheel braking. Reverse thrust is available, but accounts for only about twenty percent of the force required for deceleration. Estimating the maximum braking force available is by no means trivial. While the condition of the runway is a factor, several factors unique to each aircraft are important. This adds to the uncertainty in any projected stopping distance.

In the design of his TOPMS,¹¹ Srivatsan accounted for a litany of variables that influence the distance required for an aircraft to accelerate or decelerate, as appropriate. These included the ambient air pressure and temperature, the weight of the aircraft and its centre of gravity, the flap setting, the pitch attitude, the throttle setting and engine pressure ratio, the wind speed and direction, the rolling friction coefficient, the acceleration of the aircraft, and the calibrated airspeed. Additionally, those parameters that change throughout the takeoff roll were referenced to theoretical models. The net result of this treatment was a large uncertainty in the predicted takeoff roll, as much as five percent of the overall displacement of the aircraft. Moreover, the required instrumentation limited the applicability of the design to large passenger jet aircraft.

Several other performance monitoring systems^{12,13} have been devised. In most designs, the pilot would have been required to manually supply runway length information as well as the runway frictional coefficient provided by ground based observers. No large-scale implementation of such a device has been published. There would be much more likelihood of implementation were the system completely self-contained. More importantly, there has been no published work on a monitor specifically intended for use in the unique far-northern environment.

2.1.2 Regulatory Issues

In Canada, there are currently no regulations regarding the procedures to be followed when conducting a takeoff or landing on a gravel runway. Some aircraft performance charts include information pertaining to gravel runways, but manufacturers are not

required to provide such information. As a result, operators are left with performance charts pertaining to dry, paved runways. Moreover, in compiling such performance charts it is typically assumed that reverse thrust is unavailable. While it would be prudent to account for the reduced utility of wheel brakes on gravel runways by extending the required runway length or reducing the aircraft payload, such measures carry financial implications for operators.

At a preliminary meeting¹⁴ of officials at Transport Canada, some guidelines were established in pursuit of regulations specifically intended to govern the use of gravel runways. While it is common knowledge in the industry that the primary means of deceleration on gravel runways is through the application of reverse thrust, the preliminary guidelines state that “no credit for propeller reverse may be used in calculation of Accelerate - Stop Distance Required (ASDR) or Landing Distance Required (LDR).” To paraphrase, only wheel braking may be considered in a determination of the required runway length for takeoff or landing.

2.2 The Global Positioning System

The Global Positioning System is a satellite navigation system that provides a means of calculating time, position, and velocity data using coded signals which can be processed using a receiver.¹⁵ Four equations are required to solve for four unknowns: time and three components of three-dimensional position. Thus, signals from a minimum of four satellites are used to compute the three-dimensional position of the receiver. A GPS receiver derives position information by measuring the time required for a signal to be

transmitted from a satellite at a known position. The distance observations to each satellite are the product of the speed of light, c , and the transit time for the signal,

$$c(t-t_1) = \sqrt{(x-x_1)^2 + (y-y_1)^2 + (z-z_1)^2}, \quad (2.1)$$

$$c(t-t_2) = \sqrt{(x-x_2)^2 + (y-y_2)^2 + (z-z_2)^2}, \quad (2.2)$$

$$c(t-t_3) = \sqrt{(x-x_3)^2 + (y-y_3)^2 + (z-z_3)^2}, \quad (2.3)$$

$$c(t-t_4) = \sqrt{(x-x_4)^2 + (y-y_4)^2 + (z-z_4)^2}, \quad (2.4)$$

where: x_n, y_n, z_n, t_n are known satellite positions and times of signal transmission,

and;

x, y, z, t are the receiver location and times of receipt of each signal.

There are several sources of inaccuracy in this process including receiver noise, tropospheric delay, multipath error, satellite clock errors, orbit errors, and ionospheric delay. Until May 1, 2000 the United States Department of Defense injected intentional degradation or Selective Availability (SA) into the transmitted signal for security reasons. At the beginning of this project, SA was by far the largest contribution to position error, on the order of one hundred metres. However, this error could be described as a slow wandering bias error. The resulting velocity error from time differentiation was less than one metre per second. Further, the velocity error changed slowly resulting in a virtually negligible acceleration error. Tropospheric delay, satellite clock errors, orbit errors, and ionospheric delay contribute a relatively steady bias error on the order of a few metres and

are highly repeatable when considering time intervals of less than one second. Multipath error occurs when reflected GPS signals are misinterpreted by the GPS receiver as having come directly from the satellite. Airport runways are typically low-multipath environments as a clear view of the sky is generally available and because buildings are not within close proximity. With no multipath error in the absence of SA, position accuracy of less than ten metres is possible.

It is possible to compensate for errors other than multipath and receiver noise using Differential GPS (DGPS). The concept of DGPS involves the use of a stationary GPS receiver at a known location that is capable of transmitting corrections to a mobile receiver. Alternatively, such corrections can be stored and later used to improve data collected by a mobile receiver. Position accuracy of less than one metre, not considering the contribution of multipath error, can be achieved with DGPS if the distance between the two receivers is less than a few hundred kilometres.

The foundation for the determination of satellite range is the speed of light and the time required for transmission. The speed of light varies slightly as it passes through regions of the atmosphere, most importantly the ionosphere. The amount of the variability in speed of light also depends on the frequency of the transmitted signal. As a result of this physical property, a GPS receiver can account for the ionospheric effect if it can receive GPS signals on two different frequencies. This capability was built into the GPS design from the beginning.

2.2.1 GPS Signal Structure

Originally intended for military use, the structure of the GPS transmitted signal was designed to provide a rapid means of calculating position and velocity. Two radio carrier frequencies were selected to carry signals from GPS satellites. The primary frequency, termed L_1 , is centred at 1575.42 MHz. The secondary frequency, L_2 , is centred at 1227.60 MHz. Each satellite transmits a unique signal at both frequencies, with a characteristic repeating digital code modulated on the carrier frequency. An example of the first one hundred chips of one of the codes transmitted by space vehicle (SV) 24 is shown in Figure 2.2. Each element in a code sequence is called a “chip” as opposed to a data bit because it is not actually data being transmitted in the code. The number of chips per second is called the chipping rate. The composition of the repeating digital code generated by each satellite can be varied based on operational requirements. Normal operation is described here.

Each satellite transmits satellite navigation data pertaining to all satellites at a rate of fifty bits per second. Part of these data represent the parameters in the equations of motion for each satellite. Typically, both the L_1 and L_2 signals contain this satellite navigation message. This information is used by the receiver to determine the positions of the satellites and to provide a rough approximation of the time and date, which can in turn be used to determine which satellites should be in view from an approximate geographic location. Because the satellite navigation message is transmitted at a relatively slow rate, it takes 12.5 minutes to receive the entire message. Each frame, corresponding to an individual satellite, takes thirty seconds to transmit. Consequently, it can take several

minutes for a position fix to be calculated the first time a GPS receiver is activated.

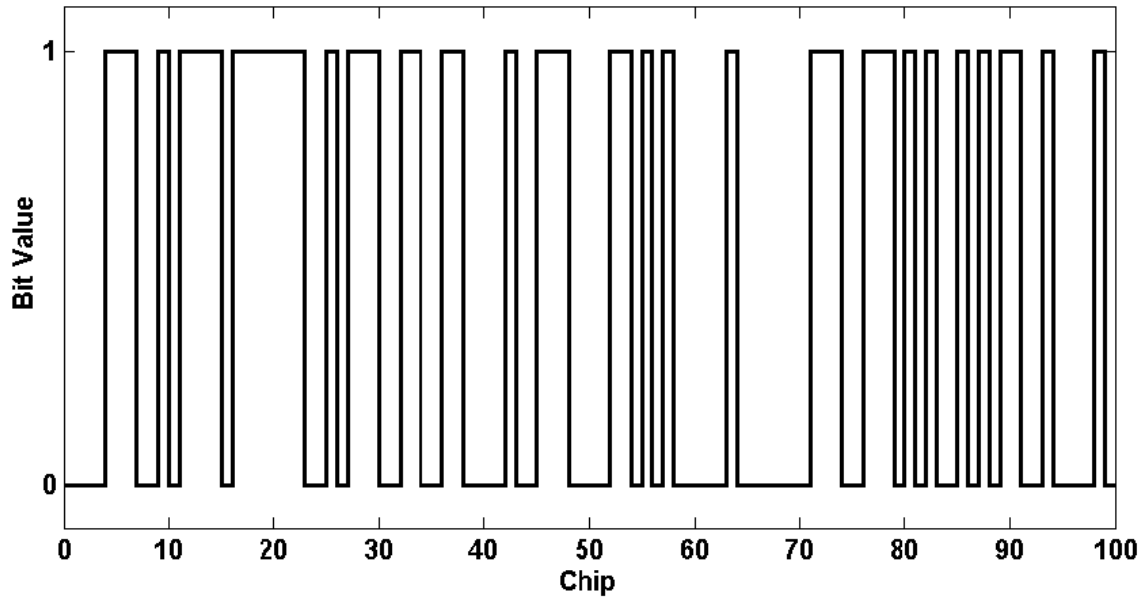


Figure 2.2 PRN Code: a Repeating Series, Characteristic of the Transmitter Satellite

The L_1 signal is also modulated with a repeating code, characteristic of the satellite from which it was sent, the purpose of which is to provide a coarse position determination. This code, called the coarse/acquisition (C/A) code, is a binary stream of 1023 chips transmitted at a rate of 1.023 Mcps so that the signal repeats once every millisecond. It is the code that allows the GPS receiver to determine the time at which the signal was sent from the satellite. A GPS receiver generates a reference signal to which the incoming signal is compared. The receiver then adjusts its estimate of time of receipt until the incoming signal and the reference signal are aligned. When this process is complete, the receiver has determined the time, accurate to less than a microsecond, but with an ambiguity of an integer multiple of a millisecond. One millisecond represents the time

required for light to travel 300 kilometres, so having observations from multiple satellites resolves this ambiguity.

Both the L_1 and the L_2 signals are also modulated with another repeating code, characteristic of the satellite from which it was sent, the purpose of which is to provide a precise determination of position. This binary data stream, called the P-code, is transmitted at 10.23 Mcps and repeats once every week. The receiver uses this code in a similar manner to that described for the C/A-code. Receiving the signal on two different frequencies allows the receiver to compensate for the change of the speed of light through the atmosphere. The length of a P-code chip is also one tenth the length of a C/A-code chip, which provides greater resolution.

The relative length of the individual constituent parts of the GPS signal provides an indication of the available accuracy. The wavelength of the L_1 signal is 19.04 centimetres. One P-code chip is 154 wavelengths or 29.33 metres. One C/A-code chip is 1540 wavelengths or 293.3 metres. Available accuracy is typically ten to fifty times better than the chip size, so C/A-code tracking leads to P-code acquisition and P-code tracking leads to resolution of the carrier cycle.

2.2.2 GPS Signal Tracking

A GPS receiver determines velocity by measuring the Doppler shift of the incoming signal from the satellite. Because the range to each satellite is continuously changing, the frequency of the received signal is slightly different for each satellite. Important to note,

for the purpose of later discussion, is the manner in which the incoming frequency is measured. A Frequency Locked Loop (FLL) is a signal tracking loop where the incoming signal is compared to a reference signal to arrive at an estimate of the incoming frequency. A Phase Locked Loop (PLL) is a signal tracking loop that incorporates the FLL capability but is intended to arrive at an estimate of the phase of the incoming signal. If the receiver has locked on to the phase of the incoming signal, then it has also locked on to the frequency. A block diagram for a PLL is shown in Figure 2.3. Phase error is fed back to a numerically controlled oscillator (NCO), which is essentially a firmware oscillator that estimates the carrier frequency and phase. The carrier frequency is the transmitted carrier frequency plus the Doppler shift resulting from the relative motion between the satellite and the receiver. The observed Doppler frequency can therefore be used to estimate receiver velocity and aid in propagating position observations from one time step to the next.

Unless the signal tracking loop is aided by some external inertial sensor, the PLL (or FLL) treats any acceleration or higher order dynamics as an unmodelled disturbance. As a result, using GPS-derived observations to determine higher order parameters may result in a performance penalty.

Once the PLL has removed the carrier from the signal, the resulting signal is the code from the satellite plus any remaining phase error. To determine range to each satellite, the GPS receiver generates the same code that the satellite has superimposed on the carrier signal. This reference code is then compared with the incoming signal in the Delay Locked Loop

(DLL) shown in Figure 2.4. The purpose of the DLL is to determine the amount of time by which the code is delayed from the receiver's reference time. This observation is used to determine the actual time with reference to the GPS datum, which is in turn used to determine the location of the satellite at the time of transmission. The location of the satellite and the time required for signal transmission is used to determine the range to the satellite and the receiver position using equations (2.1) through (2.4).

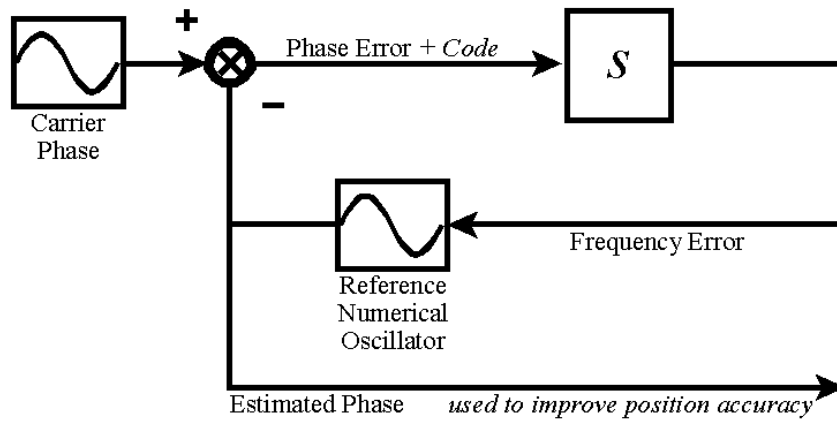


Figure 2.3 Phase Locked Loop Block Diagram

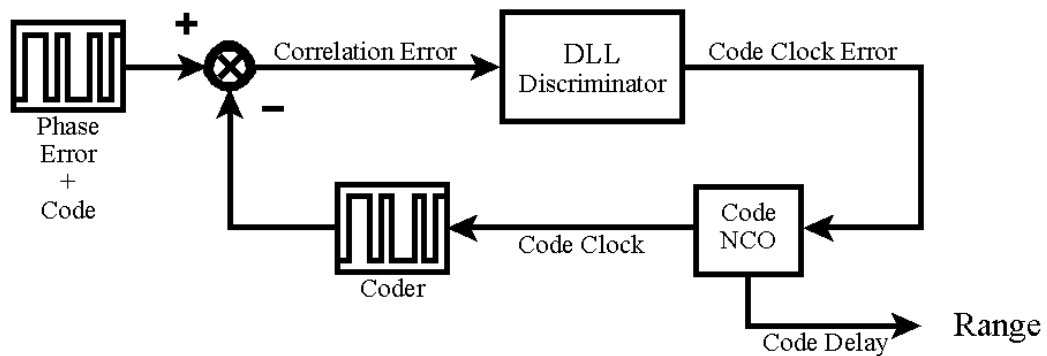


Figure 2.4 Delay Locked Loop Block Diagram

2.3 State Observers

It is not always possible to directly measure parameters of importance to a particular system of states. For example, there is no means to directly measure the acceleration of a vehicle. It is possible to measure the net force applied to a vehicle, the orientation of that force with respect to the gravity vector, and the weight of the vehicle, and then *infer* the magnitude and direction of the acceleration of the vehicle. Alternatively, the speed or position of a vehicle can be measured over time and the acceleration can be determined through differentiation. However, direct differentiation amplifies any noise present in the measured quantity. “There are methods available to estimate unmeasurable state variables without a differentiation process. Estimation of unmeasurable state variables is commonly called *observation*.”^{16*} A system of states is observable if the available measurements allow all states to be determined in a finite amount of time.

2.4 The Discrete Kalman Filter**

The purpose of a Kalman Filter is to optimally estimate states in a theoretical model based on sensor measurements. In a state-space representation such as the following, the state vector, \bar{x} , represents the actual condition of the system being observed, which includes process noise. The state transition matrix, \mathbf{A} , need not be constant¹⁸. Rather, it is the matrix which, multiplied by the states at a time, k , would result in a noiseless state vector

*The convention for nomenclature used by Ogata¹⁶ is used consistently throughout this manuscript.

**The development of the Discrete Kalman Filter appearing in this section is reproduced in its entirety¹⁷ from literature. Note also that the subscripts, k , are dropped in all equations where all arguments are at the same time step, k .

at a time, $k + 1$. Adding process noise, the states at $k + 1$,

$$\bar{x}_{k+1} = \mathbf{A}\bar{x}_k + \bar{w}_{1:k+1}, \quad (2.5)$$

are found, where the zero-mean process noise, \bar{w}_1 , is described by the covariance matrix,

$$\mathbf{Q} = E\{\bar{w}_1\bar{w}_1^T\}. \quad (2.6)$$

The measurements,

$$\bar{y} = \mathbf{C}\bar{x} + \bar{w}_2, \quad (2.7)$$

relate to the states through the matrix, \mathbf{C} , in combination with zero-mean sensor noise,

\bar{w}_2 , described by the covariance matrix,

$$\mathbf{R} = E\{\bar{w}_2\bar{w}_2^T\}. \quad (2.8)$$

Once sensor measurements are taken, the state estimates computed in the prior time step,

\hat{x}^- , can be improved based on how the measurements deviate from those the state

transition matrix would project,

$$\hat{x} = \hat{x}^- + \mathbf{K}(\bar{y} - \hat{y}^-), \quad (2.9)$$

or

$$\hat{x} = \hat{x}^- + \mathbf{K}(\bar{y} - \mathbf{C}\hat{x}^-), \quad (2.10)$$

where the observer gain matrix, \mathbf{K} , remains to be chosen. The optimal gain matrix is defined as that which would provide state estimates that deviate from the actual states by the least square error. To find this optimal gain, it is necessary to mathematically

determine the variance of the state error. It is assumed that the process noise and the sensor noise are zero-mean random processes, so the variance of the state error should also be a zero-mean process.

The state error,

$$\bar{e} = \bar{x} - \hat{x}, \quad (2.11)$$

expanded using (2.10),

$$\bar{e} = \bar{x} - \hat{x}^- - \mathbf{K}(\bar{y} - \mathbf{C}\hat{x}^-), \quad (2.12)$$

and (2.7),

$$\bar{e} = \bar{x} - \hat{x}^- - \mathbf{K}(\mathbf{C}\bar{x} + \bar{w}_2 - \mathbf{C}\hat{x}^-) \quad (2.13)$$

then rearranging,

$$\bar{e} = (\bar{x} - \hat{x}^-) - \mathbf{K}\mathbf{C}(\bar{x} - \hat{x}^-) - \mathbf{K}\bar{w}_2 \quad (2.14)$$

and collecting terms,

$$\bar{e} = (\mathbf{I} - \mathbf{K}\mathbf{C})(\bar{x} - \hat{x}^-) - \mathbf{K}\bar{w}_2 \quad (2.15)$$

or

$$\bar{e} = (\mathbf{I} - \mathbf{K}\mathbf{C})\bar{e}^- - \mathbf{K}\bar{w}_2 \quad (2.16)$$

provides a means to determine the error covariance,

$$\mathbf{P} = E\{\overline{e e^T}\}. \quad (2.17)$$

If there is no correlation between the process noise and the sensor noise, the expected values* of the terms in (2.16) are separable. Thus,

$$\mathbf{P} = E\{(\mathbf{I} - \mathbf{K}\mathbf{C})\overline{e} \overline{e}^{-T} (\mathbf{I} - \mathbf{K}\mathbf{C})^T\} + E\{\mathbf{K}\overline{w}_2 \overline{w}_2^T \mathbf{K}^T\}, \quad (2.18)$$

or

$$\mathbf{P} = (\mathbf{I} - \mathbf{K}\mathbf{C})\mathbf{P}^- (\mathbf{I} - \mathbf{K}\mathbf{C})^T + \mathbf{K}\mathbf{R}\mathbf{K}^T. \quad (2.19)$$

Expanding,

$$\mathbf{P} = (\mathbf{P}^- - \mathbf{K}\mathbf{C}\mathbf{P}^- - \mathbf{P}^- \mathbf{C}^T \mathbf{K}^T + \mathbf{K}\mathbf{C}\mathbf{P}^- \mathbf{C}^T \mathbf{K}^T) + (\mathbf{K}\mathbf{R}\mathbf{K}^T). \quad (2.20)$$

Because the covariance matrix is symmetric, it is equal to its transpose. The third term can be rewritten, which provides the error covariance matrix,

$$\mathbf{P} = \mathbf{P}^- - \mathbf{K}\mathbf{C}\mathbf{P}^{-T} - (\mathbf{K}\mathbf{C}\mathbf{P}^{-T})^T + \mathbf{K}(\mathbf{C}\mathbf{P}^- \mathbf{C}^T) \mathbf{K}^T + \mathbf{K}(\mathbf{R}) \mathbf{K}^T. \quad (2.21)$$

This represents the covariance of the state estimate error regardless of the observer gain chosen. It is desirable to minimize the state error, so the trace of the covariance matrix must be minimized.

Using the matrix differentiation formulae,

*Mathematical expectation, statistical average, and ensemble average are commonly used synonyms for expected value.¹⁹

$$\frac{d(\text{trace } \mathbf{FG})}{d\mathbf{F}} = \mathbf{G}^T, \quad (2.22)$$

$$\frac{d(\text{trace } (\mathbf{FG})^T)}{d\mathbf{F}} = \mathbf{G}^T, \quad (2.23)$$

and

$$\frac{d(\text{trace } \mathbf{FGF}^T)}{d\mathbf{F}} = 2\mathbf{FG}, \quad (2.24)$$

the derivative of the trace of the covariance matrix with respect to the observer gain matrix,

$$\frac{d(\text{trace } \mathbf{P})}{d\mathbf{K}} = -2(\mathbf{CP}^{-T})^T + 2\mathbf{K}(\mathbf{CP}^{-T}\mathbf{C}^T) + 2\mathbf{K}(\mathbf{R}) \quad (2.25)$$

is determined.

Setting the result of (2.25) to zero provides a relationship defining the point at which the trace of the covariance matrix is a minimum,

$$\mathbf{P}^{-T}\mathbf{C}^T = \mathbf{K}(\mathbf{CP}^{-T}\mathbf{C}^T + \mathbf{R}). \quad (2.26)$$

Rearranging, the observer gain,

$$\mathbf{K} = \mathbf{P}^{-T}\mathbf{C}^T(\mathbf{CP}^{-T}\mathbf{C}^T + \mathbf{R})^{-1}, \quad (2.27)$$

is found. This is the optimal observer or Kalman Gain Matrix.

In a recursive state estimator, state estimate projections,

$$\hat{x}_{k+1}^- = \mathbf{A}_k \hat{x}_k, \quad (2.28)$$

are based on the current state estimate and state transition matrix. Error projections,

$$\bar{e}^- = \bar{x} - \hat{x}^-, \quad (2.29)$$

can be used to determine an error covariance projection. Incorporating (2.5), and (2.28),

$$\bar{e}_{k+1}^- = \mathbf{A}_k \bar{x}_k + \bar{w}_{1:k+1} - \mathbf{A}_k \hat{x}_k, \quad (2.30)$$

gathering terms,

$$\bar{e}_{k+1}^- = \mathbf{A}_k (\bar{x}_k - \hat{x}_k) + \bar{w}_{1:k+1}, \quad (2.31)$$

and using (2.11),

$$\bar{e}_{k+1}^- = \mathbf{A}_k \bar{e}_k + \bar{w}_{1:k+1}, \quad (2.32)$$

a representation of the error projection vector is determined. This function can be used to determine an error covariance projection,

$$\mathbf{P}^- = E\{\bar{e}^- \bar{e}^{-T}\}. \quad (2.33)$$

Note that the first term on the right side in (2.32) includes the process noise and sensor noise from the current step, k , while the second term includes the process noise that will be present in the next step, $k+1$. If there is no correlation between the process noise from one step to the next, the expected values of the terms in (2.32) are separable. Thus,

$$\mathbf{P}_{k+1}^- = E\{\mathbf{A} \bar{e} \bar{e}^T \mathbf{A}^T\}_k + E\{\bar{w}_1 \bar{w}_1^T\}_{k+1}, \quad (2.34)$$

or

$$\mathbf{P}_{k+1}^- = \mathbf{A}_k \mathbf{P}_k \mathbf{A}_k^T + \mathbf{Q}_{k+1}. \quad (2.35)$$

Equations (2.10), (2.19), (2.27), (2.28), and (2.35) are used in the recursive Kalman Filter.

The recursion algorithm is shown graphically in Figure 2.5.

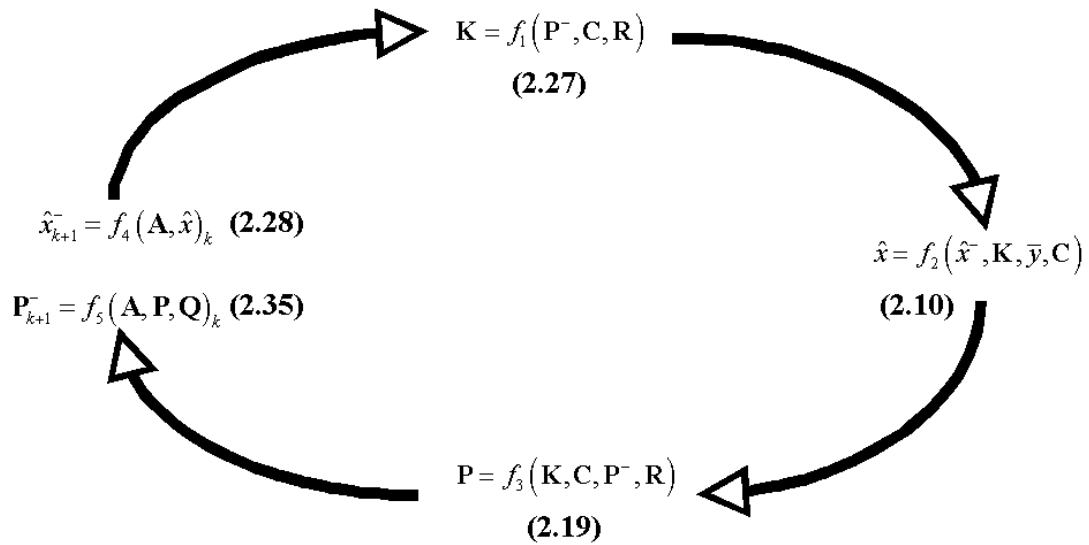


Figure 2.5 Recursive Kalman Filter Algorithm

In the recursive Kalman Filter algorithm, state estimates determined in the prior time step are improved by comparing sensor measurements with those expected from the system model. The mean square state estimate error is computed, then estimates of the expected error and states are determined for the following time step.

2.5 Applied Kalman Filtering, an Example

To demonstrate the use of a Discrete Kalman Filter, consider the interesting problem of

fusing data generated by a GPS receiver with inertial navigation systems (INS). INS instrumentation is based on the observation of linear acceleration and rotational velocity. These data can be integrated to determine position and velocity which are generally used for navigation purposes. The problem with INS instrumentation is that the error present in the sensor data is also integrated, which results in errors in position and velocity which grow over time. The error associated with GPS-derived observations of position do not grow over time, but may not be as accurate as necessary for a particular application. The fusion of data from both sources using a Kalman Filter can result in an optimal determination of position and velocity. Note that the approach described here is far simplified from common methods²⁰ of implementing a Kalman Filter for GPS/INS integration.

To construct the state vector and the state transition matrix, it is necessary to have an understanding of the dynamic range of the vehicle being navigated. Where an automobile may experience acceleration of less than eight metres per second squared and the driver may be capable of making control adjustments resulting in jerk of less than fifty metres per second cubed, a high-performance jet fighter may be capable of acceleration in excess of fifty metres per second squared and jerk in excess of one hundred metres per second cubed. In the latter instance, it may be necessary to consider higher order dynamics. For the following example, it is assumed that higher order dynamics are negligible. The kinematic equation relating position, s , velocity, v , acceleration, a , and jerk, j , from one time step to the next,

$$\bar{x}_{k+1} = \begin{bmatrix} s \\ v \\ a \\ j \end{bmatrix}_{k+1} = \begin{bmatrix} 1 & \Delta t & 0 & 0 \\ 0 & 1 & \Delta t & 0 \\ 0 & 0 & 1 & \Delta t \\ 0 & 0 & 0 & 1 \end{bmatrix} \bar{x}_k + \begin{bmatrix} 0 \\ 0 \\ 0 \\ q \end{bmatrix}_{k+1}, \quad (2.36)$$

is governed by the zero-mean random variable, q . This means that jerk is treated as a random process. In the implementation of this filter, the variance of this process noise must be chosen. In practice, assuming jerk to be a random process will be an approximation of reality. Arriving at a model to describe the system dynamics is, in the opinion of the author, the most important aspect in the design of a Kalman Filter. In this example, whether or not the system dynamics can be described by assuming jerk to be a random process is pivotal. In practice, the approach taken in the identification of noise variance in a Kalman Filter, a strategy called “tuning”, is more or less arbitrary²¹ and based primarily on the resulting performance as judged by the designer rather than adherence to the stipulations set forth in the original development of the Kalman Filter algorithm. The Kalman Filter derivation requires that the process noise be uncorrelated in time.

The measurements from a GPS receiver and from an INS,

$$\bar{y} = \begin{bmatrix} s \\ a \end{bmatrix} = \begin{bmatrix} 1 & 0 & 0 & 0 \\ 0 & 0 & 1 & 0 \end{bmatrix} \bar{x} + \begin{bmatrix} r_1 \\ r_2 \end{bmatrix}, \quad (2.37)$$

also include sensor noise represented by r_1 and r_2 . As with process noise, the variance of the sensor noise must be known or approximated. Based on these simple equations and the identification of process noise and sensor noise variances, the implementation of the

Kalman Filter is carried out through the use of the Discrete Kalman Filter equations developed earlier.

In the application described, the position, velocity, and acceleration of the vehicle is overdefined. Either sensor alone could be used to sub-optimally identify all states. The Kalman Filter essentially treats the noise variances as weighting factors to determine an improved estimate of the state variables.

Chapter 3 - Objectives

3.1 Introduction

The successful development of a system that could reduce the frequency of air transportation accidents where runway friction coefficient or limited length of runway is a critical factor would be a major achievement. In the development of such a system, a number of major studies would have to be undertaken. These could include computer modelling of the dynamics of aircraft pertaining to both flight and ground operations, and the on-board instantaneous observation of both the runway friction coefficient and the length of runway remaining. The incorporation of this and other information such as aircraft mass, measurements of inertia, and wind direction and speed, could lead in time to the development of a safe stopping distance warning system.

The specific purpose of the proposed research was to investigate the feasibility of using an observer system during the roll and takeoff phase of aircraft operation to provide to the pilot the information that is needed to manoeuvre safely. If feasible, such an observer system could be later incorporated within a takeoff performance monitoring system.

While previous work in this field focussed on the design of a takeoff performance monitoring system for use on dry, paved runways, this project examined the factors pertaining to gravel runways where reverse thrust, rather than braking, is the primary

means of deceleration.

3.2 Project Objectives

The objectives of this thesis project were:

1. to investigate, with the aid of a theoretical model, the relative importance of the various parameters influencing the estimation of stopping distance for a specific aircraft type, the British Aerospace Jetstream 31, through installation and flight testing in a typical aircraft, and;
2. to explore the sensing technologies that would be required to measure the required parameters, with special consideration for the application of the Global Positioning System in determination of aircraft acceleration, velocity, and position with respect to the end of the runway.

3.3 Methodology

To achieve the project objectives, a theoretical dynamic model of an aircraft during takeoff or landing was first determined. A practical examination using accelerometers as the source of reference data was performed to evaluate the feasibility of using Global Positioning System to measure vehicle acceleration. Finally, validation of the theoretical model was pursued through installation of a data acquisition system in an aircraft operated by a regional airline.

3.4 Scope

In this preliminary investigation of a TOPMS designed specifically for the far-northern environment, factors such as runway slope, wind velocity, wheel friction coefficient, and aircraft control settings were considered constant in the theoretical dynamic model of an aircraft in contact with the ground. While variability in any parameter considered constant by the model could influence the performance of a TOPMS, such variability was deemed beyond the scope of this project. In essence, the goal of this project was to assess the feasibility of using a GPS receiver as the sole sensor in a TOPMS.

Chapter 4 - Theoretical Prototype System

4.1 Background

Assuming that all necessary quantities can be measured, a takeoff performance monitor would require a method to project how the speed, position, and acceleration of an aircraft might change in the future based on measurements taken in the past. This necessitates the availability of a mathematical model describing how these parameters vary with respect to one another.

4.2 Parametric Model of an Aircraft During Takeoff

In the construction of such a model, each parameter need not be independently measurable, so long as the system can be observed.

The force of drag on an aircraft,

$$D = D_3 v_{/a}^2, \quad (4.1)$$

where: D_3 is a constant parameter for a given aircraft geometry, and;

$v_{/a}$ is the speed of the aircraft relative to the air.

Applying the convention that a headwind is positive while aircraft speed is positive forward,

$$D = D_3 (v_a + v)^2. \quad (4.2)$$

Expanding,

$$D = D_3 v_a^2 + 2D_3 v_a v + D_3 v^2, \quad (4.3)$$

or

$$D = D_1 + D_2 v + D_3 v^2, \quad (4.4)$$

where: D_n are constant parameters for a given aircraft geometry,

D_1 is the component of aerodynamic drag at rest,

D_2 is the component of aerodynamic drag proportional to speed,

D_3 is the component of aerodynamic drag proportional to speed squared,

v_a is the component of wind in the direction of the runway, and;

v is the speed of the aircraft relative to the ground.

Similarly, thrust,

$$T = T_0 + T_3 v_a^2, \quad (4.5)$$

where: T_0 is a parameter representing the throttle setting, and;

T_3 is a parameter to account for increased thrust at higher engine inlet pressures.

As in the derivation for drag,

$$T = T_0 + T_3 (v_a + v)^2. \quad (4.6)$$

Expanding,

$$T = T_0 + T_3 v_a^2 + 2T_3 v_a v + T_3 v^2, \quad (4.7)$$

or

$$T = T_1 + T_2v + T_3v^2, \quad (4.8)$$

where: T_n are constant parameters for a given throttle setting,

T_1 is the component of engine thrust at rest,

T_2 is the component of engine thrust proportional to speed, and;

T_3 is the component of engine thrust proportional to speed squared.

Simple relationships exist for viscous friction,

$$F = F_2v, \quad (4.9)$$

and for the component of weight in the direction of motion,

$$W = W_1, \quad (4.10)$$

where: F_2 and W_1 are constants provided that the runway slope is constant.

Note that this model applies equally to the situation that exists on both paved and gravel runways, so long as no wheel braking is used. Grouping similar parameters and applying Newton's Second Law,

$$a = \frac{\Sigma F}{m} = \frac{D_1 + T_1 + W_1}{m} + \frac{D_2 + T_2 + F_2}{m}v + \frac{D_3 + T_3}{m}v^2, \quad (4.11)$$

or

$$a = P_1 + P_2v + P_3v^2, \quad (4.12)$$

where: P_n are parameters representing the net force per unit mass acting on the aircraft,

P_1 is the component of vehicle acceleration at rest,

P_2 is the component of vehicle acceleration proportional to speed,

P_3 is the component of vehicle acceleration proportional to speed squared, and;

a is the acceleration of the aircraft in the direction of motion.

4.3 Projection of Displacement

To use this model for the prediction of later displacement requires an equation describing the displacement as a function of speed. From fundamental kinematics,

$$v = \frac{ds}{dt}, \text{ and;} \quad (4.13)$$

$$a = \frac{dv}{dt}, \quad (4.14)$$

which can be solved to describe the differential time,

$$dt = \frac{ds}{v} = \frac{dv}{a}. \quad (4.15)$$

Rearranging, an equation describing the differential displacement,

$$ds = \frac{v dv}{a}, \quad (4.16)$$

is found.

Incorporating the model,

$$ds = \frac{v dv}{P_1 + P_2 v + P_3 v^2}. \quad (4.17)$$

If the instantaneous position and speed are known, the displacement at a reference speed can be determined through integration. The displacement,

$$s_2 - s_1 = \int_{v_1}^{v_2} \frac{v dv}{P_1 + P_2 v + P_3 v^2}, \quad (4.18)$$

where: s_1 is the instantaneous position;

s_2 is the predicted position at the reference speed;

v_1 is the instantaneous speed, and;

v_2 is the reference speed.

The solution to this integral,

$$s_2 - s_1 = \frac{c \ln|v + c| - d \ln|v + d|}{P_3(c - d)} \Bigg|_{v_1}^{v_2}, \quad (4.19)$$

where:

$$c = \frac{P_2 + \sqrt{P_2^2 - 4P_1P_3}}{2P_3}, \quad (4.20)$$

and;

$$d = \frac{P_2 - \sqrt{P_2^2 - 4P_1P_3}}{2P_3}, \quad (4.21)$$

can be used to conduct an uncertainty analysis for the measured quantities in the model.

Appendix 1.03 (CD-ROM) contains the mathematical development of this solution under the “integral solution” directory.

4.4 Signal Processing Technique

Customarily, the states in a Kalman Filter are time derivatives of one another. This stems from the rigidity of the *continuous* Kalman Filter, which requires that all states be related to one another through differentiation in a homogeneous domain. The discrete Kalman Filter is not limited in this way, as shown earlier in section 2.4.

4.4.1 Standard Treatment of the Discrete Kalman Filter

Based on the dynamics pertaining to the particular application, the designer typically assigns a high derivative to be a random process. The lower states are then dependent on the random variable. Each state may also be assigned some random variability to uncouple neighbouring states. For instance, it would not be uncommon to describe the dynamics of an aircraft during its takeoff roll based on its position, s , speed, v , acceleration, a , and jerk, j ,

$$\bar{x}_{k+1} = \begin{bmatrix} s \\ v \\ a \\ j \end{bmatrix}_{k+1} = \begin{bmatrix} 1 & \Delta t & 0 & 0 \\ 0 & 1 & \Delta t & 0 \\ 0 & 0 & 1 & \Delta t \\ 0 & 0 & 0 & 1 \end{bmatrix} \bar{x}_k + \begin{bmatrix} 0 \\ 0 \\ 0 \\ q \end{bmatrix}_{k+1}, \quad (4.22)$$

where: Δt is the difference in time between k and $k + 1$, and;

q_j is a zero-mean random variable.

Such a filter functions best when jerk most closely resembles a zero-mean random process, though this is usually an approximation of reality. For small time steps, it may be considered a reasonable approximation.

4.4.2 Non-linear Manipulation of the Discrete Kalman Filter

In the model,

$$a = P_1 + P_2 v + P_3 v^2, \quad (4.23)$$

jerk can be found through differentiation,

$$j = \frac{da}{dt} = P_2 a + 2P_3 v a, \quad (4.24)$$

or,

$$j = P_1 P_2 + (P_2^2 + 2P_1 P_3) v + 3P_2 P_3 v^2 + 2P_3^2 v^3, \quad (4.25)$$

and is clearly not a zero-mean process. The higher derivatives are also non-zero.

On the other hand, velocity derivatives of the model,

$$\frac{da}{dv} = P_2 + 2P_3 v, \quad (4.26)$$

$$\frac{d^2 a}{dv^2} = 2P_3, \text{ and}; \quad (4.27)$$

$$\frac{d^3 a}{dv^3} = 0, \quad (4.28)$$

provide an alternative method of observer construction. The third velocity derivative of acceleration is a zero-mean process. Without approximation, this can be considered a random process because the sole source of variation in the observation of this quantity

would be process noise.

Based on this knowledge, an observer* built with the state transition equation,

$$\begin{bmatrix} s \\ v \\ a \\ \frac{da}{dv} \\ \frac{d^2a}{dv^2} \end{bmatrix}_{k+1} = \begin{bmatrix} 1 & \Delta t & 0 & 0 & 0 \\ 0 & 1 & \Delta t & 0 & 0 \\ 0 & 0 & 1 & \Delta v & 0 \\ 0 & 0 & 0 & 1 & \Delta v \\ 0 & 0 & 0 & 0 & 1 \end{bmatrix} \begin{bmatrix} s \\ v \\ a \\ \frac{da}{dv} \\ \frac{d^2a}{dv^2} \end{bmatrix}_k + \begin{bmatrix} 0 \\ 0 \\ 0 \\ q_4 \\ q_5 \end{bmatrix}_{k+1}, \quad (4.29)$$

was constructed. This is a model for a Kalman Filter that is capable of an optimal estimation despite reference to a non-linear model. This treatment cannot be examined in the continuous Kalman Filter.

4.5 Required Accuracy

In an operative takeoff performance monitor, the device would project the displacement that would occur while accelerating to a decision speed, V_1 . This displacement would be added to the projected displacement that would occur when decelerating from V_1 to rest. The total displacement would be compared to the instantaneous observation of the remaining runway length, and the difference would be displayed to the pilot as a margin of safety in units of distance. There are several factors that could affect the actual margin of safety, most notably the reaction time of the pilot.

*The importance of this contribution is the subject of an article in draft at the time of completion of this manuscript, formed in part by the combination of two previously published refereed conference papers.^{22,23}

Assuming that the pilot would compensate for reaction time by selecting a comfortable margin of safety, the required accuracy of the margin measurement must be selected. For larger aircraft, a larger margin would be selected. It is therefore appropriate to establish required accuracy based on the length of the aircraft. In the extreme case, a takeoff rejection is initiated at V_1 and the pilot has selected a margin of safety that would be completely consumed by the displacement of the aircraft during the reaction time of the pilot. This is explained further in the section 4.7. In the instance where no margin of safety remains, it is desirable that the runway remaining when the aircraft has come to rest is no less than one aircraft length, measured from the nose of the aircraft. The author has therefore selected the length of the aircraft, measured from nose to tail, as the required accuracy in the observation of projected displacement. The aircraft used in this experimental investigation measured fifteen metres from nose to tail.

4.6 Uncertainty Analysis

To assess the sensitivity of the theoretical model to uncertainties in the measured quantities, an uncertainty analysis was conducted.

The partial derivatives of displacement with respect to the measured quantities,

$$\frac{\partial(s_2 - s_1)}{\partial v_1} = \frac{v_2 - v_1}{P_1 + P_2 v_1 + P_3 v_1^2}, \quad (4.30)$$

$$\begin{aligned}
\frac{\partial(s_2 - s_1)}{\partial P_1} &= \frac{\partial c}{\partial P_1} \left[\frac{\ln \left| \frac{v_2 + c}{v_1 + c} \right| + \frac{c(v_1 - v_2)}{(v_1 + c)(v_2 + c)}}{P_3(c - d)} \right] \\
&- \frac{\partial d}{\partial P_1} \left[\frac{\ln \left| \frac{v_2 + d}{v_1 + d} \right| + \frac{d(v_1 - v_2)}{(v_1 + d)(v_2 + d)}}{P_3(c - d)} \right], \\
&+ \left(\frac{\partial d}{\partial P_1} - \frac{\partial c}{\partial P_1} \right) \left[\frac{c \ln \left| \frac{v_2 + c}{v_1 + c} \right| - d \ln \left| \frac{v_2 + d}{v_1 + d} \right|}{P_3(c - d)^2} \right]
\end{aligned} \tag{4.31}$$

$$\begin{aligned}
\frac{\partial(s_2 - s_1)}{\partial P_2} &= \frac{\partial c}{\partial P_2} \left[\frac{\ln \left| \frac{v_2 + c}{v_1 + c} \right| + \frac{c(v_1 - v_2)}{(v_1 + c)(v_2 + c)}}{P_3(c - d)} \right] \\
&- \frac{\partial d}{\partial P_2} \left[\frac{\ln \left| \frac{v_2 + d}{v_1 + d} \right| + \frac{d(v_1 - v_2)}{(v_1 + d)(v_2 + d)}}{P_3(c - d)} \right], \text{ and;} \\
&+ \left(\frac{\partial d}{\partial P_2} - \frac{\partial c}{\partial P_2} \right) \left[\frac{c \ln \left| \frac{v_2 + c}{v_1 + c} \right| - d \ln \left| \frac{v_2 + d}{v_1 + d} \right|}{P_3(c - d)^2} \right]
\end{aligned} \tag{4.32}$$

$$\begin{aligned}
\frac{\partial(s_2 - s_1)}{\partial P_3} &= \frac{\partial c}{\partial P_3} \left[\frac{\ln \left| \frac{v_2 + c}{v_1 + c} \right| + \frac{c(v_1 - v_2)}{(v_1 + c)(v_2 + c)}}{P_3(c - d)} \right] \\
&\quad - \frac{\partial d}{\partial P_3} \left[\frac{\ln \left| \frac{v_2 + d}{v_1 + d} \right| + \frac{d(v_1 - v_2)}{(v_1 + d)(v_2 + d)}}{P_3(c - d)} \right], \\
&\quad + \left(\frac{\partial d}{\partial P_3} - \frac{\partial c}{\partial P_3} \right) \left[\frac{c \ln \left| \frac{v_2 + c}{v_1 + c} \right| - d \ln \left| \frac{v_2 + d}{v_1 + d} \right|}{P_3(c - d)^2} \right] \\
&\quad - \left[\frac{c \ln \left| \frac{v_2 + c}{v_1 + c} \right| - d \ln \left| \frac{v_2 + d}{v_1 + d} \right|}{P_3^2(c - d)} \right],
\end{aligned} \tag{4.33}$$

together with partial derivatives,

$$\frac{\partial c}{\partial P_1} = -(P_2^2 - 4P_1P_3)^{-\frac{1}{2}}, \tag{4.34}$$

$$\frac{\partial c}{\partial P_2} = \frac{1 + P_2(P_2^2 - 4P_1P_3)^{-\frac{1}{2}}}{2P_3}, \tag{4.35}$$

$$\frac{\partial c}{\partial P_3} = \frac{-P_2 - \sqrt{P_2^2 - 4P_1P_3} - 2P_1P_3(P_2^2 - 4P_1P_3)^{-\frac{1}{2}}}{2P_3^2}, \quad (4.36)$$

$$\frac{\partial d}{\partial P_1} = (P_2^2 - 4P_1P_3)^{-\frac{1}{2}}, \quad (4.37)$$

$$\frac{\partial d}{\partial P_2} = \frac{1 - P_2(P_2^2 - 4P_1P_3)^{-\frac{1}{2}}}{2P_3}, \text{ and;} \quad (4.38)$$

$$\frac{\partial d}{\partial P_3} = \frac{-P_2 + \sqrt{P_2^2 - 4P_1P_3} + 2P_1P_3(P_2^2 - 4P_1P_3)^{-\frac{1}{2}}}{2P_3^2}, \quad (4.39)$$

form the basis of the uncertainty analysis.

To establish approximate parameter values for use in the uncertainty analysis, an empirical analysis was conducted. From (4.11) and (4.12), P_3 is a function of T_3 , D_3 , and the mass of the aircraft. As a conservative approximation, the contribution of T_3 can be neglected. The drag force acting on an object²⁴ at high Reynolds numbers,

$$D = 0.22A\rho_{air}v_{/air}^2, \quad (4.40)$$

where: A is the frontal area of the object;

ρ_{air} is the density of air, and;

$v_{/air}$ is the speed of the object relative to the air.

The frontal area of the Jetstream 31 aircraft is 14.3 metres squared. The density of air under standard sea-level conditions is 1.225 kilograms per metre cubed. The maximum allowable takeoff mass of the aircraft is 7000 kilograms. Neglecting T_3 ,

$$P_3 \approx \frac{-D}{mv_{air}^2} = -0.00055 \text{ [m}^{-1}\text{]}. \quad (4.41)$$

Similarly, a conservative approximation of P_2 can be determined by neglecting the variability of thrust and the contribution of viscous friction in the aircraft tires. This requires an approximation of a typical yet conservatively large value for the wind speed, v_a . If this value for wind speed is chosen to be equal to fifteen metres per second,

$$P_2 \approx 2P_3v_a = -0.0165 \text{ [s}^{-1}\text{]}. \quad (4.42)$$

Finally, a value for initial thrust, must be chosen. This value would depend totally on the length of the runway. Choosing a typical value for initial thrust,

$$P_1 = 3.0 \text{ [m/s}^2\text{]}. \quad (4.43)$$

Based on these conservative parameter values, partial derivative values,

$$\frac{\partial c}{\partial P_1} = -1.21 \times 10^1 \text{ [s]}, \quad (4.44)$$

$$\frac{\partial d}{\partial P_1} = 1.21 \times 10^1 \text{ [s]}, \quad (4.45)$$

$$\frac{\partial c}{\partial P_2} = -7.28 \times 10^2 \text{ [m]}, \quad (4.46)$$

$$\frac{\partial d}{\partial P_2} = -1.09 \times 10^3 \text{ [m]}, \quad (4.47)$$

$$\frac{\partial c}{\partial P_3} = -4.40 \times 10^4 \text{ [m}^2\text{/s]}, \text{ and;} \quad (4.48)$$

$$\frac{\partial d}{\partial P_3} = -9.85 \times 10^5 \text{ [m}^2\text{/s]}, \quad (4.49)$$

are obtained.

Suppose the aircraft in question has an instantaneous speed of thirty metres per second, and the reference speed is fifty metres per second. Evaluating (4.30) through (4.33), these quantities result in partial derivatives of displacement with respect to observed quantities,

$$\frac{\partial(s_2 - s_1)}{\partial v_1} = \frac{2.00 \times 10^1}{2.01} = 1.00 \times 10^1 \text{ [s]}, \quad (4.50)$$

$$\frac{\partial(s_2 - s_1)}{\partial P_1} = 37.4 \frac{\partial c}{\partial P_1} - 4.65 \frac{\partial d}{\partial P_1} = -5.07 \times 10^2 \text{ [s}^2\text{]}, \quad (4.51)$$

$$\frac{\partial(s_2 - s_1)}{\partial P_2} = 37.4 \frac{\partial c}{\partial P_2} - 4.65 \frac{\partial d}{\partial P_2} = -2.22 \times 10^4 \text{ [s} \cdot \text{m]}, \text{ and;} \quad (4.52)$$

$$\frac{\partial(s_2 - s_1)}{\partial P_3} = 37.4 \frac{\partial c}{\partial P_3} - 4.65 \frac{\partial d}{\partial P_3} + 1.12 \times 10^6 = -9.83 \times 10^5 \text{ [m}^2\text{]}. \quad (4.53)$$

The equations can be used to determine the effect of errors in the measured quantities.

The GPS receiver's manufacturer specified maximum speed error is 0.20 metres per second. As a result of (4.50), there will exist two metres of error in the projected displacement due to this speed error at the conditions outlined. This error will decrease as the reference speed is approached.

In a conventional uncertainty analysis, each measured quantity is treated independently. However, in this particular case, there exists only one real measurement, that of speed provided by the GPS receiver. The Kalman Filter described earlier observes the parameters based on a measurement of speed. As a result, any error in a single parameter will result in corresponding errors in the remaining parameters.

The worst case scenario corresponds to a sudden change in drag coefficient or wind speed that would affect one or both of the parameters P_2 and P_3 more quickly than the filter can respond. Figure 4.1 shows the resulting error in the projection of displacement that would occur as the aircraft accelerates from an instantaneous speed of thirty metres per second to a reference speed of fifty metres per second as a function of percent error in the parameters P_2 and P_3 .

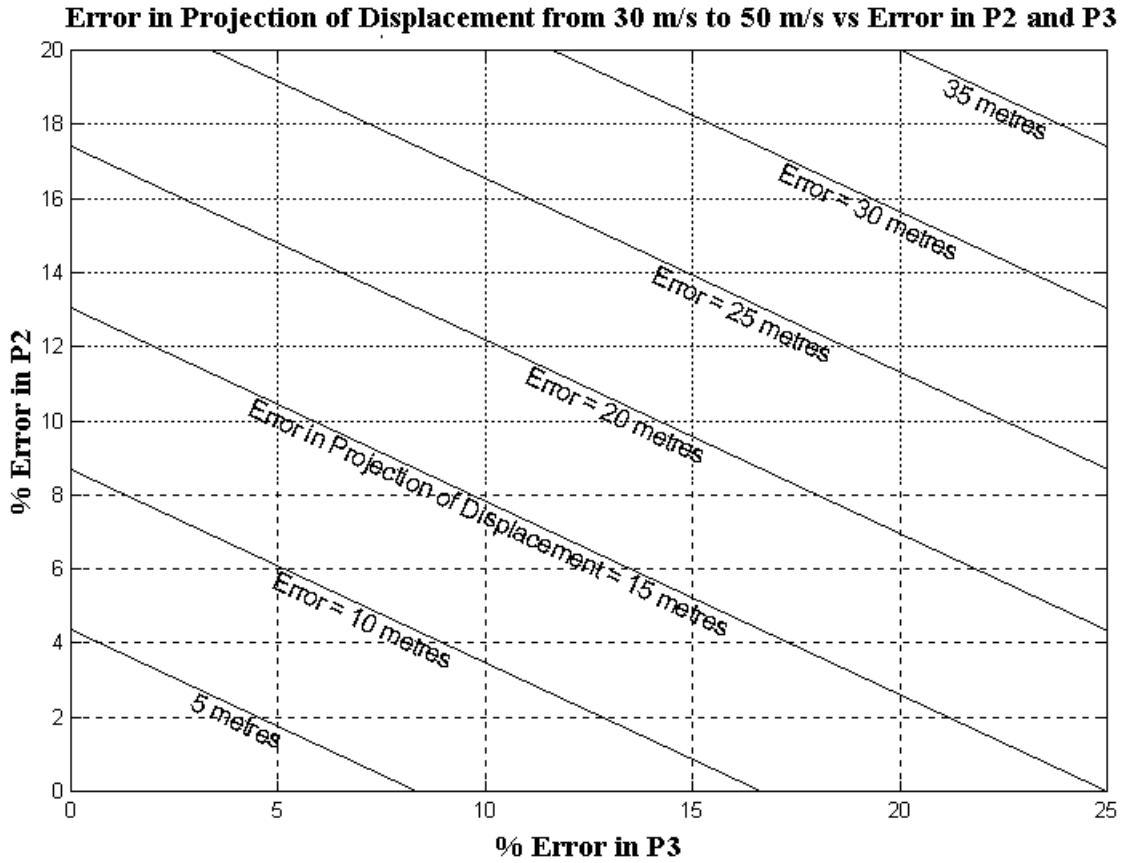


Figure 4.1 Error in Projection of Displacement as a Function of Error in P_2 and P_3

Figure 4.2 shows the error in projected displacement as a function of speed resulting from ten percent error in both P_2 and P_3 . Naturally, as the reference speed is approached, the error in the projection of the displacement that will have occurred at the reference speed approaches zero.

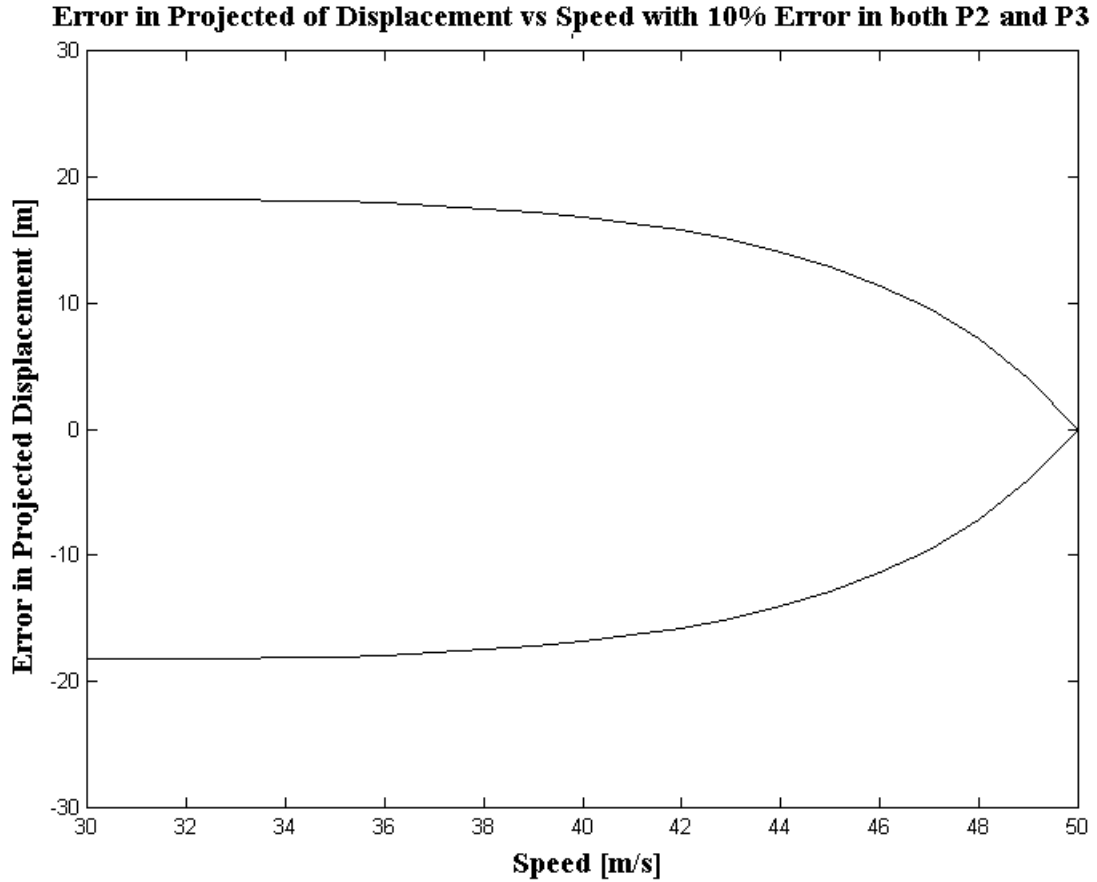


Figure 4.2 Error in Projected Displacement as a Function of Speed

In most cases, the actual error in the quantities determined by the Kalman Filter should be much less than what has been described here, because the estimation of parameters should result in observation error of far less than ten percent. Note, however, that if separate measurement systems were used to directly measure each quantity, the uncertainty in each measurement would result in a projected displacement error orders of magnitude higher. This is a clear advantage of the signal processing technique earlier described.

4.7 Takeoff Rejection Simulation using a Theoretical Model

Using the theoretical model developed in the section 4.2, a simulation routine was

developed. The purpose of this simulation was to demonstrate a simple interface that could provide information to a pilot regarding the margin of safety associated with a takeoff rejection at or near V_1 . The margin of safety is defined as the amount of runway that would remain in front of the aircraft once decelerated to rest.

The simulation routine allowed the author to examine the ability to project displacement with known parameters, and to evaluate whether the Kalman Filter introduced in the section 4.2 could, in fact, converge to the parameters in the presence of sensor and process noise. Flexibility in the simulation algorithm also allowed the author to examine the robustness of the Kalman Filter to higher order disturbances not considered in the theoretical model, such as variations in runway slope or wind velocity. The Kalman Filter was also shown to be able to converge to the parameters and thus became a candidate signal processing technique for experimental data.

Figure 4.3 shows the result of the simulation routine prior to initiation of the simulated rejection. The routine estimated a margin of safety of 380 metres. If the rejection occurred prior to reaching V_1 , a margin of safety of more than 380 metres would have existed. If the rejection occurred at or near V_1 , some of the margin of safety would have been consumed in the time required for the pilot to react.

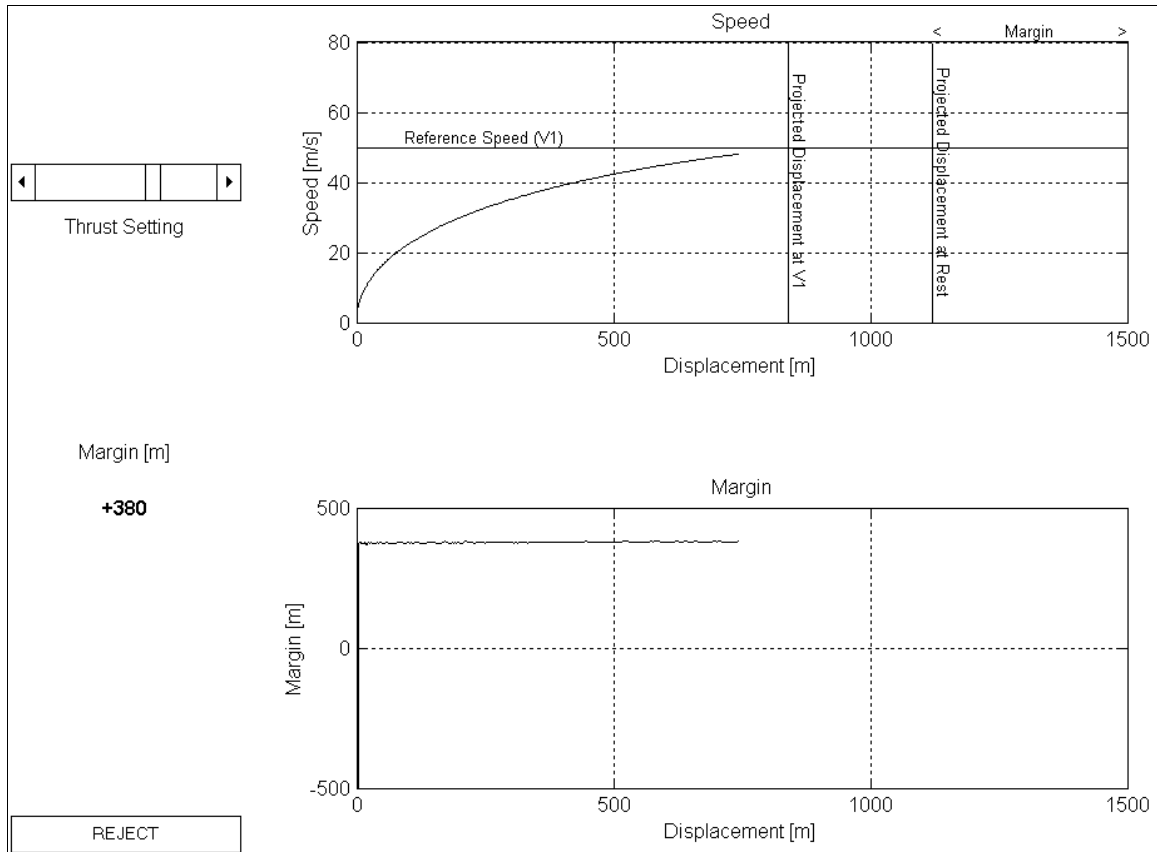


Figure 4.3 Simulation Results: Projected Displacement and Margin of Safety

Figure 4.4 depicts a simulated takeoff rejection initiated just prior to reaching V_1 . A fraction of a second later the pilot reduced thrust to idle, but some of the margin of safety had already been consumed. A couple of seconds later, reverse thrust was applied. By this time, the margin of safety had decreased to 115 metres. In the simulation routine, the availability of braking is not considered in the projection of displacement. Simulated braking is available, in the event that the pilot requires additional deceleration to improve the margin of safety after the takeoff has been rejected.

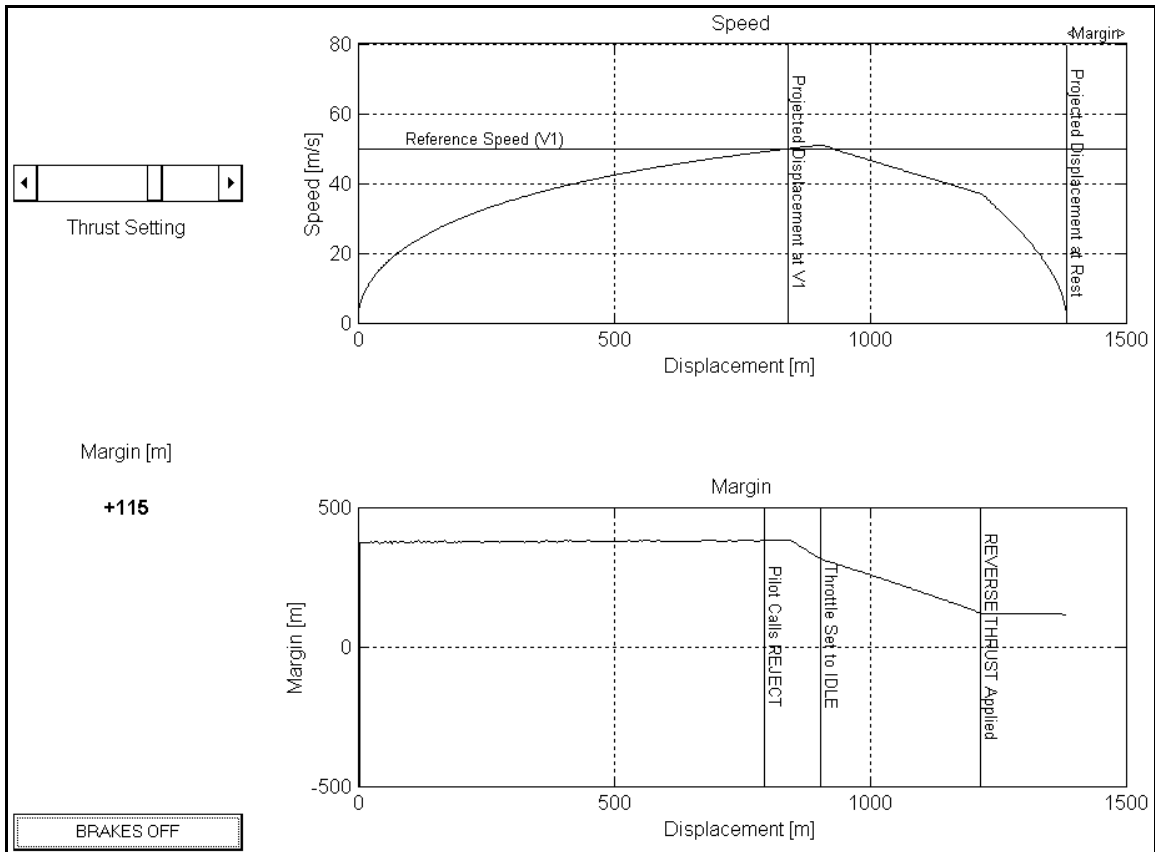


Figure 4.4 Margin of Safety during the Response to a Simulated Takeoff Rejection

The simulation is available in Appendix 1.04 (CD-ROM) under the “simulation” directory.

Note that, to completely reject a simulated takeoff, it is necessary to first call “reject” by clicking the button marked “REJECT”, then set the throttle to idle by clicking the button marked “IDLE”, then reverse thrust by clicking the button marked “REVERSE”.

Optionally, the “BRAKES OFF / BRAKES” button may be toggled to increase the margin of safety. These steps have been included to simulate the required reaction mechanism.

***Chapter 5 - Sensor Selection**

5.1 Background

At a minimum, the sensors in a takeoff performance monitor must be able to measure acceleration, speed, and position relative to a known location. This information could be used, with reference to a theoretical model, to predict how the aircraft will behave in the future.

In aircraft landing and takeoff performance monitoring, the desired acceleration observation should reflect the overall vehicular acceleration as opposed to vibration of sub-components. Accelerometers have been typically used to measure acceleration. However, because accelerometers measure gravity in addition to acceleration, some method of determining the orientation of the accelerometer with respect to the gravity vector has been required. Typically, this required the use of a gyroscope, which measured the rate of change of orientation. With time, the accuracy of a gyroscope-derived determination of orientation becomes inaccurate because small errors in the raw measurement are integrated over time to determine orientation.

The measurement from an airspeed indicator together with a recently acquired measurement of the component of wind speed in the direction of motion has been used to

*A significant portion of this chapter was previously published.²⁵

determine aircraft speed, with shortcomings in accuracy due mostly to the time varying nature of wind and the associated delay in obtaining updated measurements. Alternatively, a time-integrated observation of acceleration could be used. This leads to an accumulation of error over time, requiring re-initialization.

With the recent widespread availability of highly accurate position observations from the Global Positioning System, a GPS receiver was identified as a sensor that would provide information regarding the position of the aircraft relative to the end of the runway. A GPS receiver can also be used to measure speed relative to the ground. Of course, during a takeoff roll, speed changes. If a GPS receiver can also be used to measure acceleration with accuracy comparable to accelerometers, there is the possibility that one sensor can be used as the sole source of kinematic information for a takeoff performance monitor.

It may be necessary to include instrumentation capable of measuring the forces present in the landing gear. Such forces could reveal the magnitude of the instantaneous rolling friction, the weight of the aircraft, and the instantaneous normal force. It was decided that the need for such additional sensors would be governed by experimental results. Whether such instrumentation would be necessary would depend on the sensitivity of the system to changes in these parameters.

5.2 Acceleration From GPS

The notion of acquiring an observation of acceleration from GPS is not new. When compared to the observation obtained from an accelerometer, a GPS-derived observation

of acceleration can be used to determine the gravity vector. This technique has been used in airborne gravimetry to determine the gravitational constant with accuracies²⁶ on the order of 10^{-5} metres per second squared, but requires a substantial amount of data to filter out vibrational disturbances. More recently, it has been proposed that a GPS-derived observation of acceleration together with an accelerometer could yield a representation of the gravity vector²⁷ to be used as an attitude reference. Such an application would require a real time GPS-derived observation of acceleration if used on vehicles with rapidly changing attitude.

Although accelerometers have been historically used to determine aircraft acceleration, additional instrumentation is required to accurately measure aircraft attitude to remove the significant and adverse influence of the gravity vector. Accelerometers do not respond only to acceleration, but rather the force per unit mass on an element of known mass. The accelerometer measurement is therefore a combination of the components of gravity and acceleration in the direction of the sensing axis of the accelerometer. With reference to Figure 5.2, the accelerometer measurement,

$$a^* = a_x + g_x, \quad (5.1)$$

where: a_x is the component of acceleration in the accelerometer's direction of sensitivity,

and;

g_x is the component of gravity in the sense-direction of the accelerometer.

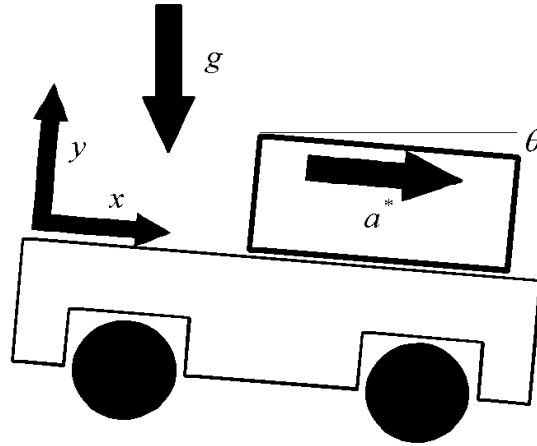


Figure 5.1 Unknown Sensor Inclination Results in “Accelerometer Gravity Error”

“Accelerometer Gravity Error” results from an accelerometer measuring a component of the gravity vector that cannot be determined without an accurate observation of the sensor inclination with respect to horizontal. Observation of inclination always requires additional instrumentation. Depending on the sensor used to measure inclination, the accuracy of the observation usually degrades over time.

The component of gravity in the direction of sensitivity,

$$g_x = g \sin \theta, \quad (5.2)$$

where: θ is the angle between the direction of sensitivity and horizontal.

Thus, for small angles, the gravity vector introduces an error of 0.171 metres per second squared per degree of inclination. This problem is avoided through the use of a GPS-derived observation. The selection of a GPS receiver as the primary source of kinematic information is an especially appropriate choice given the need to determine the location of the aircraft with respect to the end of the runway, an application to which a GPS receiver

is well suited.

5.3 Required Accuracy

The level of uncertainty in a GPS-derived observation of acceleration depends on the type of filter used to remove noise that is amplified by differentiation. In any case, the amount of error will not depend on the magnitude of the instantaneous signal. Rather, the standard deviation of noise depends primarily on the number of satellites in view.

Assuming constant deceleration, the instantaneous stopping distance of a vehicle,

$$s = \frac{v^2}{2a}, \quad (5.3)$$

where: v is the instantaneous speed of the vehicle, and;

a is the magnitude of acceleration of the vehicle.

The sensitivity of the stopping distance,

$$\Delta s = \Delta v \frac{\partial s}{\partial v} + \Delta a \frac{\partial s}{\partial a}, \quad (5.4)$$

where: Δv is the error in the observation of speed, and;

Δa is the error in the observation of acceleration.

Substituting expressions for partial derivatives,

$$\Delta s = \Delta v \frac{v}{a} - \Delta a \frac{v^2}{2a^2}. \quad (5.5)$$

Rearranging (5.3) to solve for deceleration, substituting into (5.5), and solving for deceleration uncertainty gives:

$$\Delta a = \Delta v \frac{v}{s} - \Delta s \frac{v^2}{2s^2}. \quad (5.6)$$

Instances where deceleration uncertainty has the most impact occur when the forward speed is high and when the rearward acceleration is low. To establish an acceptable level of uncertainty in the observation of deceleration, consider a modest V_1 on a long runway. Runways are seldom longer than 4000 metres. Over half of the length of the runway would be required to reach V_1 , so assume $s = 2000$ metres and $v = V_1 = 90$ metres per second.

The margin of safety in the stopping distance would need to be larger than the length of the aircraft, so the error in the estimation of stopping distance can be conservatively chosen as $\Delta s = 150$ metres. From GPS, a typical speed error determined using constant speed trials, as described in section 5.4, was $\Delta v = 1.12$ metres per second. Note that at the time of this preliminary experimental investigation, the intentional degradation described in section 2.2 was present in the GPS signal structure resulting in position errors of approximately one hundred metres.

Substituting these values into equation (5.6) yields a conservative maximum acceptable

uncertainty in the observation of deceleration:

$$\Delta a = 0.101 \text{ m/s}^2 \quad (5.7)$$

While a lower speed may apply to many aircraft, the runway length should be considered very conservative. In many cases, higher uncertainty may be acceptable. This analysis was intended only to provide a nominal uncertainty to which results could be compared.

5.4 Experimental Investigation

An experimental investigation was conducted to determine the accuracy with which a GPS receiver could measure acceleration. The GPS-derived observations collected during this investigation were compared to observations derived from carefully mounted accelerometers. A 400-metre segment of railway track together with a rail-mounted gasoline-powered vehicle having no suspension system was used in this investigation. Because the vehicle had no suspension system, the orientation of the vehicle was a function of the slope of the track at any given location. Accelerometers were used during constant-speed trials to determine the slope of the track. During trials where the vehicle speed varied, the accelerometer data were corrected for the influence of minor pitch changes by subtracting the known slope at the instantaneous position. These corrected accelerometer data were then used as truth data to which GPS-derived observations of acceleration could be compared.

A GPS receiver (NovAtel 3151RE) capable of collecting satellite range observations at a rate of twenty samples per second was selected for use in the test apparatus. Appendix

1.05 (CD-ROM) contains operating instructions for the GPS receiver* under the “novatel” directory. The receiver logged position and velocity at ten samples per second. The velocity observation from the GPS receiver in the test apparatus was derived from time differentiation of position or carrier phase Doppler observations owing to the manufacturer's proprietary algorithm. The acceleration observation was a filtered time differentiation of this velocity observation, obtained using a Kalman Filter. In this Kalman Filter, the third derivative of position was considered to be a random process. This is of course untrue, but was a reasonable approximation of the dynamics.

In state-space form, the system dynamics,

$$\begin{bmatrix} s \\ v \\ a \\ j \end{bmatrix}_{k+1} = \begin{bmatrix} 1 & \Delta t & 0 & 0 \\ 0 & 1 & \Delta t & 0 \\ 0 & 0 & 1 & \Delta t \\ 0 & 0 & 0 & 0 \end{bmatrix} \begin{bmatrix} s \\ v \\ a \\ j \end{bmatrix}_k + \begin{bmatrix} 0 \\ 0 \\ 0 \\ q_k \end{bmatrix}, \quad (5.8)$$

and the measurements,

$$y_k = [0 \quad 1 \quad 0 \quad 0] \begin{bmatrix} s \\ v \\ a \\ j \end{bmatrix}_k + v_k, \quad (5.9)$$

where: s , v , a , and j are position, speed, acceleration, and jerk, respectively, form the foundation of the Kalman Filter. This filter requires identification of the variance of the two random variables. The measurement noise is easily approximated during

*Copyright NovAtel Incorporated

constant speed trials as later discussed. This leaves one variance, that of the process noise, to be chosen.

Testing was undertaken to verify the accuracy of the acceleration observation derived from GPS data. The apparatus consisted of a rail-mounted GPS receiver, a bank of accelerometers (Analog Devices ADXL 202) mounted with parallel axes of measurement, and a data acquisition system. Appendix 1.06 (CD-ROM) contains specifications for the accelerometers under the “accelerometer” directory. Four identical accelerometers were used to provide a confident measure of the acceleration.

The data acquisition system collected these data at a rate of twenty samples per second, electrically synchronized with the GPS receiver’s collection of raw satellite signals. The data acquisition system for the accelerometers, which used an analog-to-digital data acquisition computer card, was separate from the data collection system for the GPS receiver, which used serial communications. The GPS receiver was equipped with strobe pins for both input and output triggering. One of these strobes fired on receipt of raw satellite data. This strobe was used to trigger the collection of data from the accelerometers. Another strobe connection allowed the GPS receiver to log the time at which it received an input voltage step. This strobe was used to record the times at which accelerometer data collection began and ended. In this way, the data from both the accelerometers and from the GPS receiver could be synchronized in time.

During constant-speed trials, the accelerometers were used to determine the slope of the

rail surface so that the influence of the gravity vector could be calculated. This slope information was cross matched with geographic location through the use of differential GPS. Twenty constant-speed trials were conducted, yielding a reliable observation of slope. This method of accounting for rail slope implicitly accounted for any bias errors present in the accelerometers. During trials where the vehicle speed was varied, the accelerometer data were corrected for the influence of minor pitch changes by subtracting the known slope at the instantaneous position. Both observations of acceleration were filtered using the same algorithm. The GPS-derived acceleration observation was then compared with acceleration data from the bank of accelerometers, after accounting for the effect of gravity. This is shown schematically in Figure 5.2.

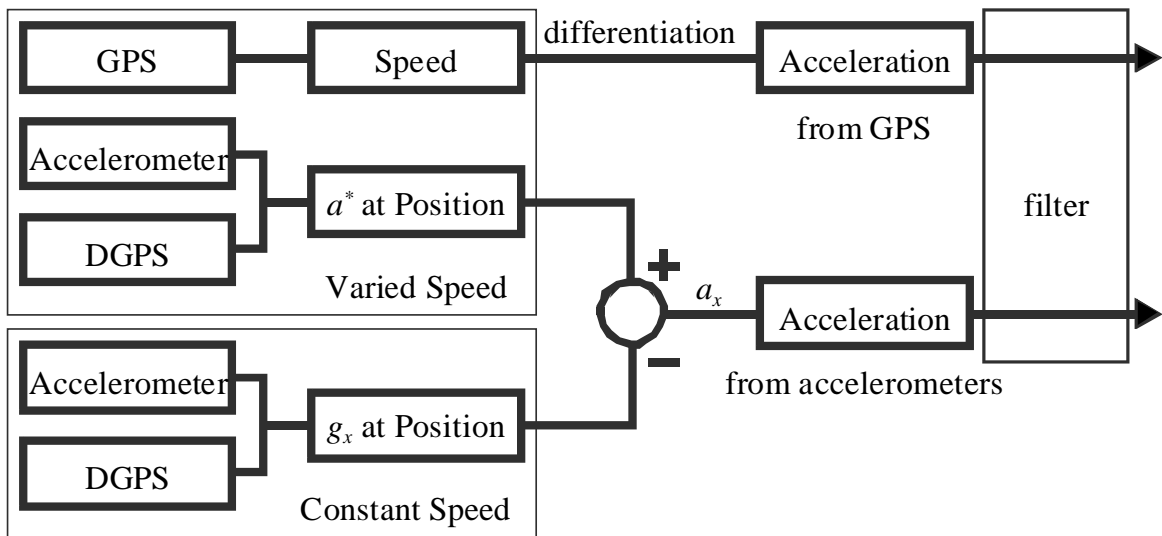


Figure 5.2 Accelerometer and GPS-derived Acceleration Observation Processing

5.5 Results and Discussion

Figure 5.3 shows the speed of the vehicle obtained from a GPS receiver, in the presence of selective availability, and acceleration computed using the Kalman Filter. This observation of acceleration can be compared to an observation obtained from a bank of

accelerometers.

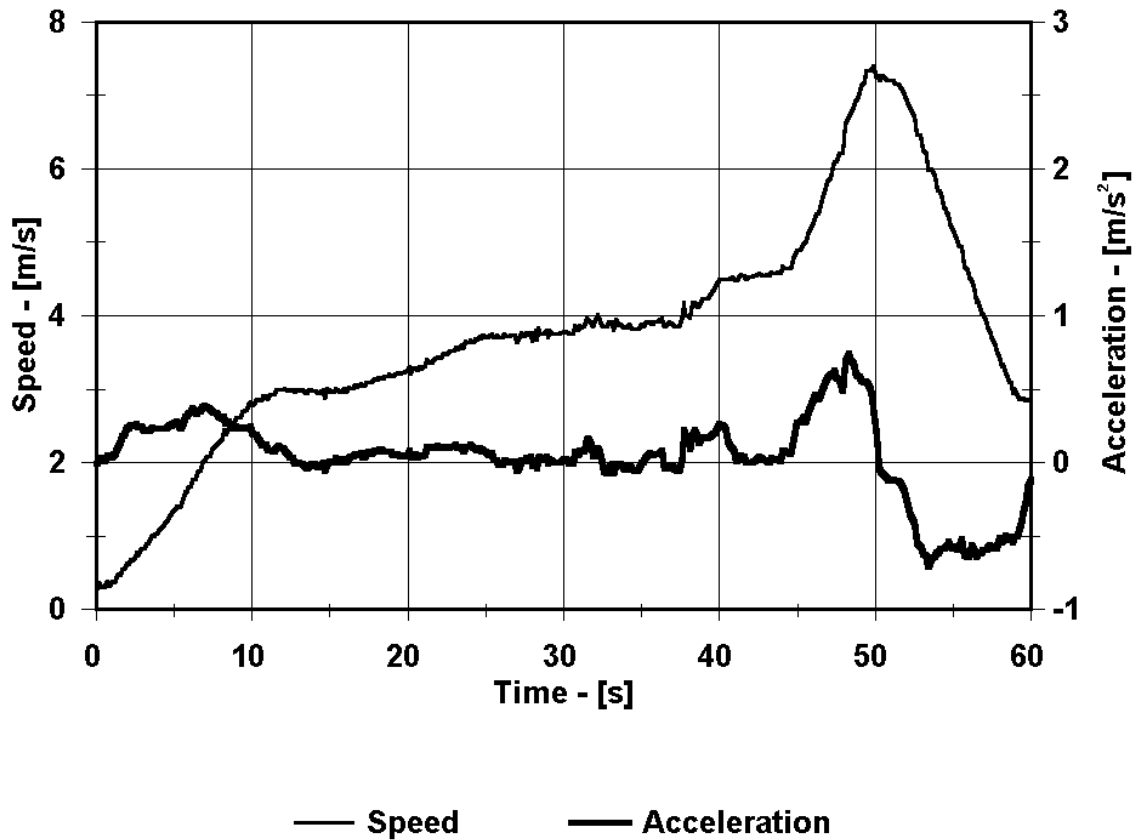


Figure 5.3 Speed and Acceleration of the Test Vehicle vs Time

Speed and acceleration of a test vehicle were derived from GPS data in the presence of selective availability. The observation of acceleration required filtering to remove noise due to differentiation.

The use of redundant accelerometers provided increased confidence in the observation of acceleration. Measurements from each of the four accelerometers used in the experimental apparatus agreed with one another very well. The covariance matrix

describes how the data collected from each sensor varied from one another. In completely uncorrelated data, off diagonal values would be zero. In completely correlated data, all values would be equal. For the collected accelerometer data, a covariance matrix,

$$\text{cov} = \begin{bmatrix} 1.779 & 1.776 & 1.775 & 1.772 \\ 1.776 & 1.779 & 1.775 & 1.776 \\ 1.775 & 1.775 & 1.779 & 1.773 \\ 1.772 & 1.776 & 1.773 & 1.779 \end{bmatrix} \text{m}^2/\text{s}^4, \quad (5.10)$$

was determined.

It can be concluded that the accelerometer data, while being variable with a standard deviation on the order of 1.33 metres per second squared, were highly correlated. This demonstrated that the accelerometer data represented a confident measure of the acceleration of the vehicle component to which the accelerometers were attached.

Figure 5.4 shows a comparison of the GPS-derived acceleration with that from the accelerometers for one of ten trials where the speed of the vehicle was varied. Other trials yielded similar results. While both observations of acceleration were filtered in exactly the same manner, there is clearly no superiority in the accelerometer observation over the GPS-derived observation of acceleration. It had been expected that given the care with which the accelerometer data were corrected, an approach that would not be feasible in practice, the GPS-derived acceleration would be notably time-delayed and would contain noise. Conversely, it would appear that in those instances where the vehicle acceleration changed quickly, such at the period between twenty seconds and twenty-five seconds, the

two observations were in agreement.

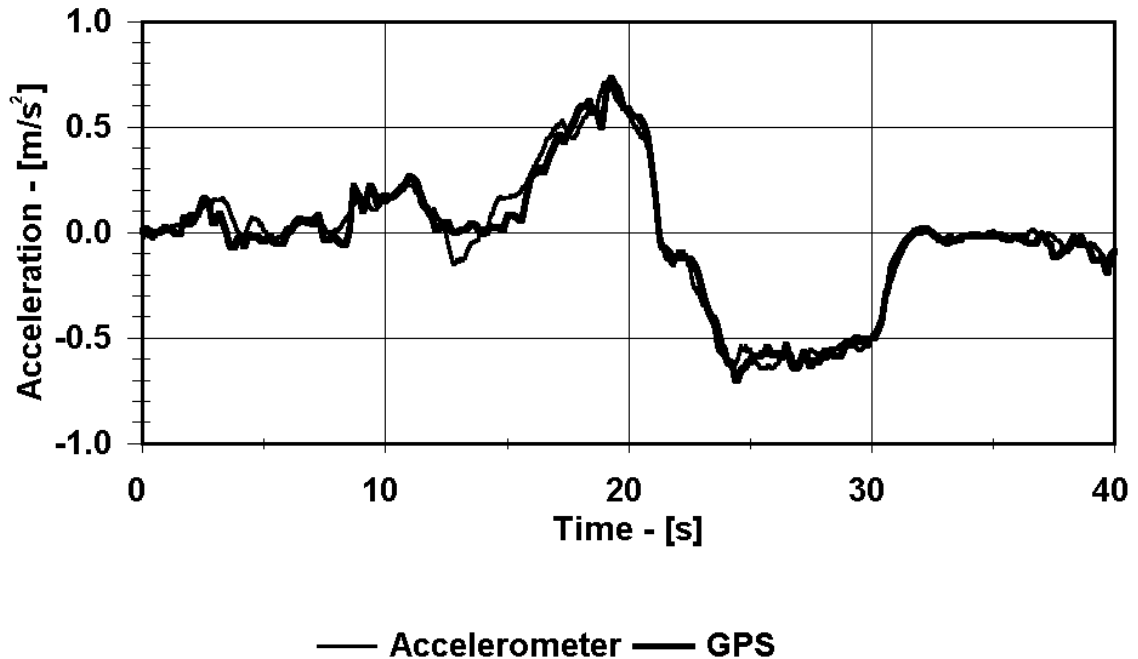


Figure 5.4 GPS-derived Acceleration Data Agree with Accelerometer Data

Observations of the acceleration of the test vehicle derived from GPS data were compared with accelerometer-derived observations. While the GPS-derived observation required filtering to remove noise due to differentiation, the accelerometer-derived observation required filtering to remove measurements of vibration.

Figure 5.5 shows the calculated difference, for the same trial, between the two observations of acceleration. This does not represent the error in the GPS-derived observation, as the accelerometer observation also lags the “real” acceleration because of filtering. The standard deviation of the difference was 0.054 metres per second squared.

This falls well within the established conservative maximum uncertainty of 0.101 metres per second squared. Closer analysis showed that the calculated difference falls within the maximum uncertainty over ninety percent of the time.

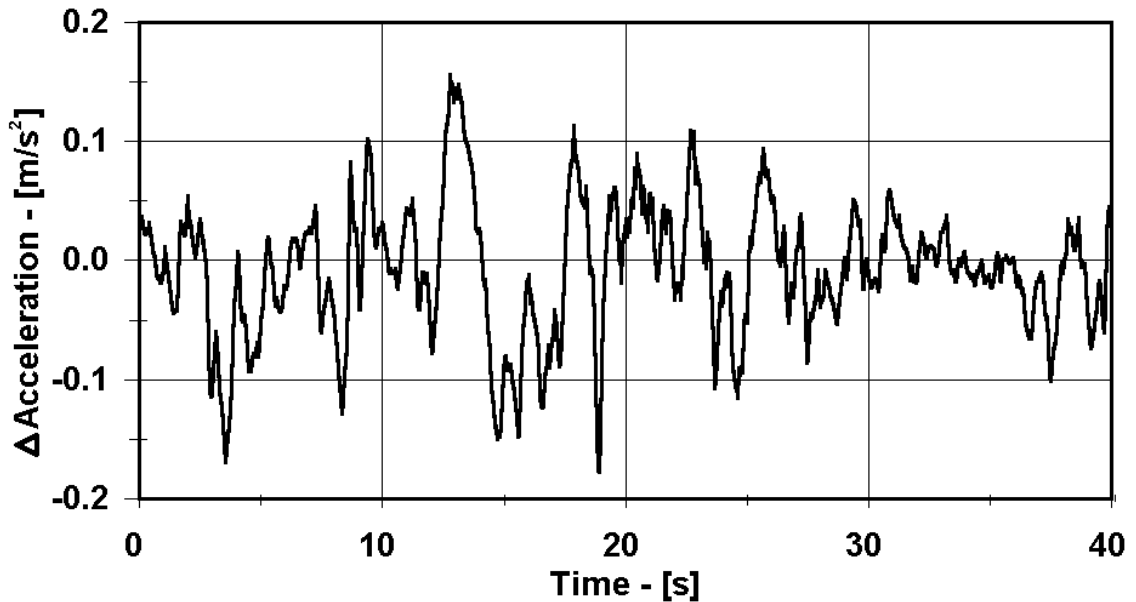


Figure 5.5 Difference between GPS-derived Acceleration and Accelerometer Data

With regard to the dynamic range of this investigation, it should be noted that the acceleration and speed associated with aircraft takeoff and landing are typically larger than those investigated. In the investigation, speeds in excess of ten metres per second were not experienced and acceleration was typically 0.5 metres per second squared. This difference in dynamic range should have little effect on the accuracy or resolution of the GPS-derived speed observation, which is governed by jerk. Because the corresponding accuracy of the acceleration observation was dependent on the ratio of speed accuracy to

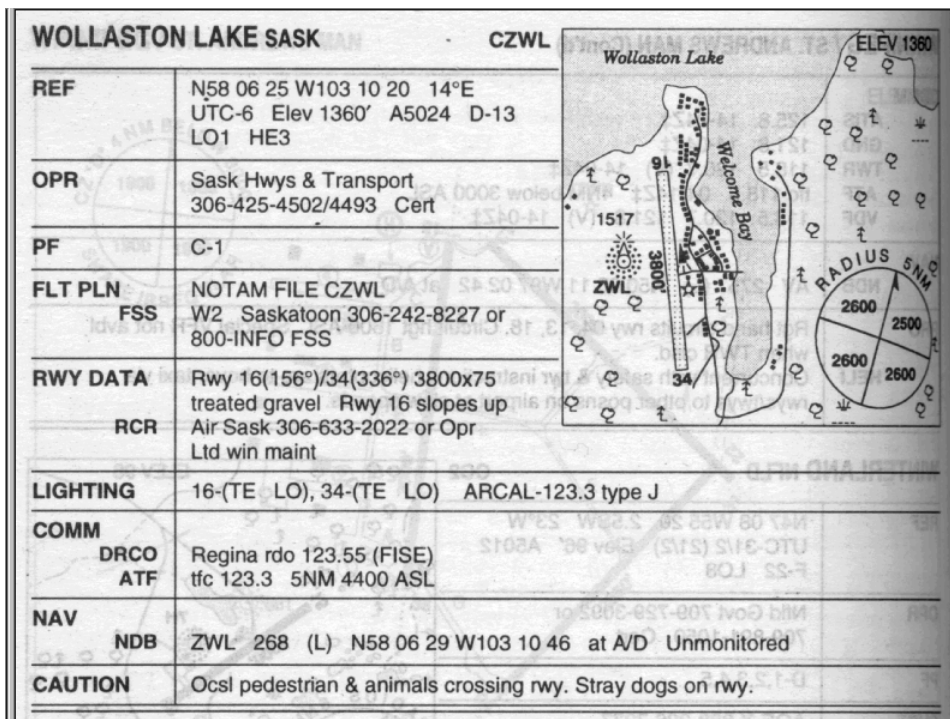
the change in speed, this accuracy should improve at higher accelerations.

It has been demonstrated that the Global Positioning System is able to provide an observation of vehicle speed that is sufficiently reliable to determine acceleration with an uncertainty of under 0.10 metres per second squared. This accuracy should be achievable for acceleration in excess of 0.5 metres per second squared. Accelerometers are well suited to measurement of vibration, where the influence of gravity need not be removed from the measurement, but a GPS-based observation is clearly superior in stable, slowly changing vehicular acceleration. Clear advantages in using a GPS receiver over the more conventional sensor, an accelerometer, include insusceptibilities to the gravity vector, vibrational disturbances, and temperature fluctuations.

Chapter 6 - Model Validation through Experimental Investigation

6.1 Introduction

For the experimental investigation in this phase of the project, the data collected represented normal operating conditions aboard an aircraft. Tranwest Airlines cooperated in the research project. The airline operated four twin turboprop Jetstream 31 aircraft. The airports visited by these aircraft on a daily basis included locations as far north as Uranium City, Saskatchewan, located at north latitude of 59.56 degrees, and as secluded and underserved as Wollaston Lake, Saskatchewan, shown in Figure 6.1.



© 2002 Her Majesty the Queen in Right of Canada with permission of Natural Resources Canada.

Figure 6.1 Wollaston Lake Airport: an Unmonitored and Uncontrolled Airport

The model developed in section 4.2 applies theoretically to any turboprop aircraft operated in the absence of braking during takeoff or landing on a constant slope runway with fixed control settings. The runway surface type would affect whether the pilot would elect to use wheel braking during a normal landing or during the rejection of a takeoff. The Jetstream 31, also known as the British Aerospace 3112, is a nineteen-passenger pressurized turboprop aircraft. One of the four aircraft operated by the airline was already equipped with a navigational GPS receiver where the antenna was mounted above the cockpit on the exterior of the aircraft. Appendix 1.07 (CD-ROM) contains photographs of this aircraft under the “c-fsew” directory. Because the principle of operation of a GPS receiver requires a straight line view of GPS satellites, such an externally mounted antenna was very useful in collecting data for this experiment, if not an absolute necessity.

6.2 Materials and Methods

A fundamental principle in dealing with a commercial airline was established very early in the project. It was absolutely crucial that the design of the experimental system require minimal modification to existing aircraft systems. Adherence to this principle would not only minimize the time required to install the necessary components, but would also simplify the process of obtaining permission from Transport Canada.

A more detailed examination of the selected aircraft revealed the existence of a docking station for a processor in a traffic collision avoidance system (TCAS), that had been removed due to serviceability problems. Appendix 1.08 (CD-ROM) contains excerpts from the TCAS installation manual under the “tcas manual” directory. While needed in

more populated areas, the use of such a device in Canada in the 1990s was not a regulatory requirement. Upon further examination,²⁸ it was determined that the TCAS docking station was equipped with a dedicated circuit breaker as well as connections to antennas both on the belly of the aircraft and over the cockpit a short distance behind the antenna for the GPS receiver. The radio frequency used by the TCAS was in the same band as that used by the GPS receiver, and the characteristic attenuation of the coaxial cable between the TCAS docking station and the overhead antenna was similar to GPS receiver requirements. It was decided that a commercially available GPS antenna signal splitter would be used to share the signal from the existing GPS antenna with the navigational GPS receiver and the project test equipment. Appendix II, the type certificate application, describes this in further detail.

With the physical and electrical constraints for the test equipment dictated by the existing hardware in the aircraft, a data collection system was designed and constructed. The only modifications required in the aircraft were the insertion of a GPS antenna signal splitter and the reconnection of a TCAS antenna cable.

The design and implementation of test equipment for this phase of the project required considerable care. With the knowledge that the most invasive aspect of the project would be the sharing of a navigational GPS antenna, testing was undertaken to verify that no adverse effects would be experienced. The process of obtaining Transport Canada certification for the installation required adherence to airworthiness regulations and conformity testing.

6.2.1 Certification

The certification process involved showing compliance with airworthiness regulations through testing or evaluation. Transport Canada provided a list of regulations to which adherence would have to be demonstrated. As well, an explanation of the purpose of the modification, together with an outline of mechanical and electrical considerations, was required.

The basis of certification for the test aircraft was the United States Federal Aviation Administration's Federal Airworthiness Regulation Part 23, which applies to commuter aircraft that are "propeller-driven, multiengine airplanes that have a seating configuration, excluding pilot seats, of 19 or less, and a maximum certificated takeoff weight of 19,000 pounds or less."²⁹

The purpose of the modification was to collect position and velocity data during takeoff of a Jetstream 31. These data were to be used to investigate the feasibility of a landing and takeoff performance monitoring system for passenger aircraft that frequently travel to airports with gravel runways in the Far North. The required equipment consisted of a unit containing a portable computer and a GPS receiver (NovAtel OEM2), and an antenna splitter used to acquire the signal from an existing GPS antenna.

Under this effort, the Global Positioning Data Recorder (GPDR) system was designed to be minimally invasive and to take advantage of existing equipment wherever possible. Transwest Airlines (formerly Air Sask Aviation) agreed to carry the equipment onboard

the aircraft registered C-FSEW, a Jetstream 31 equipped with a GPS receiver (Bendix / King KLN 0089B). Appendix 1.09 (CD-ROM) contains excerpts from the installation manual for this GPS receiver under the “nav gps” directory. A GPS antenna splitter was employed to acquire the signal from the existing GPS antenna.

The existing configuration of the aircraft included the hardware for a TCAS (Bendix / King CAS 66) installation. The TCAS processor had been removed due to serviceability problems as it was not a required instrument. It was decided that the tray for the TCAS processor would be used as the station for the data recorder. The TCAS infrastructure was used to supply power to the unit. There was coaxial cable running from the TCAS tray to an unused antenna mounted at station 130,³⁰ just aft of the cockpit bulkhead as shown in Figure 6.2. The existing GPS antenna was within a few centimetres of this location.

6.2.2 Mechanical Considerations

An aluminum enclosure was constructed that contained the portable computer and the GPS receiver. The unit weighed 5.0 kilograms. It was secured in place using hold down pins on the existing TCAS processor tray, located just aft of the rear right side passenger seats, as shown in Figure 6.3.

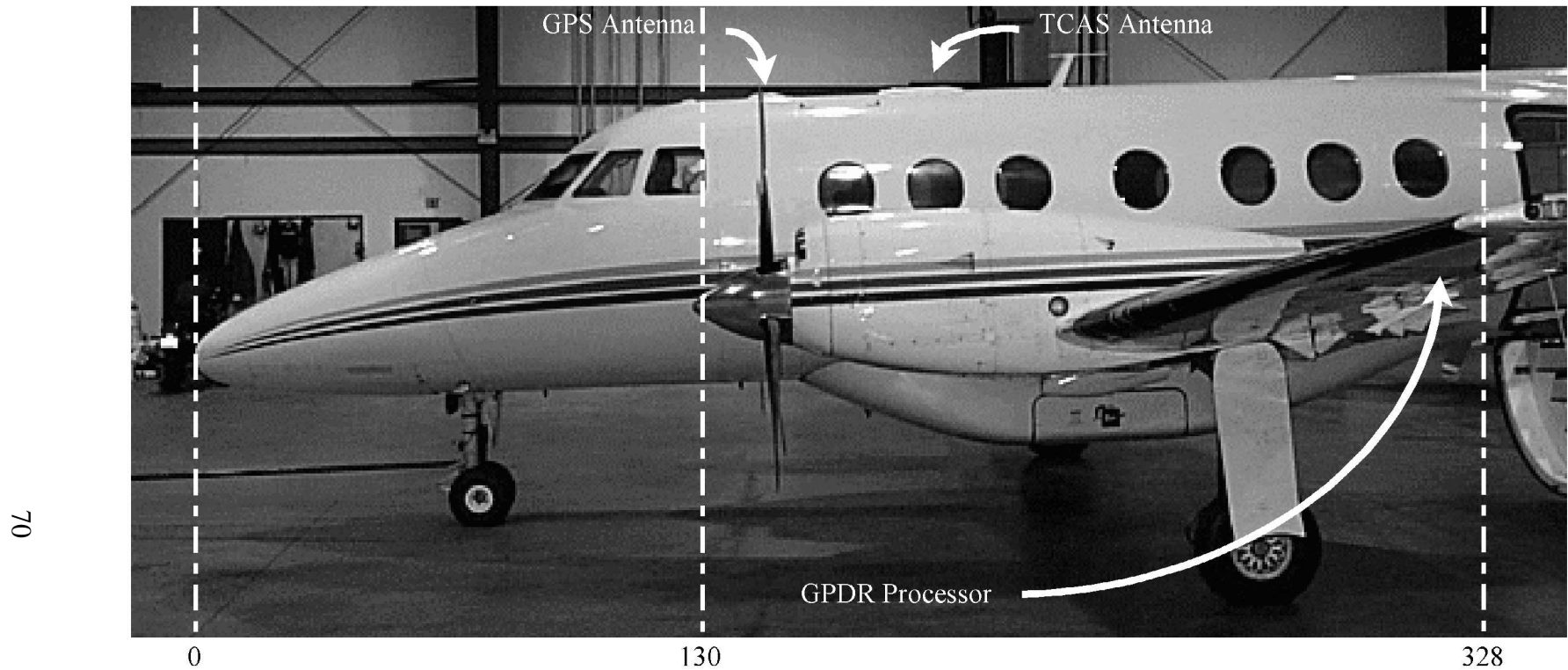


Figure 6.2 Left Side View of Aircraft

The positions of the navigational GPS antenna and the TCAS antenna are shown. The GPDR processor was installed inside the aircraft behind the rear passenger seats as indicated. Numbers along the bottom of the photograph indicate distances, in inches, from the nose of the aircraft. These distances are also known as “stations” for purposes of weight and balance.

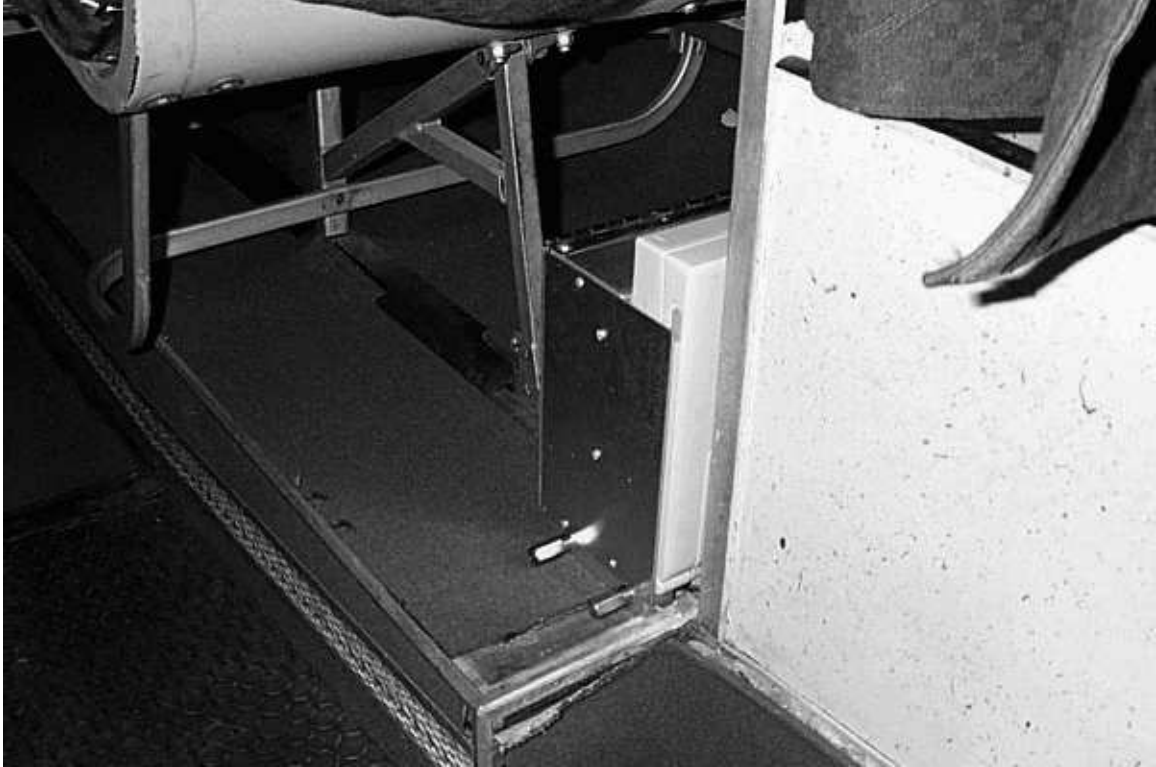


Figure 6.3 GPDR Installed in the Tray belonging to the Removed TCAS Processor

The GPS antenna splitter, shown in Figure 6.4, weighed 0.15 kilograms and was attached to the GPS antenna using a TNC male-to-male elbow adaptor. The coaxial cable supplying the navigational GPS receiver was connected to the primary branch of the splitter using the existing TNC connector. One of four coaxial cables that ran between the TCAS tray and the TCAS directional antenna was connected to the secondary branch of the splitter using the existing TNC connector.

6.2.3 Electrical Considerations

There was a dedicated five-Ampere circuit breaker for the TCAS tray at the auxiliary avionics circuit breaker panel. This circuit drew power from the 28 VDC main avionics bus. The recorder unit drew 1.8 Amperes at 28 VDC and was internally protected with a

three-Ampere normal blow fuse. This level of power consumption was identical to that of the removed TCAS processor.

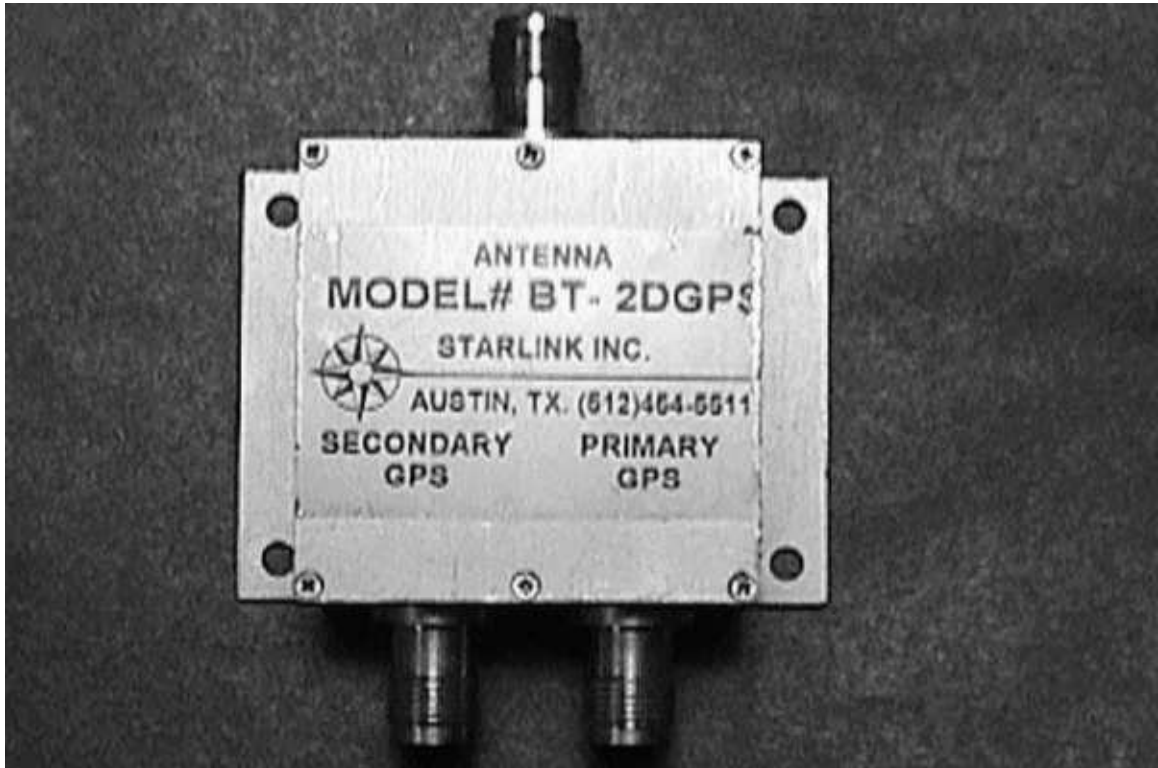


Figure 6.4 Antenna Splitter used to Share the Signal of the Existing GPS Antenna

Power was supplied to the GPS antenna internal amplifier circuitry by the existing GPS receiver through the primary branch of the antenna splitter which allowed DC current to pass. The second receiver acquired the antenna signal from the secondary branch. The splitter provided isolation in excess of twenty decibels between the primary and secondary branches. Testing that was completed to prove non-interference of the antenna splitter is found in Appendix III.

6.2.4 Installation

The navigational GPS antenna was located just forward of the cockpit bulkhead, directly overhead. The overhead cockpit circuit breaker panel was removed to gain access to the antenna. There was one coaxial cable attached to the GPS antenna with a TNC-male connector. This cable led to the navigational GPS receiver. The receiver coaxial cable was detached. The TNC-male adaptor of the antenna splitter assembly was attached to the GPS antenna. Test C2 was then successfully performed. Test C2 required that, when installed, the combined structure of the antenna splitter, TNC male-to-male elbow adaptor, and GPS antenna be shown to withstand a force applied vertically down at the centre of the antenna splitter of no less than 7.0 Newtons without permanent deformation of the structure at any location. The purpose of this test was to show that the new hardware would be able to withstand the maximum certified acceleration that the aircraft might experience. A small test mass was used for this purpose.

The receiver coaxial cable was then attached to the “Primary GPS” connector on the antenna splitter. The TCAS directional antenna was located just aft of the cockpit bulkhead, directly overhead. The overhead cabin panelling was removed to gain access to the antenna. There were four coaxial cables attached to the TCAS directional antenna with TNC-male connectors. The forward connector was colour-coded yellow. The yellow coaxial cable was detached, drawn forward, then attached to the “Secondary GPS” connector on the antenna splitter. The overhead cabin panelling and the circuit breaker panel were then replaced.

The GPDR processor was installed in the TCAS processor tray just aft of the right side passenger seats. The TCAS processor hold-downs were used to secure the GPDR processor in place. Test C1 was then successfully performed. Test C1 required that, when installed, the GPDR processor be shown to withstand a force applied vertically down of no less than 230 Newtons without permanent deformation of the processor structure or separation from the tray. The purpose of this test was to show that the new hardware would be able to withstand the maximum certified acceleration that the aircraft might experience.

6.2.5 System Summary

The prototype monitor was certified³¹ for use as a Global Positioning Data Recorder (GPDR) and was installed in a nineteen-passenger British Aerospace 3112 operated by an airline servicing far-northern Canadian airports. The full text of the Supplemental Type Certificate Application including instructions for the installation and testing of the GPDR is available in Appendix II. Appendix 1.10 (CD-ROM) contains the basis of certification under the “type certificates” directory. Appendix 1.11 (CD-ROM) contains the full text of the type certificate application together with all appendices under the “gpdr lstc” directory. The particular aircraft was equipped with a navigational GPS receiver (Bendix King KLN 89B) with a permanent active patch antenna (Bendix King KA 92) installed over the cockpit with a clear view of the sky. A signal splitter (Starlink BT-2DGPS) was installed that allowed the GPS antenna signal to be shared by the navigational GPS receiver and the GPDR. Figure 6.5 depicts the electrical configuration of the complete system. Figure 6.6 shows the internal configuration of the GPDR. The receiver contained

in the GPDR logged position and velocity at a rate of ten samples per second to a portable computer that stored the data to a disk drive. Appendix 1.12 (CD-ROM) contains information regarding the portable computer under the “laptop manual” directory. The velocity observation from the GPS receiver in the test apparatus was derived from time differentiation of position or carrier phase Doppler observations owing to the manufacturer's proprietary algorithm.

6.2.6 Data Collection Software

Custom serial data collection software was programmed to extract the necessary information from the GPS receiver in the GPDR. When an aircraft is taxied before takeoff or after landing, speeds can be similar to the first few seconds of a takeoff. The amount of time spent taxiing, however, is nearly one hundred times more than the amount of time spent accelerating for takeoff. To avoid excess data collection, a technique for recording only data pertaining to takeoff and landing was required.

It was necessary to develop logic that would decide, based on speed and acceleration, whether a takeoff or landing was occurring. Only takeoff and landing information was recorded. The software functioned in a completely autonomous mode, capable of collecting several months of data at a time without human intervention. Appendix 1.13 (CD-ROM) contains source code and executables for all software used to collect and process data under the “software” directory.

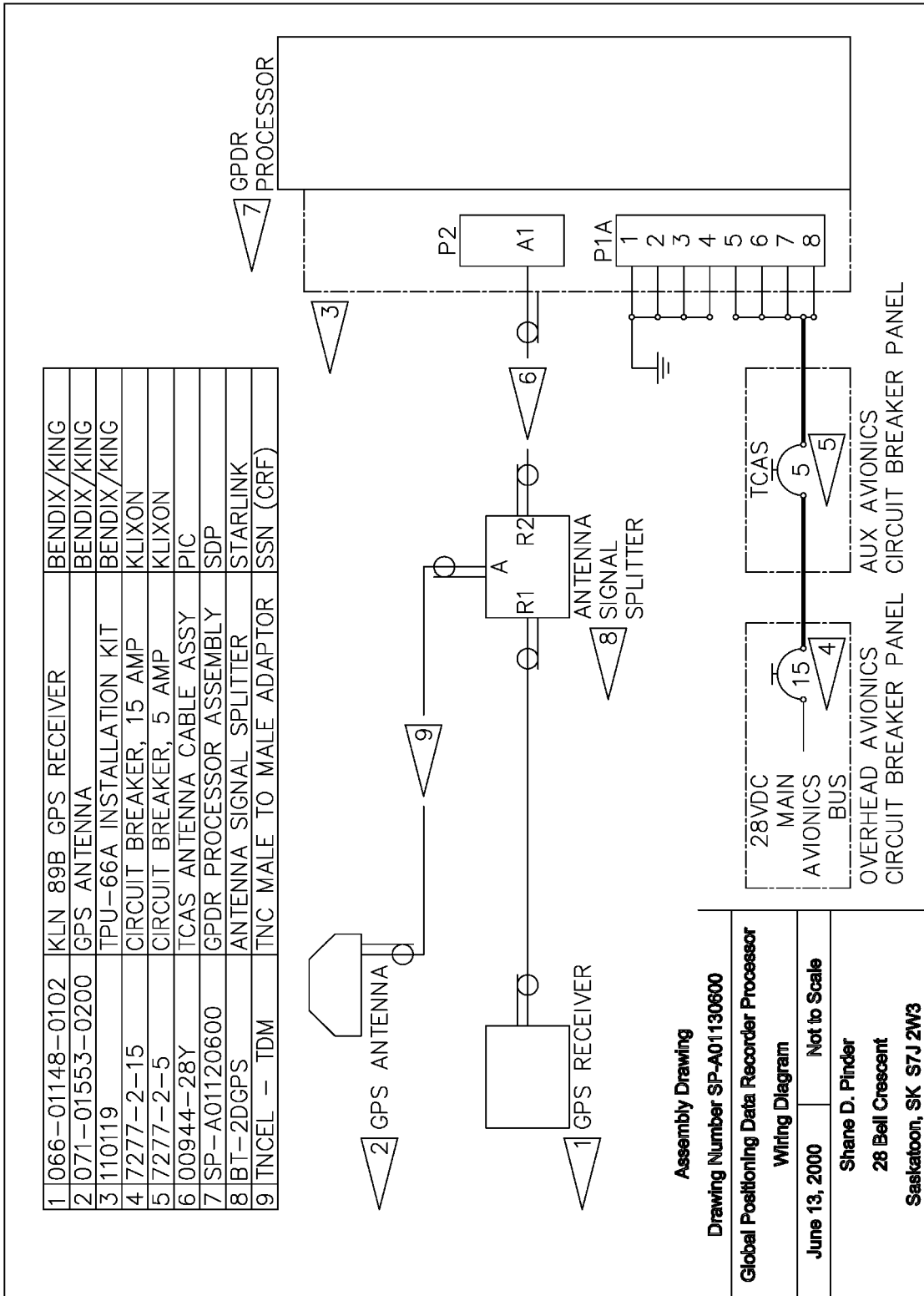


Figure 6.5 Global Positioning Data Recorder - System Electrical Schematic

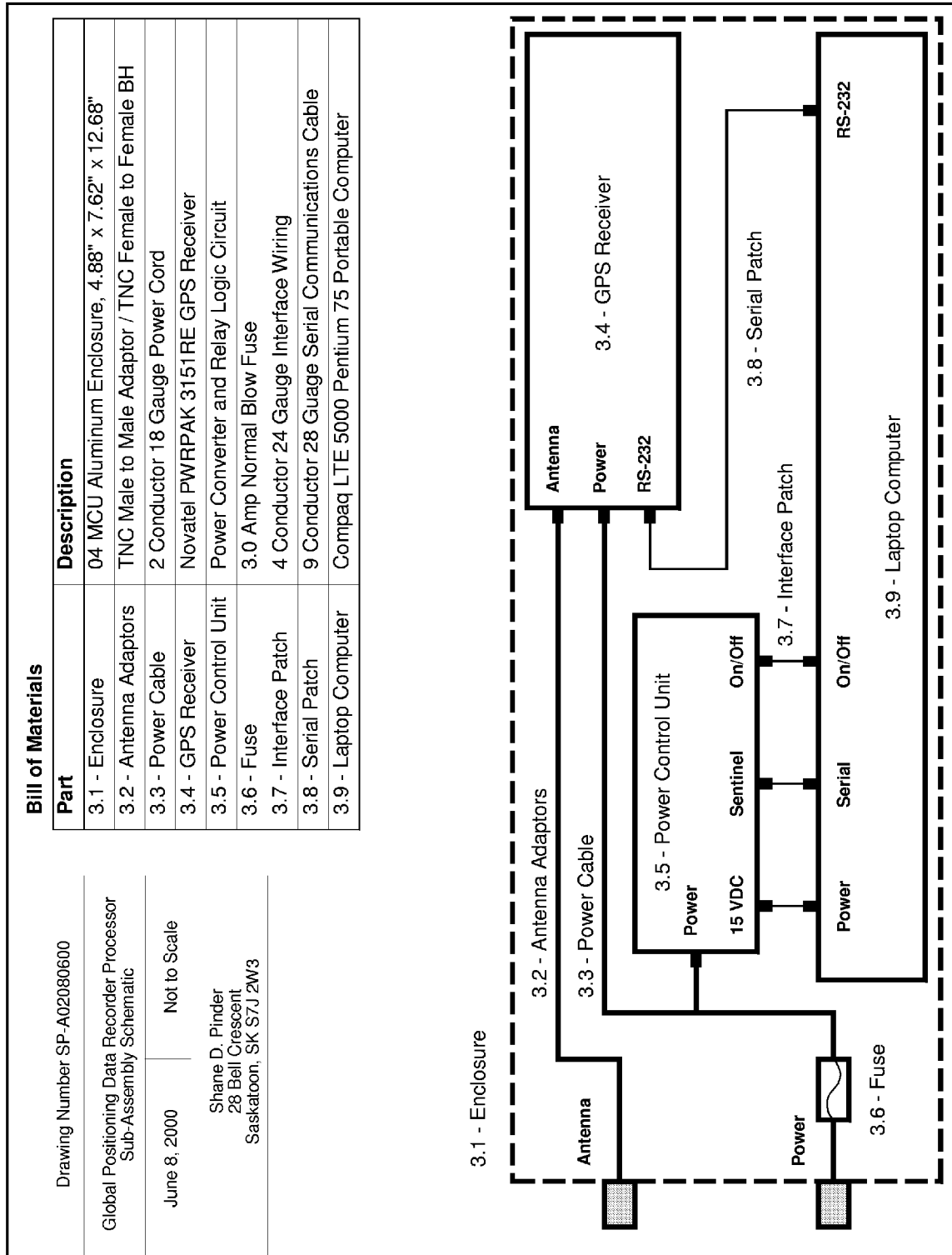


Figure 6.6 Internal Configuration of Global Positioning Data Recorder

6.3 Results and Discussion

The test aircraft used for this project visited several airports on a daily basis. Of the 175 takeoffs recorded, eighteen took place from gravel runways. The remainder took place on paved runways. The model developed in section 4.2 does not account for the use of wheel brakes during deceleration. Data pertaining to landings on paved runways cannot be modelled using a theoretical model developed without consideration for wheel braking, because pilots typically elect to make use of wheel braking during deceleration on paved runways. This did not affect the utility of the data collected during the takeoff phase, where the model applies equally well to both paved and gravel surfaced runways.

Between September 15, 2000 and December 12, 2000, data pertaining to 175 takeoffs were recorded. Raw data for all takeoffs are contained in Appendix 1.14 (CD-ROM) under the “data” directory. During a typical takeoff, the pilot adjusted control settings until the aircraft reached a speed of twenty-five metres per second. In view of this, the signal processing technique was designed to determine model parameters with iterations beginning after the aircraft reached a speed of thirty metres per second. This allowed the dynamics of the aircraft to be reasonably determined with reference to the theoretical model. Once this speed had been reached, the signal processing algorithm continuously projected the displacement that the aircraft *would have* at an arbitrary speed of fifty metres per second. This speed was chosen as a common reference for all takeoffs as it was always less than the takeoff speed of the aircraft. The projected displacement was then compared with the actual displacement of the aircraft once it reached a speed of fifty metres per second. Figure 6.7 shows the projected displacement as a function of the

instantaneous speed for a typical takeoff. Note that the algorithm continued to calculate a value for “projected” displacement after the speed of the aircraft exceeded fifty metres per second. This was included to demonstrate that the performance of the algorithm would not be affected if a different arbitrary speed were chosen.

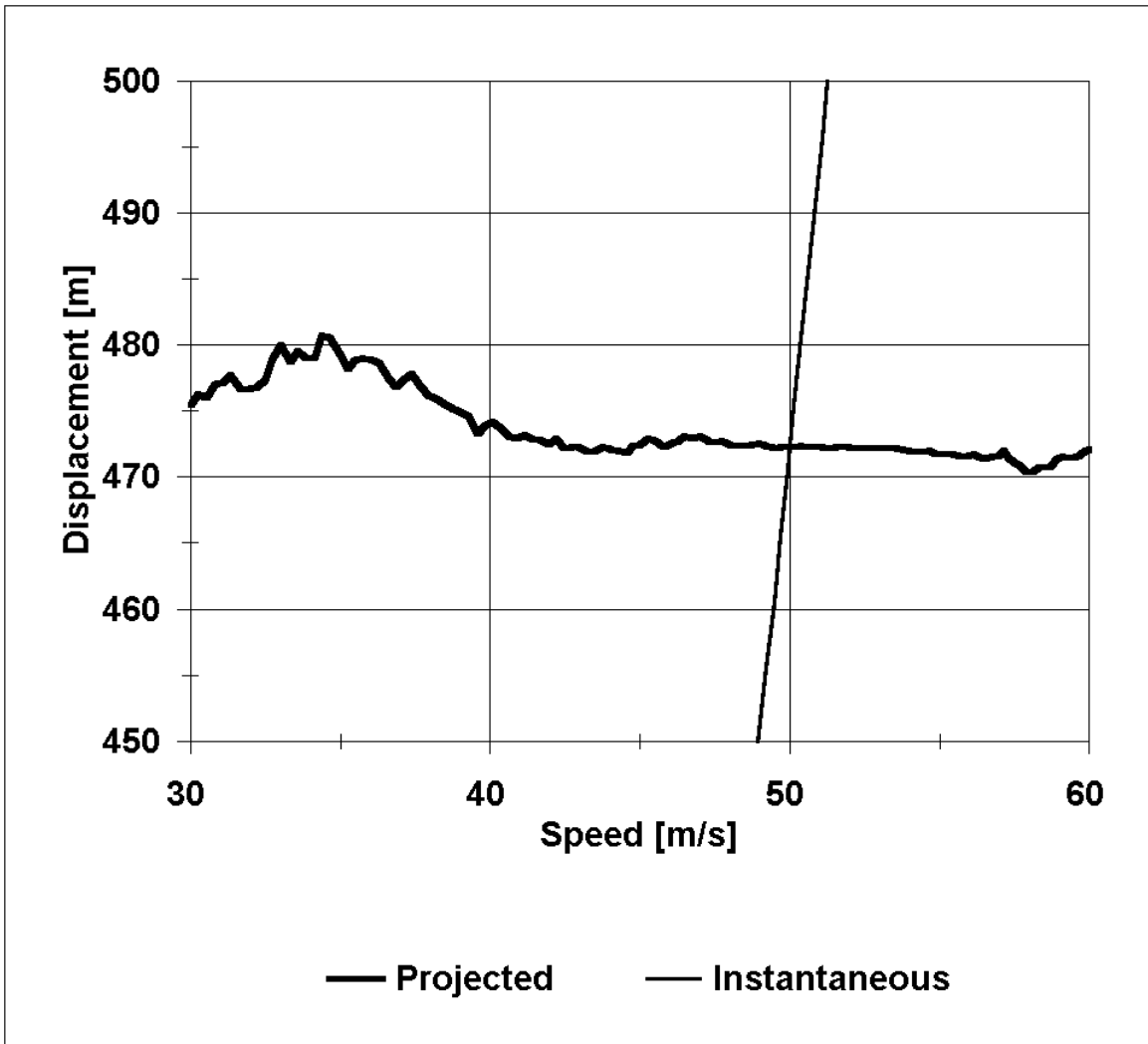


Figure 6.7 The projection of displacement in a typical takeoff converged to within ten metres of the actual future displacement a few seconds after control settings were fixed.

The projected displacement converged to a value accurate to within ten metres before the

aircraft had reached a speed of thirty-five metres per second. The projected displacement error was the amount by which the displacement at a speed of fifty metres per second differed from the instantaneous predicted displacement as a function of speed.

Figure 6.8 shows the results of parameter estimation and stopping distance projection for another typical takeoff. Note that variations in the projected displacement corresponded to variations caused by noisy segments in the acceleration filter. Note also that the noise present in the unfiltered acceleration appears to have been correlated in time. This indicates that either sensor noise or process noise was time correlated. Recall from the discussion of the discrete Kalman Filter in section 2.4 that process noise must be uncorrelated in time for the Kalman Filter to yield an optimal result. There is no such restriction on sensor noise.

With regard to the parameter values, note that the model developed in section 4.2 specified that each of the parameters are influenced by factors that are constant for each takeoff, such as control settings, runway slope, wind speed, and aircraft mass. Consequently, the value of each parameter should be expected to change from one takeoff to the next, but should be relatively constant for a given takeoff. A change in the value of a parameter during a takeoff could indicate a change in a control setting by the pilot, a sudden change in wind direction or speed, or a change in runway slope as the aircraft displaced.

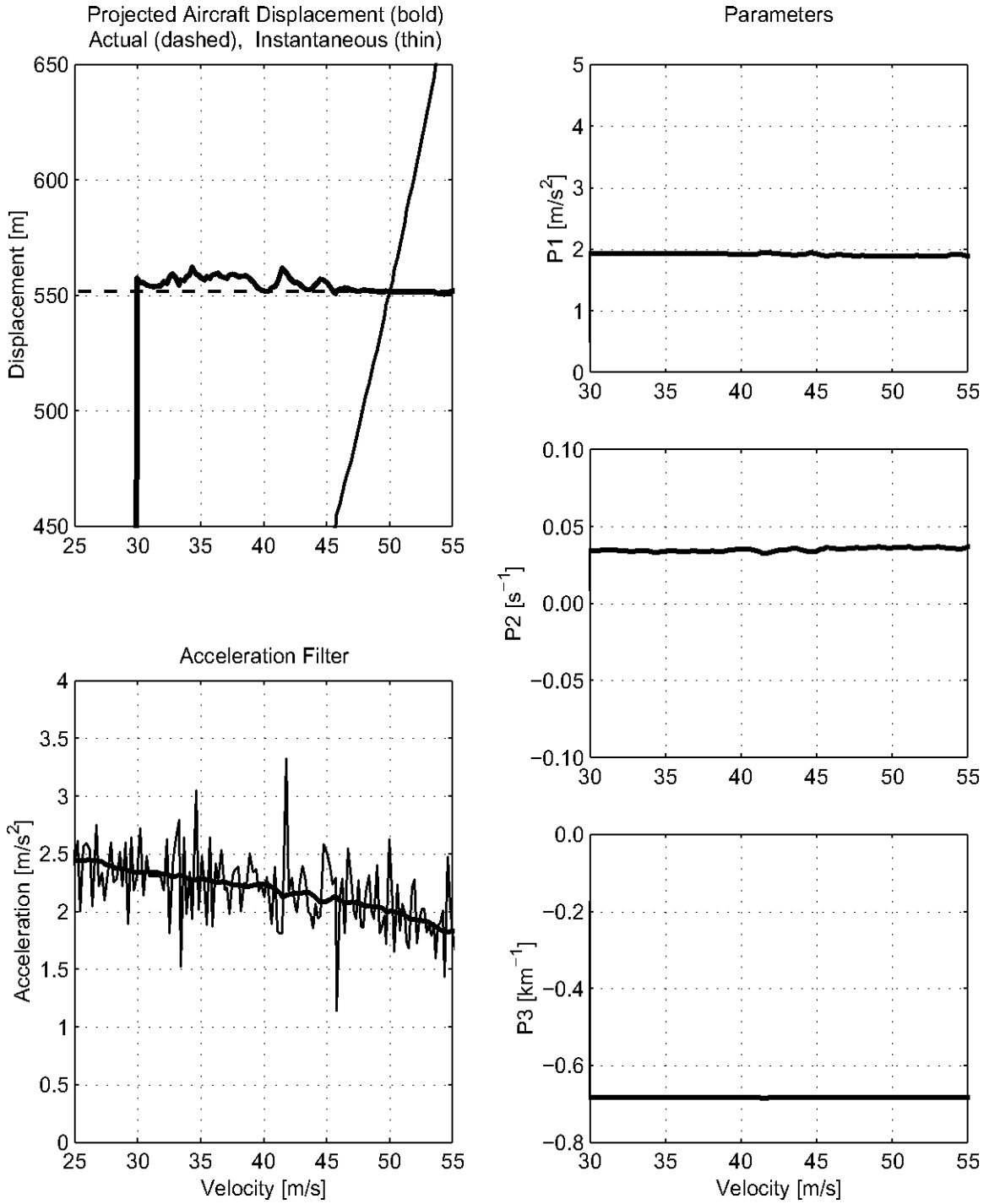


Figure 6.8 Parameter Estimation in a Typical Takeoff

Figure 6.9 shows the results of parameter estimation for another typical takeoff. Note that there was a gradual decrease in the estimated value for the parameter, P_2 , corresponding

to the convergence of the prediction of displacement to the actual displacement that occurred when the aircraft reached fifty metres per second. Note also that the unfiltered acceleration observations were again time correlated. Finally, note the lack of variation in the estimation of the value of the parameter, P_1 , which was calculated each iteration after all other parameters were determined. This indicated that the theoretical model was consistent with the measurement data.

Figure 6.10 shows the results of parameter estimation for another typical takeoff. Most notable in this example is the level of noise present in the unfiltered acceleration values. This resulted in slow convergence of the parameter, P_2 , which in turn resulted in slow convergence of the projection of aircraft displacement. Note that in this far less than ideal situation, the projection of displacement was in error by twenty metres when the aircraft was travelling at thirty metres per second. By the time the aircraft had reached a speed of thirty-seven metres per second, the error in the projection of displacement was less than fifteen metres.

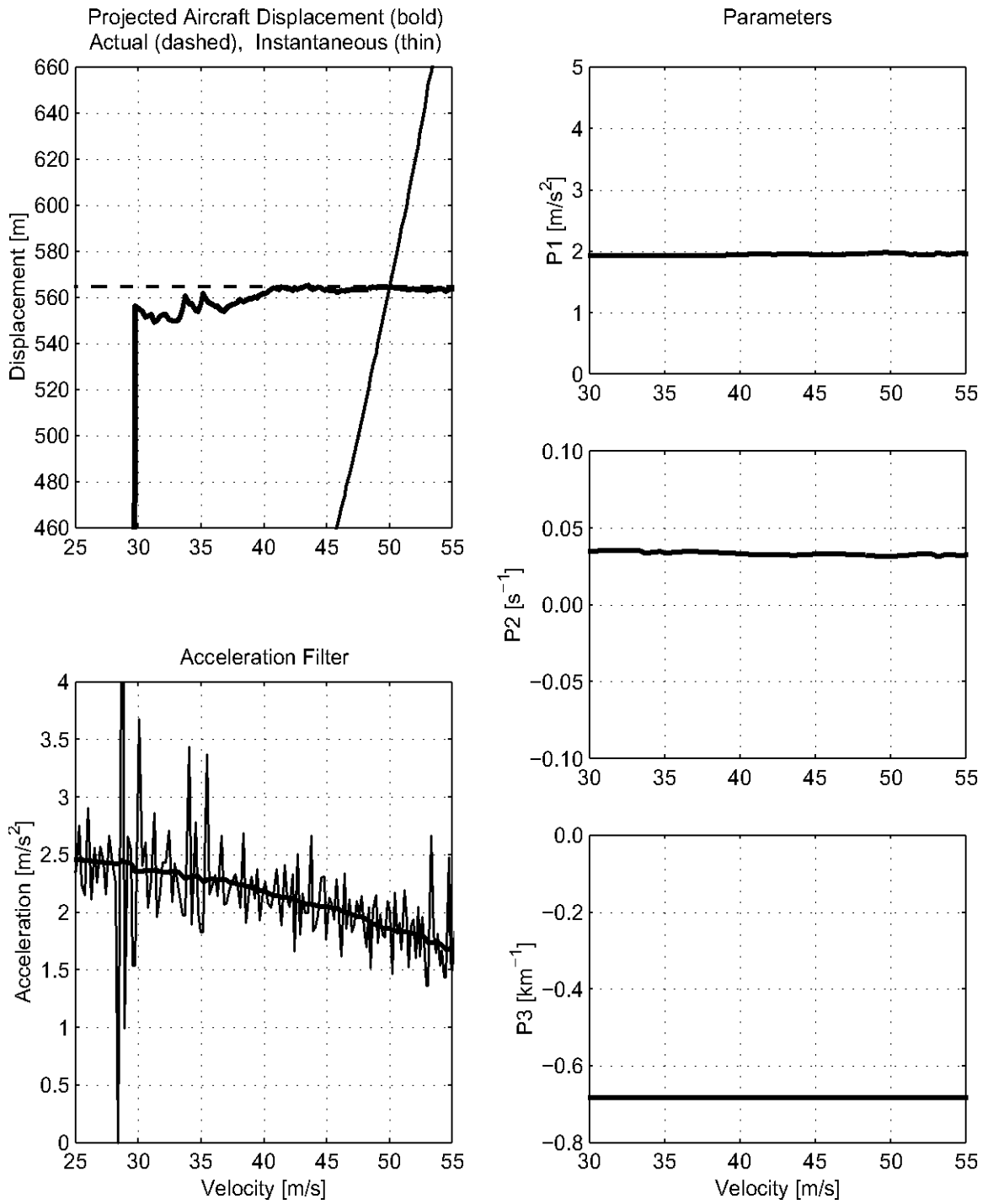


Figure 6.9 Parameter Estimation in a Typical Takeoff - Model Validation

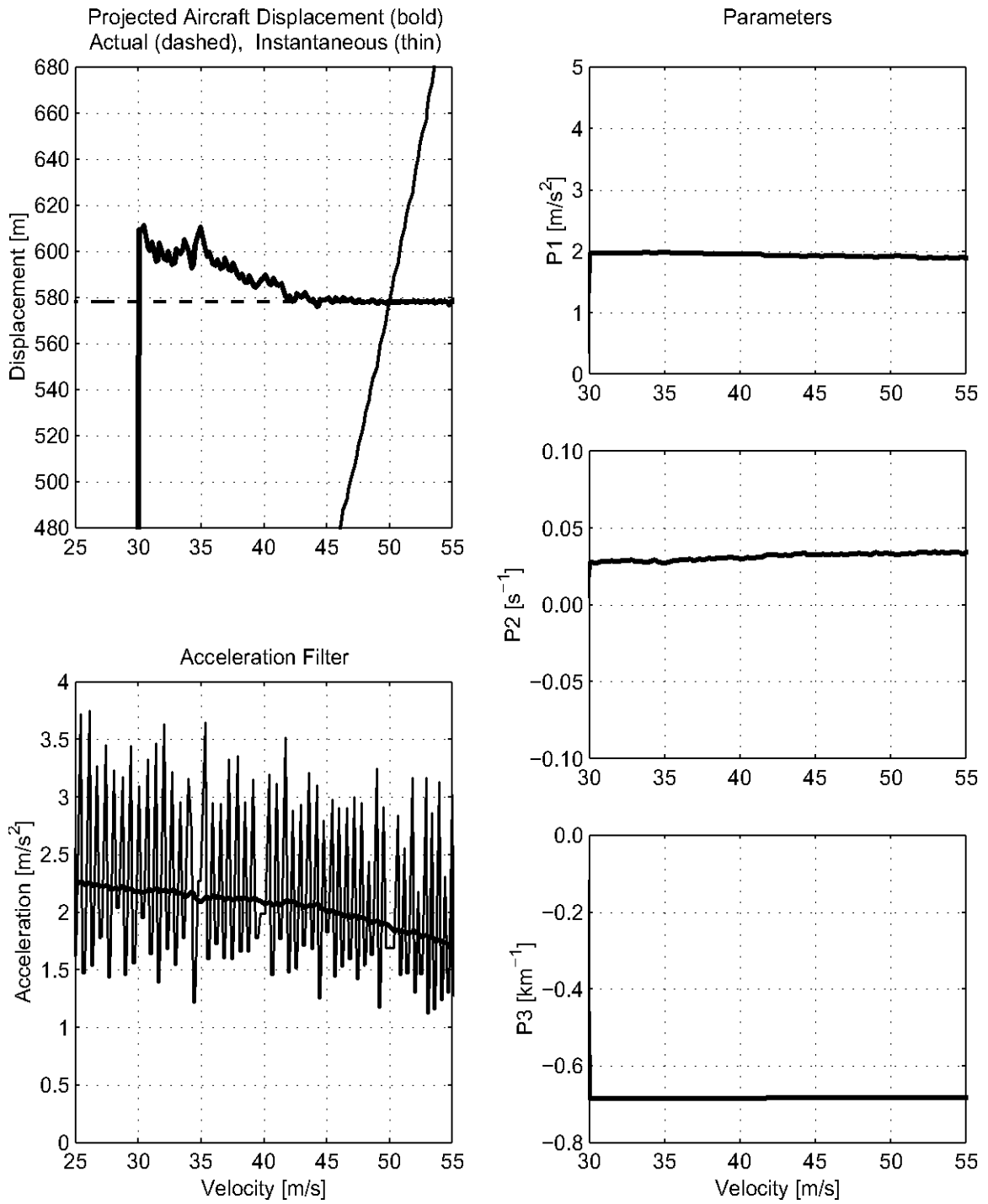


Figure 6.10 Parameter Estimation in a Typical Takeoff - Acceleration Noise

Data were collected over several months. Figure 6.11 shows a scatter plot of all data collected during 175 takeoffs. The solid lines represent the standard deviation of error as a function of speed. Note that, in all cases, the error in projection of displacement was less than fifteen metres by the time the aircraft reached forty-one metres per second. Figure 6.12 shows a histogram indicating the number of takeoffs in which the fifteen-metre standard is met as a function of aircraft speed. Data pertaining to a subset of individual takeoffs are contained in Appendix IV. Data for all takeoffs are contained in Appendix 1.15 (CD-ROM) in the “parameters” directory.

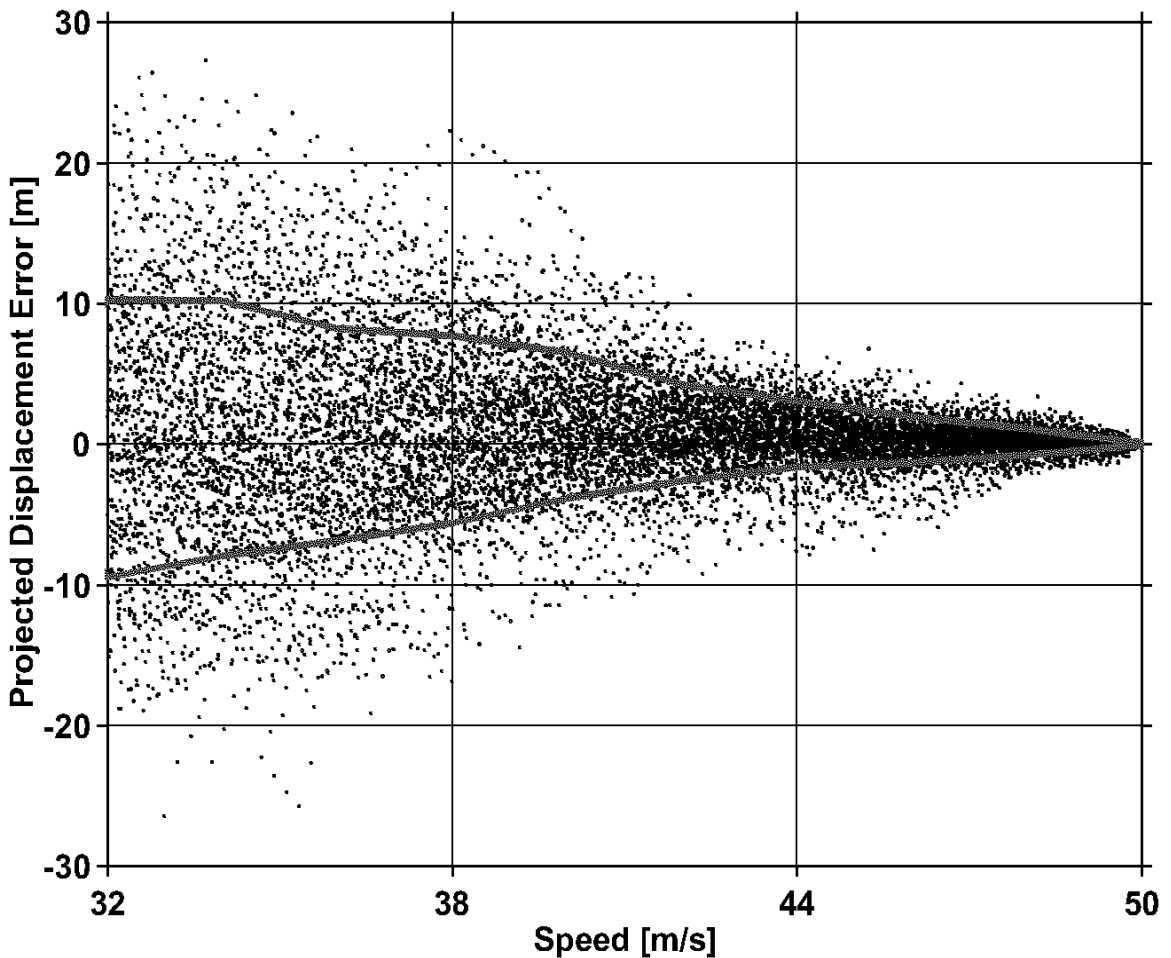


Figure 6.11 Scatter Plot of All Projections of Displacement over 175 Takeoffs

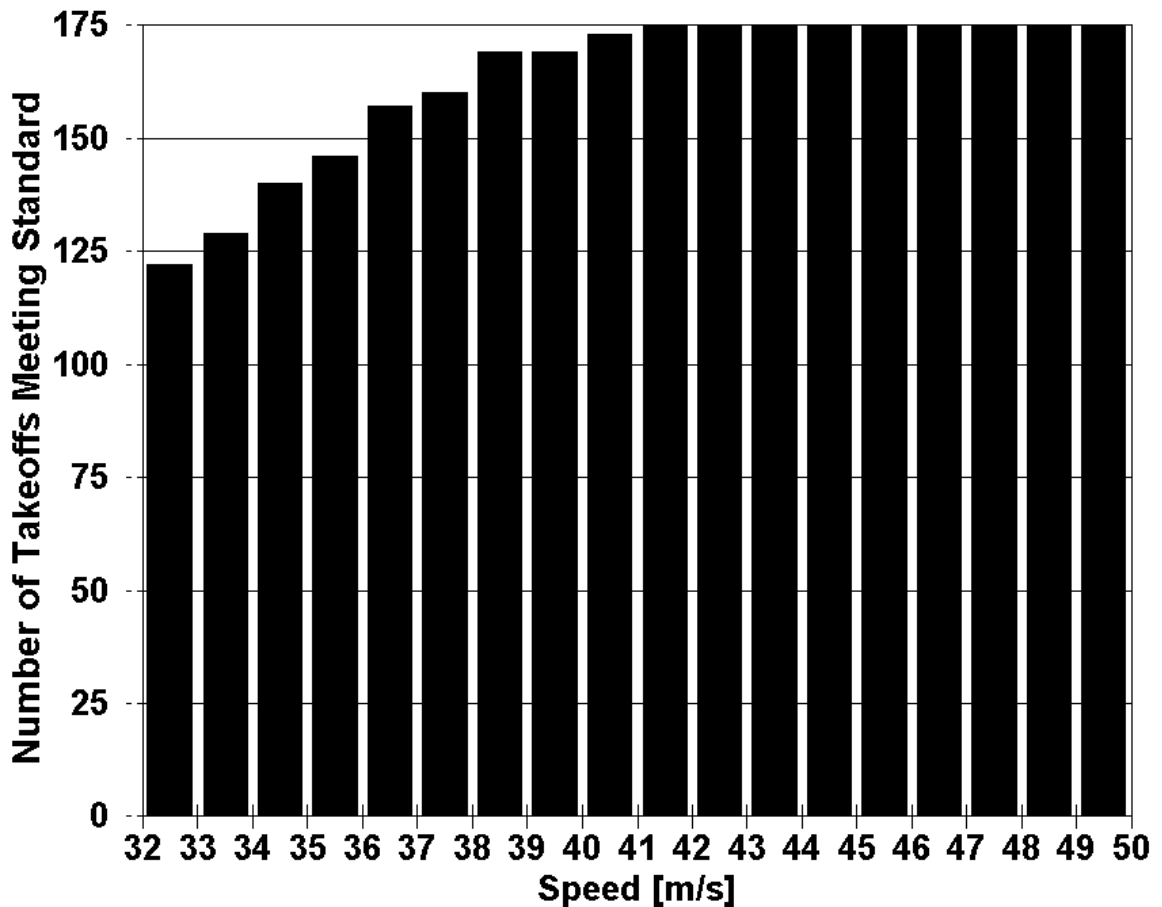


Figure 6.12 The number of takeoffs in which the error in projection of displacement was less than fifteen metres increased to 175 by a speed of forty-one metres per second.

With regard to the parametric model, it was hypothesized that the parameter, P_3 , would be a characteristic of the aircraft engines and is therefore a parameter that would change slowly, rendering this parameter a constant for any single takeoff. A filter with an effective time constant of several takeoffs in length was used to identify this parameter. In theory, the parameter, P_2 , combines the effects of runway characteristics, weather conditions, and wheel bearing friction. A filter with a time constant a few seconds in length was used to identify this parameter. The convergence of the remaining parameter, P_1 , showed that this was an entirely acceptable treatment of the parameters, P_3 and P_2 .

The aircraft used in this experimental investigation measured fifteen metres from nose to tail. From the data collected, it was concluded that a projection of displacement can be determined to within an uncertainty of fifteen metres in sufficient time to alert the pilot of an unsafe situation.

Chapter 7 - Major Conclusions and Recommendations

The feasibility of constructing a takeoff performance monitor that can project the displacement of an aircraft has been demonstrated. Improvements in the theoretical model should result in an improvement of the accuracy of the projection and an associated improvement in the time to convergence of a solution.

7.1 Major Findings

It was demonstrated that the Global Positioning System is able to provide an observation of vehicle speed that is sufficiently reliable to determine acceleration with an uncertainty of less than 0.10 metres per second squared. This accuracy should be achievable for acceleration in excess of 0.5 metres per second squared. Clear advantages in using a GPS receiver over the more conventional sensor, an accelerometer, include insusceptibilities to the gravity vector, vibrational disturbances, and temperature fluctuations.

The theoretical dynamic model derived in section 4.2 was validated using data collected under normal operating conditions of a nineteen-passenger turboprop aircraft. The signal processing technique that was used performed well enough to project the displacement of the aircraft to within fifteen metres, a distance equal to the length of the aircraft, in sufficient time to alert the pilot of an unsafe situation. If separate observation systems were used to directly measure each quantity in the theoretical model as has been the case

in earlier work in this field, the uncertainty in each measurement would result in a projected displacement error orders of magnitude higher. This improvement in the observation of projected displacement is a clear advantage of both the modelling of the combined effect of multiple factors in the grouped parameter approach described in section 4.2 and of the signal processing technique that was described in section 4.4.2.

7.2 Takeoff Performance Monitoring - Future Work

It has been demonstrated that the development of a TOPMS for use in the far-northern region using a GPS receiver as the sole sensor is technically feasible. To assess the feasibility of large-scale implementation of such a device, the following recommendations are put forward.

7.2.1 Modular Device Development

It is recommended that a prototype TOPMS be constructed for potential integration in candidate test aircraft. The hardware for such a device could be a commercial aviation GPS receiver which would include a display. The integration of TOPMS algorithms could be performed through modification of existing firmware within the GPS receiver. Such a device would include a graphical user interface which would alert the pilot of the instantaneous margin of safety.

7.2.2 Target Environment Testing

Medical ambulance aircraft in the far-northern region encounter marginal conditions more often than commercial airlines. This arises primarily due to the varied airports that are

visited by medical ambulance aircraft, and the infrequency with which the same airport is visited. In some cases, the length of the runway would not allow acceleration to V_1 followed by safe deceleration to rest. It is recommended that medical ambulance aircraft be used in target environment testing. It is expected that the data that could be collected on such a platform would represent a worst case scenario from which refinements to the TOPMS algorithm could be made.

7.3 Device Development - Future Work

There are likely many refinements that could be made to the proposed device configuration that could result in a technically improved TOPMS. For example, a fully integrated commercial INS could easily improve the performance of a TOPMS, but at prohibitively excessive expense. The following recommendations are put forward as areas where cost effective refinements could be most easily realized and where safety improvement is most significantly addressed.

7.3.1 GPS/INS Sensor Integration

The integration of GPS with inertial sensors is by no means new technology. While inertial measurements can provide an accurate determination of acceleration and angular rate, the time integration of these measurements required for positioning results in drift error due to the inevitable time integration of measurement errors. On the other hand, GPS measurements can provide bounded position and velocity information, but do not respond quickly to platform acceleration. In extreme cases, platform acceleration can cause a GPS receiver to lose signal lock.

The fusion of measurements from GPS and inertial sources results in an improvement over the measurements from either source alone. To date, the successful fusion of GPS with INS measurements has been confined to system level integration. In other words, the output from GPS and the output from an INS are combined in a separate observer.

Since the original design of GPS technology, it has been hypothesized that an improved measurement could be obtained if inertial aiding from an inertial measurement unit (IMU) were used within the tracking loops in the GPS receiver, as shown in Figure 7.1.

As described in section 2.2.2, a GPS receiver typically treats any acceleration as an unmodelled disturbance within the tracking loops. As a result, the tracking loops *filter away* the effects of acceleration and any higher order dynamics. In extreme cases, such as when high acceleration is experienced, this can cause the receiver to lose signal lock because the receiver *expects* that it is moving at a constant speed. If inertial aiding of the tracking loops were successful, this loss of lock could be avoided.

Inertial aiding of GPS tracking loops would also improve the estimation of parameters within the takeoff performance monitoring algorithm. Like acceleration, higher order dynamics such as the velocity derivatives of acceleration are also filtered away by the tracking loops in a typical GPS receiver.

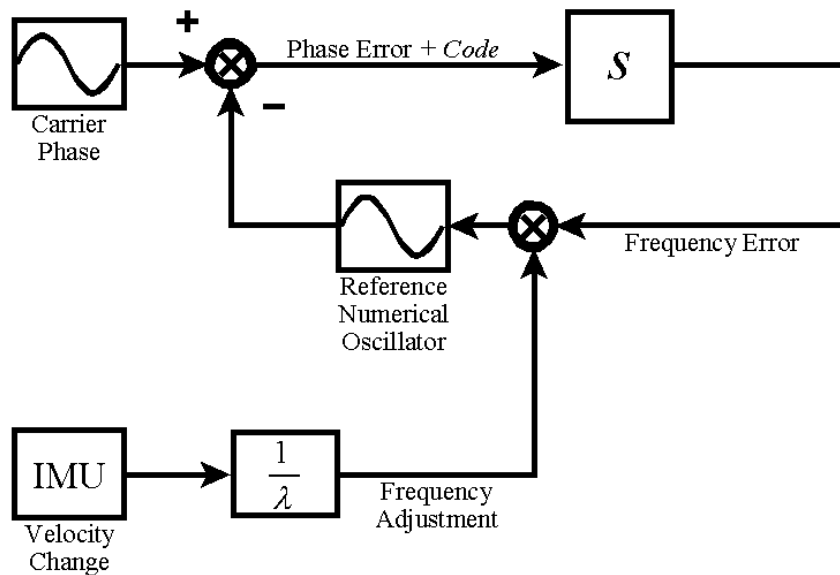


Figure 7.1 Phase Locked Loop with Inertial Aiding

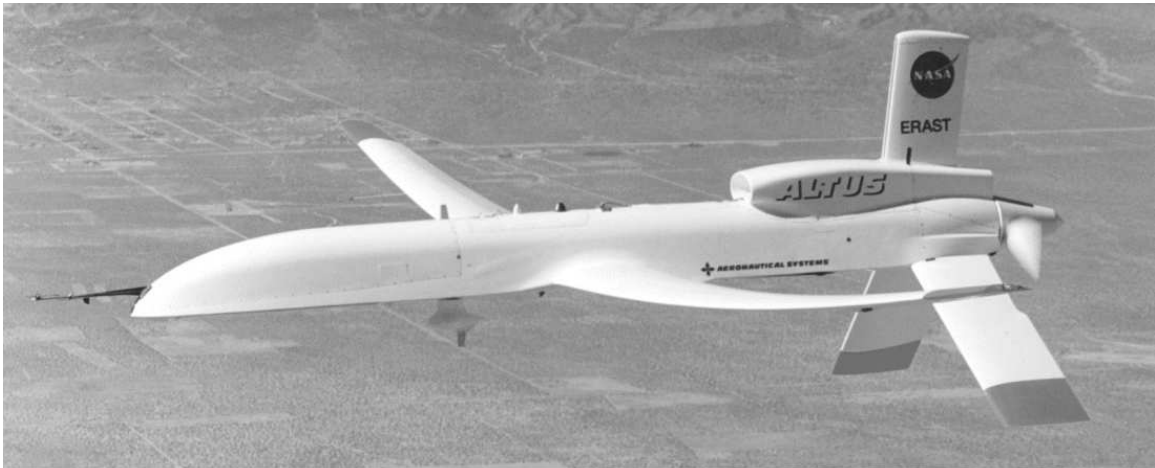
7.3.2 Actuator Integration - Automatic Deceleration Systems

In the long term, the successful development of a system that could reduce the frequency of air transportation accidents where runway friction coefficient or limited length of runway is a significant problem would be a major achievement. Such a system may require a fully automated deceleration system to overcome problems associated with pilot reaction time. This would effectively remove the pilot from the control loop at a time when an immediate procedural response is required. The development of such a system would require significant industrial support, which is not currently available. There are, however, other applications where a similar system would be advantageous.

7.4 Other Applications - Unmanned Aerial Vehicles (UAVs)

UAVs are currently used in military applications for aerial surveillance and, in limited

capacity, as an attack vehicle. The Altus II, similar in design to the Predator UAV, is shown in Figure 7.2. Aircraft of this sort are piloted remotely into hostile environments.



NASA Dryden Flight Research Center Photo Collection
<http://www.dfrc.nasa.gov/gallery/photo/index.html>
NASA Photo: EC98-44684-1 Date: 29 Jun 1998 Photo by: General Atomics

Altus II aircraft flying over southern California desert

Figure 7.2 Altus II: an Operational Unmanned Aerial Vehicle

The next generation of military UAVs will extend the attack capability to the extent available from fighter aircraft. Unmanned Combat Air Vehicles (UCAVs), such as Boeing's X-45A shown in Figure 7.3, are similar in size, instrumentation, and cost to a typical fighter aircraft and are almost completely autonomous. Consequently, onboard control systems will have the capability to reproduce the control reliability of a human pilot during all phases of flight, including takeoff and landing. This would be the ideal proving ground for a fully automated takeoff performance monitor and control system. As well, given the high dynamics that such a vehicle would exhibit, inertial aiding of GPS tracking loops will be essential.

If the development of UCAV technology progresses as expected, the spinoffs will benefit commercial aviation. Once proven in an unmanned vehicle, the adoption of takeoff performance monitoring technology in passenger aircraft will be able to proceed with much less skepticism than is currently attached to such devices.



NASA Dryden Flight Research Center Photo Collection
<http://www.dfrc.nasa.gov/gallery/photo/index.html>
NASA Photo: EC01-0292-9 Date: October 24, 2001 Photo by: Tony Landis

DARPA, U.S. Air Force, Boeing X-45A UCAV at NASA Dryden

Figure 7.3 Boeing X-45A UCAV: the Next Generation of Unmanned Air Vehicle

REFERENCES

1. Transportation Development Centre, "Aircraft Takeoff Performance and Risks for Wet and Contaminated Runways in Canada," TP 10888E, July 1991.
2. Wagenmakers, J., *Aircraft Performance Engineering*, Prentice Hall, 1991.
3. Transportation Safety Board of Canada, Report Number A95H0015, "Rejected Takeoff / Runway Overrun, Canadian Airlines International, McDonnell Douglas DC-10-30ER, C-GCPF, Vancouver International Airport, British Columbia," Minister of Public Works and Government Services Canada, 1996.
4. Sully, P. R., "Take-off Performance Monitoring Systems - Review and Prospects," Flight Research Laboratory, Institute for Aerospace Research, National Research Council of Canada, 1993.
5. Transportation Safety Board of Canada, "TSB Statistical Summary, Aviation Occurrences," Minister of Public Works and Government Services Canada, 1997.
6. Society of Automotive Engineers, "SAE Aerospace Standard AS 8044, Minimum Performance Standards for Airplane Takeoff Performance Monitors," August 1987.
7. Srivatsan, R., "Takeoff Performance Monitoring," doctoral thesis, University of Kansas, 1986.
8. Middleton, D. B., Srivatsan, R., and Person, L.H., "Simulator Evaluation of Displays for a Revised Takeoff Performance Monitoring System," NASA TP-3270, December 1992.
9. Middleton, D. B., Srivatsan, R., and Person, L.H., "Flight Test of Takeoff Performance Monitoring System," NASA TP-3403, May 1994.
10. Wallace, L.E., "Airborne Trailblazer - Two Decades with NASA Langley's 737 Flying Laboratory," NASA SP-4216, 1993.
11. Srivatsan, R., Downing, D.R., and Bryant, W. H., "Development of a Takeoff Performance Monitoring System," NASA TM-89001, August 1986.
12. Milligan, M.W., Zhao, M.M., and Wilkerson, H. J., "Monitoring Airplane Takeoff Performance: Prototype Instrument with Learning Capability," **AIAA Journal of Aircraft**, Vol. 32, No. 4, 1995.
13. Khatwa, R., "The Development of a Takeoff Performance Monitor," doctoral thesis, University of Bristol, 1991.
14. Decision Record for a Meeting of the Performance Standards Working Group, Transport Canada, Ottawa, October 18, 2000.
15. Spilker, J.J., "Overview of GPS Operation and Design," *Global Positioning System: Theory and Applications, Vol. I*, edited by Parkinson, B.W. and Spilker, J.J. Jr., American Institute of Aeronautics and Astronautics, 1996, pp. 29-56.

16. Ogata, K., *Modern Control Engineering, Second Edition*, Prentice Hall, 1990.
17. Brown, R.G. and Hwang, P.Y.C., *Introduction to Random Signals and Applied Kalman Filtering*, Second Edition, John Wiley & Sons, 1992.
18. Kalman, R.E., "A New Approach to Linear Filtering and Prediction Problems," **Transactions of the ASME-Journal of Basic Engineering**, Vol. 82, Series D, 1960., pp. 35-45.
19. Lukesh, J., "Random Processes: Basic Concepts," Appendix to Kalman, R.E., "A New Approach to Linear Filtering and Prediction Problems," reproduced, 2002.
20. Biezad, D.J., "Kalman Filter Inertial Navigation System Flight Applications," *Integrated Navigation and Guidance Systems*, edited by Przemieniecki, J.S. et al., American Institute of Aeronautics and Astronautics, 1999, pp. 95-107.
21. Axelrad, P. and Brown, R.G., "GPS Navigation Algorithms," *Global Positioning System: Theory and Applications, Vol. I*, edited by Parkinson, B.W. and Spilker, J.J. Jr., American Institute of Aeronautics and Astronautics, 1996, pp. 409-433.
22. Pinder, S.D., Crowe, T.G., and Nikiforuk, P.N., "A Practical Investigation of a Takeoff Performance Monitor for Turboprop Aircraft," *Proceedings of the AIAA Guidance, Navigation, and Control Conference*, August 6-9, 2001, Montreal, PQ.
23. Pinder, S.D., Crowe, T.G., and Nikiforuk, P.N., "A Lumped Parameter Model of Turboprop Aircraft Operating on Gravel Runways," *Proceedings of the AIAA Modeling and Simulation Technologies Conference*, August 6-9, 2001, Montreal, PQ.
24. Gaskell, D.R., *An Introduction to Transport Phenomena in Engineering*, Macmillan Publishing Company, New York, 1992, p. 160.
25. Pinder, S.D., Crowe, T.G., and Nikiforuk, P.N., "Application of the Global Positioning System in Determination of Vehicular Acceleration," **AIAA Journal of Aircraft**, Vol. 38, No. 5, 2001, pp. 856-859.
26. Van Dierendonck, K.J., Cannon, M.E., Wei, M., and Schwarz, K.P., "Error Sources in GPS-determined Acceleration for Airborne Gravimetry," *Proceedings of the Institute of Navigation National Technical Meeting*, January 24-26, 1994, San Diego, CA, pp. 811-820.
27. Psiaki, M.L., Powell, S.P., and Kintner, P.M. Jr., "The Accuracy of the GPS-derived Acceleration Vector, A Novel Attitude Reference," *Proceedings of AIAA 1999 Guidance, Navigation, and Control Conference*, August 9-11, 1999, Portland, OR, pp. 751-760.
28. AlliedSignal Commercial Avionics Systems, "Bendix/King CAS 66A TCAS I Installation Manual," July, 1997.
29. United States Federal Aviation Regulation Part 23, Amendment 23-50, 1996.

30. AMR Combs, Inc., "Installation of a Bendix/King CAS-66 TCAS I System," Supplemental Type Certificate Number SA00071DE-D, 1994.
31. Pinder, S.D., "Installation of a Global Positioning Data Recorder," Transport Canada Limited Supplemental Type Certificate Number LSA00-016, August 29, 2000.

Appendix I - CD-ROM

Directory

1.01 CAI Flight 17
1.02 airports
1.03 integral solution
1.04 simulation
1.05 novatel
1.06 accelerometer
1.07 c-fsew
1.08 tcas manual
1.09 nav gps
1.10 type certificates
1.11 gpdr lstc
1.12 laptop manual
1.13 software
1.14 data
1.15 parameters
1.16 publications
1.17 copyright_releases
1.18 manuscript

Contents

description of a rejected takeoff at Vancouver Airport
flight supplement sheets for airports in dataset
derivation of the integral used to project displacement
interactive takeoff performance monitor simulation
user's manual for the GPS receiver contained in the GPDR
datasheet for accelerometers used in railway testing
photographs of the test aircraft containing the GPDR
install manual for the TCAS contained in the test aircraft
user's manual for the aircraft GPS receiver
Canadian and U.S. type certificates for the Jetstream 31
supplemental type certificate application for the GPDR
user's manual for the laptop computer used in the GPDR
source code for GPDR and post-processing algorithms
raw and formatted data collected from the GPDR
post-processing datasheets for 175 takeoffs
publications resulting from studies within this project
copyright releases for various reproduced materials
searchable copy of manuscript

Appendix II - Limited Supplemental Type Certificate Application

This appendix contains the original Limited Supplemental Type Certificate Application that was submitted to Transport Canada for approval prior to the installation of the Global Positioning Data Recorder and the subsequent period of data collection. This document outlines the rationale used to show compliance with various airworthiness regulations pertaining to the design, construction, and installation of the device as well as any potential interference with existing aircraft systems.



Department of Transport

Limited Supplemental Type Certificate

This approval is issued to:

Shane Pinder
28 Bell Crescent
Saskatoon, SK
S7J 2W3

Approval Number: C-LSA00-016

Issue Number: 1

Date of Approval: August 29, 2000

Date of Issue: August 29, 2000

Responsible Office: Prairie and Northern Region (Winnipeg)

Aircraft/Engine Type/Model: British Aerospace 3112

Registration/Serial No.: C-FSEW/764

Canadian Type Certificate
or Equivalent: A-154

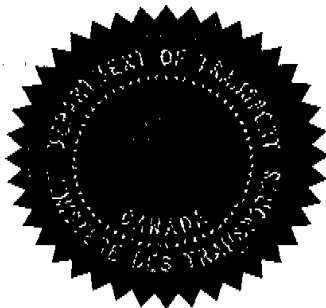
Description of Design Change: Installation of a Global Positioning Data Recorder

Installation/Operating Data,
Required Equipment and
Limitations: Modification to be completed in accordance with Shane
Pinder Master Drawing List Number L01160600 Revision B
or later DOT Approved Revision.

NOTE:

Approval is for Mechanical and Electrical provisions only.
System Circuit Breaker must be tripped and collared.

Conditions: This approval is only applicable to the type/model of
aeronautical product specified therein. Prior to incorporating this
modification, the installer shall establish that the interrelationship
between this change and any other modification(s) incorporated will not
adversely affect the airworthiness of the modified product.



Marc Malo

Aircraft Certification Engineer
For Minister of Transport

Canada



Department of Transport

Limited Supplemental Type Certificate

This approval is issued to:

Shane Pinder
28 Bell Crescent
Saskatoon, SK
S7J 2W3

Approval Number: C-LSA00-016

Issue Number: 2

Date of Approval: August 29, 2000

Date of Issue: September 14, 2000

Responsible Office: Prairie and Northern Region (Winnipeg)

Aircraft/Engine Type/Model: British Aerospace 3112

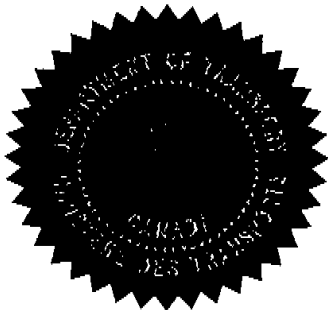
Registration/Serial No.: C-FSEW/764

Canadian Type Certificate
or Equivalent: A-154

Description of Design Change: Installation of a Global Positioning Data Recorder

Installation/Operating Data,
Required Equipment and
Limitations: Modification to be completed in accordance with Shane
Pinder Master Drawing List Number L01160600 Revision B
or later DOT Approved Revision.

Conditions: This approval is only applicable to the type/model of
aeronautical product specified therein. Prior to incorporating this
modification, the installer shall establish that the interrelationship
between this change and any other modification(s) incorporated will not
adversely affect the airworthiness of the modified product.



Marc Malo

Aircraft Certification Engineer
For Minister of Transport

Canada



TRANSPORT CANADA
Aircraft Certification (RAWD)
Box 8550, 344 Edmonton Street
Wpg, Mb, Canada, R3C 0P6

Date: August 29, 2000

File: 2195-00

MEMO

From: Marc Malo (RAWD)

Telephone: (204) 983-4228

Fax: (204) 984-6021

To: Shane Pinder

Telephone: (306) 222-0782

Fax: (306) 664-2595

Attention: Shane Pinder

Subject: Installation of Global Positioning Data Recorder in Jetstream 3112

Reference: File 2195-00

Mr. Pinder,

Please find enclosed the following approved documents:

1. Limited Supplemental Type Certificate, C-LSA00-016, Issue 1, Installation of Global Positioning Data Recorder in Jetstream 3112
2. Letter of LSTC Transmittal
3. Approved Master Drawing List
4. Approved Modification Data List

Regards,

Marc Malo, P.Eng.
Aircraft Certification Engineer
Prairie & Northern Region
RAWD

Canada

Ph: 204-983-4228

FAX: 204-984-6021

E-Mail: malom@tc.gc.ca



TRANSPORT CANADA
Aircraft Certification (RAWD)
Box 8550, 344 Edmonton Street
Wpg, Mb, Canada, R3C 0P6

Date: September 14, 2000

File: 2195-00

MEMO

From: Marc Malo (RAWD)

Telephone: (204) 983-4228

Fax: (204) 984-6021

To: Shane Pinder

Telephone: (306) 222-0782

Fax: (306) 664-2595

Attention: Shane Pinder

Subject: Installation of Global Positioning Data Recorder in Jetstream 3112

Reference: File 2195-00

Mr. Pinder,

Please find enclosed the following approved documents:

1. Limited Supplemental Type Certificate, C-LSA00-016, Issue 2, Installation of Global Positioning Data Recorder in Jetstream 3112
2. Letter of LSTC Transmittal

Regards,

Marc Malo, P.Eng.
Aircraft Certification Engineer
Prairie & Northern Region
RAWD



Transport
Canada

Transports
Canada

Civil Aviation
Prairie and Northern Region

Aviation civile
Région des prairies et du nord

Aircraft Certification
2-344 Edmonton Street
Box 8550
Winnipeg, Manitoba
R3C 0P6

Your file Votre référence

Our file Notre référence

File: 2195-00
Telephone: (204) 983-4228
Date: August 29, 2000

Shane Pinder
28 Bell Crescent
Saskatoon, SK
S7J 2W3

Attention: Shane Pinder

Issue of Limited Supplemental Type Certificate C-LSA00-016 Issue #1

Aircraft: British Aerospace 3112
Subject: Installation of Global Positioning Data Recorder
Registration: C-FSEW/764

This is to confirm the Transport Canada Certificate number C-LSA00-016 Issue #1 has been assigned for the subject changes and the LSTC is enclosed.

Please ensure that the approval number is recorded in the aircraft logbooks.

The transfer of this document in the name of another person requires a prior approval from the Minister. For further details, refer to Airworthiness Manual Advisory 513/5, which defines the privileges, responsibilities and obligation of an LSTC holder, and specifies LSTC transfer procedures.

An LSTC holder is responsible for reporting any service problem experienced with their product. Therefore, should you become aware of any defect, malfunction or failure resulting from the effected design change, it is your responsibility to submit a Service Difficulty Report to Transport Canada in accordance with Chapter 591 of the Airworthiness Manual.

Yours truly,

Marc Malo, P.ENG
Aircraft Certification
Prairie & Northern Region (Winnipeg)

MM/wh

encl.

HolderLSTC016Marc.doc



Transport
Canada

Transports
Canada

Civil Aviation
Prairie and Northern Region

Aviation civile
Région des prairies et du nord

Aircraft Certification
2-344 Edmonton Street
Box 8550
Winnipeg, Manitoba
R3C 0P6

Your file Votre référence

Our file Notre référence

File: 2422-00
Telephone: (204) 983-4228
Date: September 14, 2000

Shane Pinder
28 Bell Crescent
Saskatoon, SK
S7J 2W3

Attention: Shane Pinder

Issue of Limited Supplemental Type Certificate C-LSA00-016 Issue #2

Aircraft: British Aerospace 3112
Subject: Installation of Global Positioning Data Recorder
Registration: C-FSEW/764

This is to confirm the Transport Canada Certificate number C-LSA00-016 Issue #2 has been assigned for the subject changes and the LSTC is enclosed.

Please ensure that the approval number is recorded in the aircraft logbooks.

The transfer of this document in the name of another person requires a prior approval from the Minister, For further details, refer to Airworthiness Manual Advisory 513/5, which defines the privileges, responsibilities and obligation of an LSTC holder, and specifies LSTC transfer procedures.

An LSTC holder is responsible for reporting any service problem experienced with their product. Therefore, should you become aware of any defect, malfunction or failure resulting from the effected design change, it is your responsibility to submit a Service Difficulty Report to Transport Canada in accordance with Chapter 591 of the Airworthiness Manual.

Yours truly,

Marc Malo, P.ENG
Aircraft Certification
Prairie & Northern Region (Winnipeg)
MM/wh
encl.
HolderLSTC016#2Marc.doc

Canada

FAX COVER

Message:

Date : 23/08/2000

Attached please find the final revision of a Modification Approval Request Application for a Global Positioning Data Recorder. The flight test has been eliminated from the Test Plan as discussed.

Tentatively, I would like to proceed with installation on the evening of Wednesday, August 30.

Best regards,



Shane Pinder
Control Systems Laboratory
University of Saskatchewan

To: Marc Malo

From : Shane Pinder

Company : Transport Canada

Company :

Fax Number : 1-204-984-6021

Fax Number : 1-306-664-2595

Pages including this cover page: 24

Subject : Modification Approval Request



Transport Canada / Transports Canada

DESIGN CHANGE APPROVAL APPLICATION

DEMANDE D'APPROBATION MODIFICATION DE LA CONCEPTION

See Instructions on reverse side

Voir les instructions au verso

1. Name and address of applicant - Nom et adresse du demandeur Shane Pinder 28 Bell Crescent Saskatoon, SK S7J 2W3		2. Name and address of prospective holder - Nom et adresse du titulaire éventuel La Ronge Aviation Services Limited Box 320 La Ronge, SK S0J 1L0						
3. Identification of aeronautical product - Identification du produit aéronautique Make - Marque: Jetstream		Model - Modèle: 3112	Registration - Immatriculation: C-FSEW	Serial No. - N° de série: 764				
4. Request for (check appropriate box) - Objet de la demande (Cocher la case appropriée)								
A. <input type="checkbox"/> Supplemental Type Certificate (STC) Certificat de type supplémentaire (CTS)		B. <input type="checkbox"/> STC Revision Révision d'un CTS		STC No. _____ Issue Edition _____				
C. <input checked="" type="checkbox"/> Limited STC (LSTC) CTS restreint (CTSR)		D. <input type="checkbox"/> Limited STC Revision Révision de CTS restreint		LSTC No. _____ N° CTSR _____ Issue Edition _____				
E. <input type="checkbox"/> Repair Design Certificate (RDC) Certificat de conception de réparation (CCR)		F. <input type="checkbox"/> RDC Revision Révision de CCR		RDC No. _____ N° CCR _____ Issue Edition _____				
G. <input type="checkbox"/> FAA STC CTS de la FAA		H. <input type="checkbox"/> FAA STC Revision Révision de STC FAA		STC No. _____				
I. <input type="checkbox"/> Type design examination of a foreign change Examen de définition de type modification étrangère		FAA STC: CTS de la FAA: _____		Other: Autre: _____				
5. Title of modification or repair - Titre de la modification ou réparation Installation of a Global Positioning Data Recorder								
6. Brief description of modification or repair, including effects of changes (use additional pages if necessary) Description succincte de la modification ou des réparations comprenant les effets des changements (utilisez des feuilles supplémentaires si nécessaire) A portable computer and GPS receiver are used to collect position and velocity data using the signal from an existing GPS antenna.								
7. Applicable Canadian or FAA Type Certificate (TC) - Certificat de type (CT) canadien ou de la FAA pertinent								
A. Canadian TC No - N° de CT canadien: A-154		B. FAA TC No - N° de CT FAA: _____		C. Others (specify) - Autres (préciser): _____				
8. Proposed basis of certification - Critères de certification proposés								
A. <input checked="" type="checkbox"/> Same as Cdn TC Identiques à ceux du CT canadien		B. <input type="checkbox"/> Same as FAA TC Identiques à ceux du CT FAA		C. <input type="checkbox"/> Others (specify) Autres (préciser): _____				
9. Documentation to be submitted Documentation à soumettre		Submitted Soumise		For TCCA use - Réservé à TCAC				
		Yes - Oui	No - Non	Required Requis		Received Reçus		Date (Y/A-M-D/J)
Compliance program		<input checked="" type="checkbox"/>						
Master drawing or top drawing list		<input checked="" type="checkbox"/>						
Flight manual supplement			<input checked="" type="checkbox"/>					
Maintenance/repair manual supplement			<input checked="" type="checkbox"/>					
Instructions for continuing airworthiness			<input checked="" type="checkbox"/>					
Airworthiness limitations			<input checked="" type="checkbox"/>					
Engineering reports		<input checked="" type="checkbox"/>						
Design drawings		<input checked="" type="checkbox"/>						
Manufacture drawings & installations instructions		<input checked="" type="checkbox"/>						
Electrical load analysis			<input checked="" type="checkbox"/>					
Draft STC, LSTC or RDC			<input checked="" type="checkbox"/>					
Weight and moment change data			<input checked="" type="checkbox"/>					
Flight test data								
Others (specify)								
10. Applicant's remarks - Remarques du demandeur The applicant is a Ph.D. student in Mechanical Engineering at the University of Saskatchewan and holds a licence as a Professional Engineer in the Province of Ontario.								
11. I agree to pay charges as prescribed in CAR, Part 1, Subpart 4 (CAR 104-Charges) and/or to reimburse Transport Canada incremental expenses as prescribed in Civil Aviation Directive No. 3, as applicable.		Je m'engage à payer les redevances prescrites à la sous-partie 4 de la partie 1 du RAC (sous-partie 104 du RAC - Redevances) et/ou à rembourser à Transports Canada les dépenses supplémentaires telles qu'exigées dans la Directive de l'Aviation civile n° 3, selon le cas.						
Signature of Applicant - Signature du demandeur:		Title - Poste: _____		Date (Y/A-M-D/J): 16 Jun 2000				
12. Signature of responsible project engineer Aircraft Certification - Signature de l'ingénieur responsable du projet, Certification des aéronefs				Date (Y/A-M-D/J): _____				

Modification Approval Request

Global Positioning Data Recorder (GPDR)

Table of Contents

Compliance Program - Rev. 1, 23 Aug 00	2 / 14
Purpose and Scope	2 / 14
Mechanical Considerations	3 / 14
Electrical Considerations	3 / 14
Substantiation Report - Rev. 1, 23 Aug 00	4 / 14
Subpart D, Design and Construction	4 / 14
Subpart F, Equipment	4 / 14
Test Plan - Rev. 1, 23 Aug 00	7 / 14
Subpart C, Structure	7 / 14
Test C1:	7 / 14
Test C2:	7 / 14
Subpart F, Equipment	8 / 14
Test F1:	8 / 14
Test F3:	8 / 14
Installation Instructions - Rev. 1, 12 Jul 00	9 / 14
Detailed Test Plan - Rev. 1, 23 Aug 00	10 / 14
Test C1	10 / 14
Test C2	10 / 14
Test F1	10 / 14
Test F3	14 / 14
Master Drawing List	Attached
Drawing Number SP-A01130600 - Rev. 1, Wiring Diagram	Attached
Drawing Number SP-A01120600 - Rev. 1, Processor Mechanical Assembly	Attached
GPS Antenna Signal Evaluation (Splitter Test Report)	Attached

1 / 14



Purpose and Scope

The purpose of the proposed modification is to collect position and velocity data during takeoff and landing of a Jetstream 31. These data will be used in support of a research project at the University of Saskatchewan investigating the feasibility of a landing and takeoff performance monitoring system for passenger aircraft that frequently travel to airports with gravel runways in the Far North. The equipment required consists of a unit containing a portable computer and a NovAtel GPS receiver, and an antenna splitter used to acquire the signal from an existing GPS antenna.

The proposed Global Positioning Data Recorder (GPDR) system is designed to be minimally invasive and to take advantage of existing equipment wherever possible. Air Sask Aviation has agreed to carry the proposed equipment onboard C-FSEW, a Jetstream 31 equipped with a Bendix / King KLN 0089B GPS receiver. A GPS antenna splitter would be employed to acquire the signal from the existing GPS antenna.

The existing configuration of the aircraft includes the hardware for a Bendix / King CAS 66 TCAS I installation. The TCAS processor has been removed due to serviceability problems as it was not a required instrument. It is proposed that the existing tray for the TCAS processor be used as the station for the proposed data recorder. The existing infrastructure would be used to supply power to the unit. There is existing coaxial cabling that runs from the TCAS tray to an unused antenna mounted at station 130, just aft of the cockpit bulkhead. The existing GPS antenna lies within a few inches of this location.

Table 1: GPDR Processor Specifications

CHARACTERISTIC	DESCRIPTION
Form Factor	4 MCU (1/2 long ATR)
Overall Dimensions	12.750" x 9.125" x 5.000"
Weight	11 pounds
Power Requirements	
Voltage	Nominal: +28 Vdc Range: +17 to +40 Vdc
Current	Nominal: 1.8 A Maximum Operating: 2.0 A Bootup: 2.2 A
Power	56 watts
Temperature Range	
Operating	10 ° C to +35 ° C
Storage	-30 ° C to +60 ° C
Cooling	Convection

Mechanical Considerations

An aluminum enclosure has been constructed that will contain the portable computer and the GPS receiver. The unit weighs 11 pounds. It will be secured in place using hold down pins on the existing TCAS processor tray, located just aft of the rear R/H passenger seats.

The GPS antenna splitter, which weighs 0.3 pounds, will be attached to the GPS antenna using a TNC male to male elbow adaptor. The coaxial cable supplying the navigational GPS receiver will be connected to the primary branch of the splitter using the existing TNC connector. One of four coaxial cables that run between the TCAS tray and the TCAS directional antenna will be connected to the secondary branch of the splitter using the existing TNC connector.

Electrical Considerations

There is a dedicated 5 A circuit breaker for the TCAS tray at the auxiliary avionics circuit breaker panel. This circuit draws power from the 28 VDC main avionics bus. The recorder unit draws 1.8 A at 28 VDC, internally protected with a 3 A normal blow fuse. This level of power consumption is identical to that of the removed TCAS processor.

Power is supplied to the GPS antenna internal amplifier circuitry by the existing GPS receiver through the primary branch of the antenna splitter which allows DC current to pass. The second receiver acquires the antenna signal from the secondary branch. The splitter provides isolation in excess of 20 dB between the primary and secondary branches.

Table 2: Compliance Matrix

Item	Reference	Title	Means of Compliance
1	23.303	Factors of Safety	Test
2	23.305	Strength and Deformation	Test
3	23.307 (a)	Proof of Structure	Test
4	23.603	Materials & Workmanship	Evaluation
5	23.605	Fabrication Methods	Evaluation
6	23.1301 (a-c)	Function and Installation	Evaluation
7	23.1301 (d)	Function and Installation	Test
8	23.1309 (a)	Equipment, Systems & Installations	Test
9	23.1309 (b)	Equipment, Systems & Installations	Analysis
10	23.1357 (a)	Circuit Protective Devices	Evaluation
11	23.1365 (a)	Electric Cables and Equipment	Analysis
12	23.1431 (a-b)	Electronic Equipment	Test

3/14

Substantiation Report - Rev. 1, 23 Aug 00

Subpart D, Design and Construction

Sec. 23.603

Sec. 23.605

The enclosure for the GPDR processor is constructed with 1/16" aluminum, in accordance with ARINC 404A material and dimension requirements. The processor will be tested in accordance with Subpart C as described in the Test Plan, Test C1.

The TNC male to male elbow adaptor will be tested in accordance with Subpart C as described in the Test Plan, Test C2.

Subpart F, Equipment

Sec. 23.1301

The GPDR processor consists of a portable computer and a GPS receiver contained in a removable module. The manufacturer's specifications have been used to determine specific operating limitations as described in Table 1.

The antenna splitter is a commercial product designed for the purpose of providing two GPS receivers with the signal from a common antenna. Tests have been performed to verify the continued proper function of the navigational GPS receiver. Further tests will be performed in accordance with Subpart and F as described in the Test Plan, Test F1.

Applicable Regulations

Sec. 23.603

Materials and workmanship.

- (a) The suitability and durability of materials used for parts, the failure of which could adversely affect safety, must--
 - (1) Be established by experience or tests;
 - (2) Meet approved specifications that ensure their having the strength and other properties assumed in the design data, and;
 - (3) Take into account the effects of environmental conditions, such as temperature and humidity, expected in service.
- (b) Workmanship must be of a high standard.

Sec. 23.605

Fabrication methods.

- (a) The methods of fabrication used must produce consistently sound structures. If a fabrication process (such as gluing, spot welding, or heat-treating) requires close control to reach this objective, the process must be performed under an approved process specification.
- (b) Each new aircraft fabrication method must be substantiated by a test program.

Sec. 23.1301

Function and installation.

Each item of installed equipment must--

- (a) Be of a kind and design appropriate to its intended function;
- (b) Be labeled as to its identification, function, or operating limitations, or any applicable combination of these factors, and;
- (c) Be installed according to limitations specified for that equipment.

Substantiation Report (continued)

Subpart F, Equipment Sec. 23.1309

The Global Positioning Data Recorder is designed purely for the purpose of collecting kinematic data for empirical research. It will not be used to provide information to the crew. It will not be used as a safety device. Compliance with Sec. 23.1309 is therefore limited to any possible effects that the GPDR may have on other aircraft systems.

Possible Modes of Failure

- (a) electromagnetic interference with navigational or communication equipment
- (b) interruption of the operation of the navigational GPS receiver through structural failure of the cable assembly

Electromagnetic interference will be assessed through ground testing in accordance with Subpart F as described in the Test Plan, Test F1.

The integrity of the cable assembly, including the strength of the TNC male to male adaptor, will be assessed through loading in accordance with Subpart C as described in the Test Plan, Test C2.

Applicable Regulations (continued)

Sec. 23.1309

Equipment, systems, and installations.

- (b) The design of each item of equipment, each system, and each installation must be examined separately and in relationship to other airplane systems and installations to determine if the airplane is dependent upon its function for continued safe flight and landing and, for airplanes not limited to VFR conditions, if failure of a system would significantly reduce the capability of the airplane or the ability of the crew to cope with adverse operating conditions. Each item of equipment, each system, and each installation identified by this examination as one upon which the airplane is dependent for proper functioning to ensure continued safe flight and landing, or whose failure would significantly reduce the capability of the airplane or the ability of the crew to cope with adverse operating conditions, must be designed to comply with the following additional requirements:
 - (1) It must perform its intended function under any foreseeable operating condition.
 - (2) When systems and associated components are considered separately and in relation to other systems--
 - (i) The occurrence of any failure condition that would prevent the continued safe flight and landing of the airplane must be extremely improbable, and;
 - (ii) The occurrence of any other failure condition that would significantly reduce the capability of the airplane or the ability of the crew to cope with adverse operating conditions must be improbable.
 - (3) Warning information must be provided to alert the crew to unsafe system operating conditions and to enable them to take appropriate corrective action. Systems, controls, and associated monitoring and warning means must be designed to minimize crew errors that could create additional hazards.

5/14

Substantiation Report (continued)

Other Possible Modes of Failure

- (a) GPDR software failure
- (b) GPDR disk write error due to vibration or excessive loading

These possible modes of failure pertain primarily to the intended operation of the GPDR. While some refinement of the operation of the portable computer may be required, this will in no way affect other aircraft systems.

Subpart F, Equipment Sec. 23.1357 Sec. 23.1365

The GPDR processor will draw power through a 5 A dedicated circuit breaker and associated electric connecting cable originally installed to provide power to a TCAS processor that drew nominally 1.8 A. The GPDR processor will draw an identical amount of power through the existing cable. The GPDR processor includes redundant internal fuses for added protection.

Applicable Regulations (continued)

- (4) Compliance with the requirements of paragraph (b)(2) of this section may be shown by analysis and, where necessary, by appropriate ground, flight, or simulator test. The analysis must consider--
 - (i) Possible modes of failure, including malfunctions and damage from external sources;
 - (ii) The probability of multiple failures and the probability or undetected faults;
 - (iii) The resulting effects of the airplane and occupants, considering the stage of flight and operating conditions, and;
 - (iv) The crew warning cues, corrective action required, and the crew's capability of determining faults.

Sec. 23.1357

Circuit protective devices.

- (a) Protective devices, such as fuses or circuit breakers, must be installed in all electrical circuits other than--
 - (1) Main circuits of starter motors used during starting only, and;
 - (2) Circuits in which no hazard is presented by their omission.

Sec. 23.1365

Electric cables and equipment.

- (a) Each electric connecting cable must be of adequate capacity.

Test Plan

- Rev. 1, 23 Aug 00

Subpart C, Structure

Sec. 23.303

Sec. 23.305

Sec. 23.307

The maximum positive vertical load factor of the Jetstream 31 is 3.05g. The weight of the GPDR processor is 11 pounds. The weight of the antenna splitter is 0.3 pounds.

Test C1: When installed, the GPDR processor will be shown to withstand a force applied vertically down of no less than 50 pounds without permanent deformation of the processor structure or separation from the tray.

Test C2: When installed, the combined structure of the antenna splitter, TNC male to male elbow adaptor, and GPS antenna will be shown to withstand a force applied vertically down at the centre of the antenna splitter of no less than 1.5 pounds without permanent deformation of the structure at any location.

Tests C1 and C2 will be performed at the time of installation.

Applicable Regulations

Sec. 23.303

Factor of safety.

Unless otherwise provided, a factor of safety of 1.5 must be used.

Sec. 23.305

Strength and deformation.

- (a) The structure must be able to support limit loads without detrimental, permanent deformation. At any load up to limit loads, the deformation may not interfere with safe operation.
- (b) The structure must be able to support ultimate loads without failure for at least three seconds, except local failures or structural instabilities between limit and ultimate load are acceptable only if the structure can sustain the required ultimate load for at least three seconds. However, when proof of strength is shown by dynamic tests simulating actual load conditions, the three second limit does not apply.

Sec. 23.307

Proof of structure.

- (a) Compliance with the strength and deformation requirements of Sec. 23.305 must be shown for each critical load condition. Structural analysis may be used only if the structure conforms to those for which experience has shown this method to be reliable. In other cases, substantiating load tests must be made. Dynamic tests, including structural flight tests, are acceptable if the design load conditions have been simulated.

Test Plan (continued)

Subpart F, Equipment

Sec. 23.1301

Sec. 23.1309

Sec. 23.1431

Test F1: After installation of the GPDR equipment, the normal operation of the navigational GPS receiver will be verified in accordance with chapter 2.4 of the Bendix / King KLN 89/89B GPS RNAV Installation Manual, Revision 3, May, 1999.

Test F2: This test has been deleted.

Test F3: After the first flight, the data collected by the GPDR processor will be examined to verify its intended function.

Applicable Regulations (continued)

Sec. 23.1301

Function and installation.

Each item of installed equipment must--

(d) Function properly when installed.

Sec. 23.1309

Equipment, systems, and installations.

(a) Each item of equipment, each system, and each installation:

(1) When performing its intended function, may not adversely affect the response, operation, or accuracy of any--

(i) Equipment essential to safe operation, or;

(ii) Other equipment unless there is a means to inform the pilot of the effect.

(2) In a single-engine airplane, must be designed to minimize hazards to the airplane in the event of a probable malfunction or failure.

(3) In a multi-engine airplane, must be designed to prevent hazards to the airplane in the event of a probable malfunction or failure.

(4) In a commuter category airplane, must be designed to safeguard against hazards to the airplane in the event of their malfunction or failure.

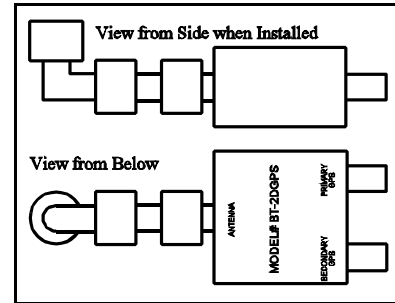
Sec. 23.1431

Electronic equipment.

(a) In showing compliance with Sec. 23.1309(b)(1) and (2) with respect to radio and electronic equipment and their installations, critical environmental conditions must be considered.

(b) Radio and electronic equipment, controls, and wiring must be installed so that operation of any unit or system of units will not adversely affect the simultaneous operation of any other radio or electronic unit, or system of units, required by this chapter.

1. The GPS antenna is located just forward of the cockpit bulkhead, directly overhead. Remove the overhead cockpit circuit breaker panel to gain access to the antenna.
2. There is one coaxial cable attached to the GPS antenna with a male TNC connector. This cable leads to the GPS receiver. Detach the receiver coaxial cable.



Antenna Splitter Assembly

3. Attach the TNC male adaptor of the antenna splitter assembly to the GPS antenna.

Test C2: When installed, the combined structure of the antenna splitter, TNC male to male elbow adaptor, and GPS antenna will be shown to withstand a force applied vertically down at the centre of the antenna splitter of no less than 1.5 pounds without permanent deformation of the structure at any location.

4. Perform Test C2. (Refer to Detailed Test Plan.) Pass / Fail: _____
5. Attach the receiver coaxial cable to the antenna splitter “Primary GPS” connector.
6. The TCAS directional antenna is located just aft of the cockpit bulkhead, directly overhead. Remove the overhead cabin panelling to gain access to the antenna.
7. There are four coaxial cables attached to the TCAS directional antenna with male TNC connectors. The forward connector is colour coded yellow. Detach the yellow coaxial cable.
8. Draw the yellow coaxial cable forward. Attach the yellow coaxial cable to the “Secondary GPS” connector on the antenna splitter.
9. Replace the overhead cabin panelling and the circuit breaker panel.
10. Install the GPDR processor in the TCAS processor tray just aft of the R/H passenger seats. Use the TCAS processor hold-downs to secure the GPDR processor in place.

Test C1: When installed, the GPDR processor will be shown to withstand a force applied vertically down of no less than 50 pounds without permanent deformation of the processor structure or separation from the tray.

11. Perform Test C1. (Refer to Detailed Test Plan.) Pass / Fail: _____

Detailed Test Plan

- Rev. 1, 23 Aug 00

Tests C1 and C2 are to be conducted during the installation procedure. (Refer to Installation Instructions.)

Test C1: When installed, the GPDR processor will be shown to withstand a force applied vertically down of no less than 50 pounds without permanent deformation of the processor structure or separation from the tray.

Place the 50 pound distributed test mass (P/N SP-T01120700) on the top surface of the GPDR processor. Verify that no permanent deformation results. Remove the test mass and examine the structure for signs of deformation.

Pass / Fail: _____

Comments:

Test C2: When installed, the combined structure of the antenna splitter, TNC male to male elbow adaptor, and GPS antenna will be shown to withstand a force applied vertically down at the centre of the antenna splitter of no less than 1.5 pounds without permanent deformation of the structure at any location.

Attach the 1.5 pound inline test mass (P/N SP-T02120700) to the primary and secondary outputs of the antenna splitter. Allow the test mass to hang supported only by the antenna and splitter assembly. Verify that no permanent deformation results. Remove the test mass and examine the structure for signs of deformation.

Pass / Fail: _____

Comments:

Test F1 will be conducted after the installation is complete with the aircraft parked in a location offering a clear view of the sky.

Test F1: After installation of the GPDR equipment, the normal operation of the navigational GPS receiver will be verified in accordance with chapter 2.4 of the Bendix / King KLN 89/89B GPS RNAV Installation Manual, Revision 3, May, 1999.

The following tests will be conducted with the GPDR equipment installed and energized. These tests include provisions to verify the absence of EMI/RFI and to verify the proper function of the GPS receiver and associated peripherals.

The following is an excerpt from chapter 2.4 of the Bendix / King KLN 89/89B GPS RNAV Installation Manual, Revision 3, May, 1999:

2.4.3 INSTALLATION CHECK OUT

- C. Manipulate the controls as necessary to display the Set 1 Page on the right half of the screen.

On the Set 1 Page, enter the airport name or the present position (latitude and longitude) for the installation location accurate to within 60 nautical miles.

Display the Set 2 Page. Verify that the date and time are correct to within 10 minutes and update if necessary.

Pass / Fail: _____

Comments:

- D. At this point the aircraft will have to be moved to a location known to have reasonable GPS signal coverage. This implies an outside location away from tall structures that could mask low elevation satellites. (To speed up the next test it is helpful to turn unit power off then on again once the system is away from structures.)

- E. Proceed to the 0TH 1 page. The State shown on the display should change to Acquire (ACQ) from INIT and after a period of not more than 5 minutes, (typically two minutes depending on the satellite coverage,) the unit should display Latitude and Longitude values on the Nav 2 Page that are correct for the installation location. If the unit has not been turned on for 6 months, the unit will take up to 20 minutes to calculate a position.

Pass / Fail: _____

Comments:

- F. Select the 0TH 2 page, verify that no asterisks appear next to any satellite with an elevation greater than 25°. Select 121.15 MHz on COMM 1. Transmit on COMM 1 for a period of 20 seconds and verify that no asterisks appear indicating satellites with an elevation of greater than 25°. Repeat for the following frequencies 121.175, 121.20, 131.250, 131.275 and 131.30 MHz. Repeat the above procedure for all VHF COMM's on board the aircraft.

Pass / Fail: _____

Comments:

2.4.4 INTEGRATED INSTALLATION CHECK OUT

The following paragraphs define checkout procedures for all possible Input/Output signals that can be connected to the KLN 89/89B. It should be clearly determined which of the signals are intended to be used in any given installation and then only the paragraphs pertaining to those signals should be performed.

2.4.4.1 All Installations

Perform all steps defined in Paragraph 2.4.3 and leave the system energized with a valid GPS signal being received.

2.4.4.2 CDI/HSI Interface

Cycle the power on the KLN 89/89B which will cause the self test page to be displayed. Verify that the CDI needle, after it has settled, is indicating half scale right deflection. Verify that the TO/FROM flag is indicating FROM. Verify that the nav flag is pulled from view.

Pass / Fail: _____

Comments:

Verify the selected course from the CDI/HSI is interfaced properly to the KLN 89/89B in the OBS Mode.

Pass / Fail: _____

Comments:

You must create an active waypoint on the Flightplan 0 page to check the following function. The OBS/LEG selection is controlled through the OBS button located on the front panel of the KLN 89/89B. Pressing this button toggles between LEG and OBS with the normal position being LEG. During OBS mode, the LEG indication (located left of the vertical page divider) will change to a three digit course value.

Pass / Fail: _____

Comments:

Verify that the selected course value agrees with the value displayed on the HSI Course Pointer. Change the selected course value on the HSI or CDI using the OBS knob. Verify that the selected course value displayed on the KLN 89/89B tracks the new value selected.

Pass / Fail: _____

Comments:

In the OBS mode with the GPS displayed on the CDI/HSI, the resolver is disconnected from the NAV converter. Verify that the KNS 80 or 81 groundspeed is still functional and the Radial display for the KX 165 or KNS 81 is still functional. These units must have jumpers or resistors across them when the resolver is removed.

Pass / Fail: _____

Comments:

In the OBS mode with the GPS not displayed on the CDI/HSI the resolver is reconnected to the NAV converter. Verify that change in the OBS resolver will not affect the selected OBS on the KLN 89/89B.

Pass / Fail: _____

Comments:

2.4.4.3 Gray Code Altitude Inputs

With gray code altitude being supplied by a compatible encoding altimeter, verify that the proper altitude is indicated on the ALT page (provided no other altitude sources are active and that proper baro setting has been entered).

Pass / Fail: _____

Comments:

Verify that there is no interference between the KLN 89/89B, transponder, and any other loads on the encoding altimeter output. Remove power from each of the loads on the encoder to verify that the remaining equipment still performs properly. If interference exists, one or more of the units are not diode isolated and isolation diodes will need to be added to the aircraft wiring.

Pass / Fail: _____

Comments:

2.4.4.7 External Annunciators

Recycle the power on the KLN 89/898 which will cause the Self Test Page to be displayed. Verify that all external annunciators are energized. Cycle the KLN 89/89B display past all initialization pages. Verify all external annunciators are extinguished. If the message light comes on, view the Message Page to verify that there is a message. If any other annunciator remains lighted, review the status of the KLN 89/89B to determine if the lighted annunciator is justified.

This concludes the reference to chapter 2.4 of the Bendix / King KLN 89/89B GPS RNAV Installation Manual, Revision 3, May, 1999

Pass / Fail: _____

Comments:

Test F2: This test has been deleted.

Test F3: After the first flight, the data collected by the GPDR processor will be examined to verify its intended function.

This test will be performed at the University of Saskatchewan.

Pass / Fail: _____

Comments:

Master Drawing List

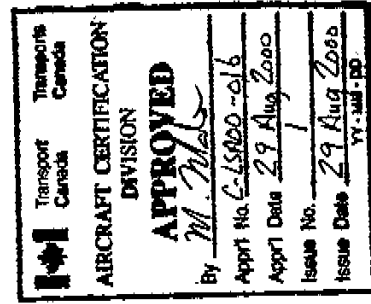
List Number L01160600 Revision B
28 Aug 2000

Stume Pinder
28 Bell Crescent
Saskatoon, SK S7J 2W3

A/C Make: Jetstream
A/C Model: 3112
A/C Serial Number: 764
A/C Registration: C-FSEW

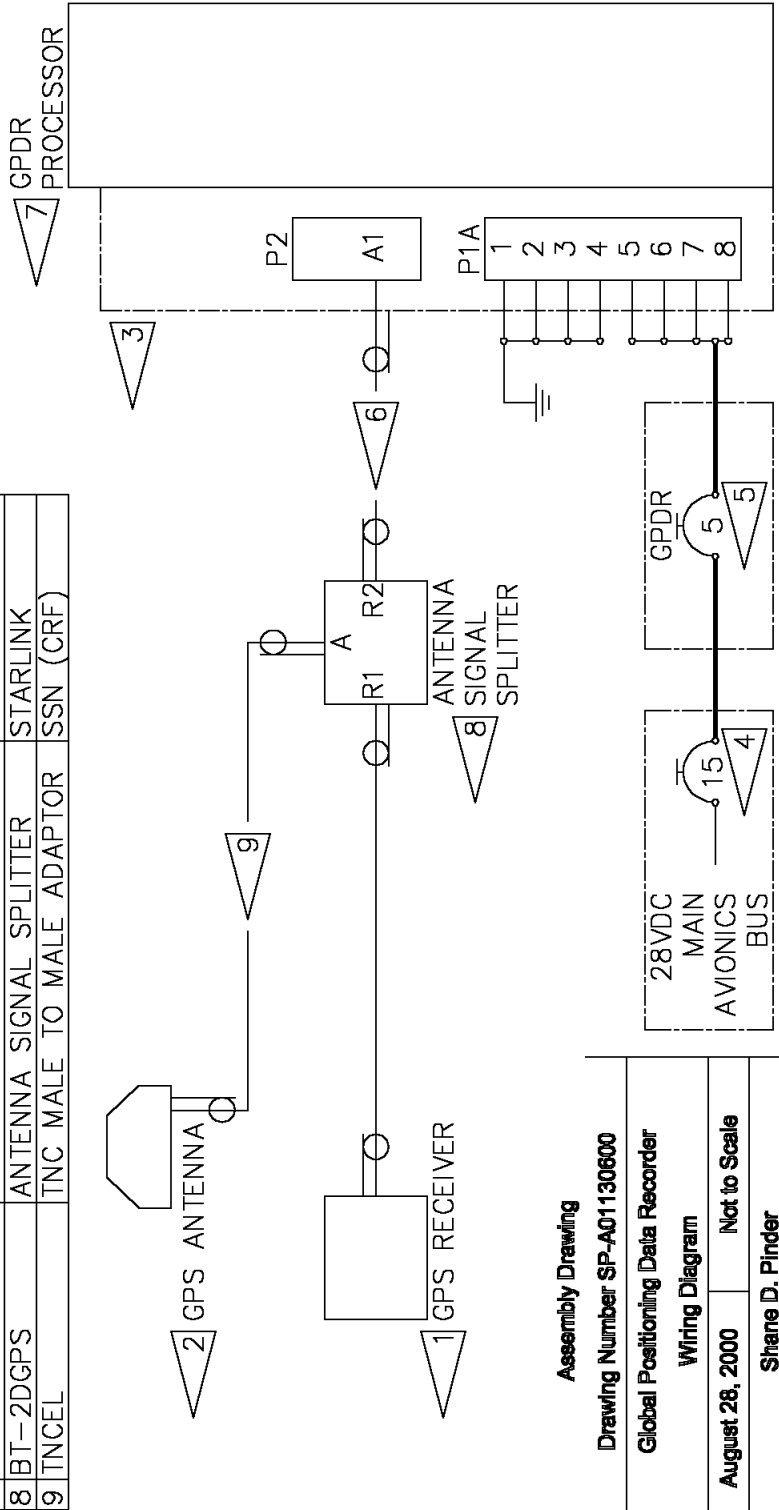
A/C Owner / Operator:
La Rouge Aviation Services Limited
Box 320
La Rouge, SK S0J 1L0

Drawing Number	Revision	Date	Type	Title
SP-A01120600	1	12 Jul 2000	Assembly	Global Positioning Data Recorder Processor Assembly
SP-A01130600	2	28 Aug 2000	Assembly	Global Positioning Data Recorder Wiring Diagram



REVISIONS	
1	Title Amended 120700
2	GPDR Breaker Named 280800

1	066-01148-0102	KLN 89B GPS RECEIVER	BENDIX/KING
2	071-01553-0200	GPS ANTENNA	BENDIX/KING
3	110119	TPU-66A INSTALLATION KIT	BENDIX/KING
4	7277-2-15	CIRCUIT BREAKER, 15 AMP	KLIXON
5	7277-2-5	CIRCUIT BREAKER, 5 AMP	KLIXON
6	00944-28Y	TCAS ANTENNA CABLE ASSY	PIC
7	SP-A01120600	GPDR PROCESSOR ASSEMBLY	SDP
8	BT-2DGPS	ANTENNA SIGNAL SPLITTER	STARLINK
9	TNCEL	TNC MALE TO MALE ADAPTOR	SSN (CRF)



Assembly Drawing

Drawing Number SP-A01130600

Global Positioning Data Recorder

Wiring Diagram

August 28, 2000 Not to Scale

Shane D. Pinder

28 Bell Crescent

Saskatoon, SK S7J 2W3

REVISIONS	
1	Holddown Detail Corrected 120700

Assembly Drawing

Drawing Number SP-A01120600

Global Positioning Data Recorder Processor

Mechanical Assembly

July 12, 2000 1 : 3

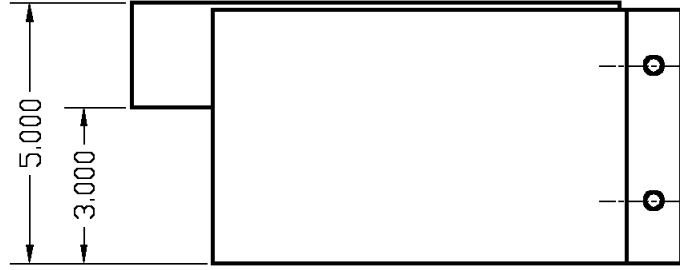
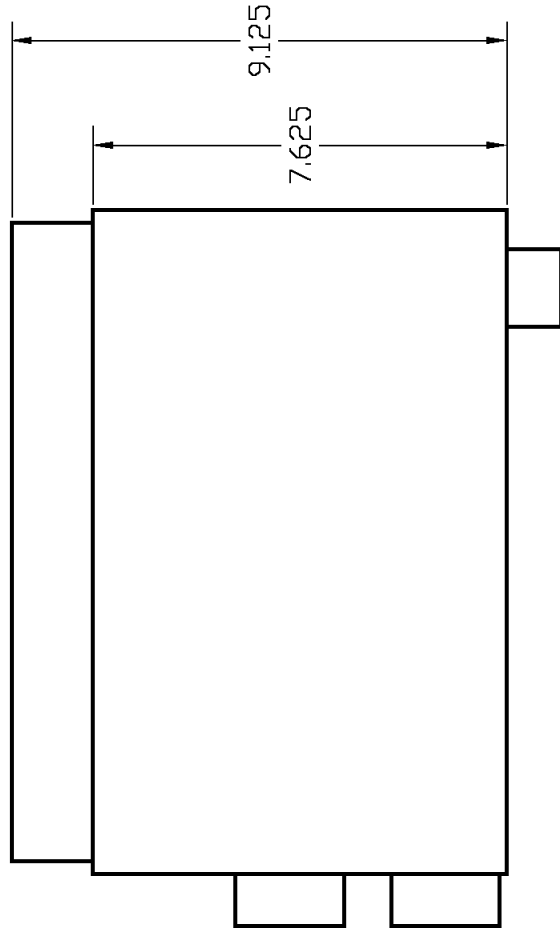
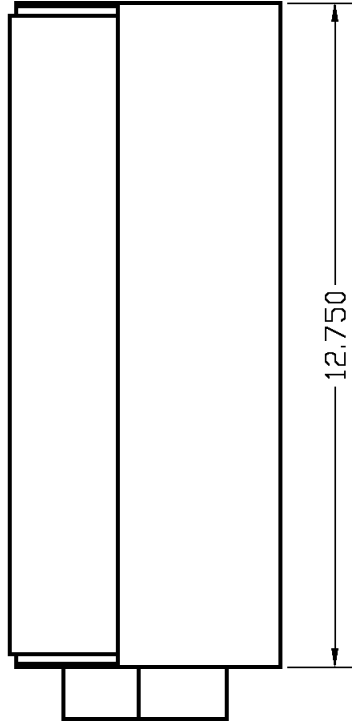
Shane D. Pindler

28 Bell Crescent

Saskatoon, SK S7J 2W3

All Dimensions in Inches

All Tolerances $+0.000$
 -0.125



Appendix III - Antenna Splitter Evaluation

A critical component of the Global Positioning Data Recorder system was a signal splitter that was used to share the signal from the existing aircraft GPS antenna. Because a failure of this component could result in the loss of the navigational GPS receiver used by the pilot, it was necessary to show that the use of the signal splitter would not risk degraded performance. This appendix describes the test that was performed to evaluate the antenna signal splitter.

Introduction

A simple test was performed to evaluate the integrity of a GPS antenna signal when split between two GPS receivers. The carrier to noise ratio pertaining to individual satellites was measured by two GPS receivers. A comparison was made between the carrier to noise ratio obtained while employing the signal splitter to that obtained in a single receiver configuration.

Materials and Methods

A schematic of the experimental apparatus is shown in Figure II.1.

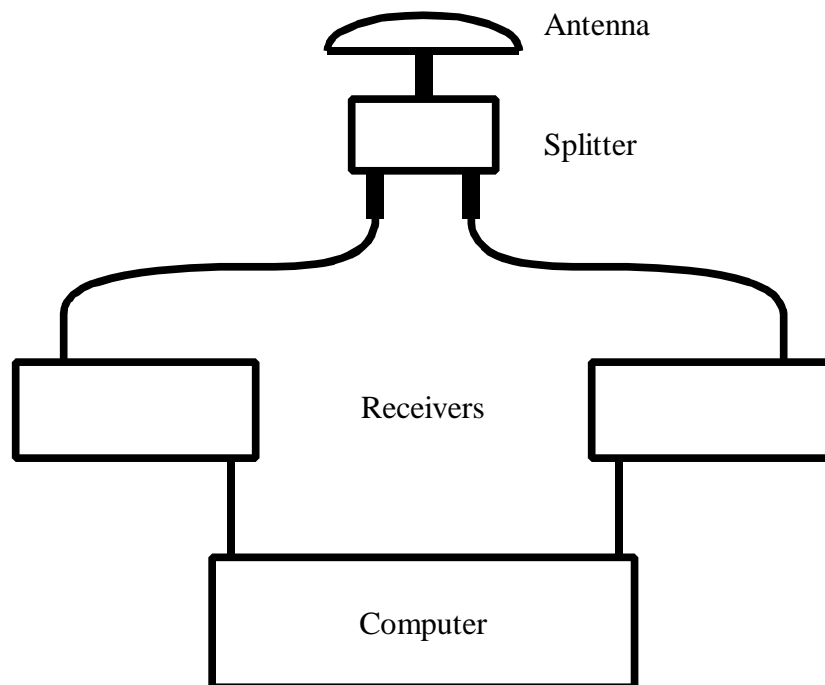


Figure II.1 Splitter Evaluation Experimental Apparatus

The equipment used for this test included two GPS receivers (NovAtel OEM2, NovAtel OEM3), a GPS antenna (NovAtel Model 531), an antenna signal splitter (Starlink BT-2DGPS), and the necessary cabling. One five-metre TNC male-to-male RG223/U coaxial cable assembly was used to connect the OEM2 receiver to the secondary GPS connection of the antenna splitter. One five-metre TNC male-to-male RG223/U coaxial cable assembly was used to connect the OEM3 receiver to the primary GPS connection of the antenna splitter. Power from this receiver was used to activate the amplification circuitry in the GPS antenna.

The GPS antenna was connected to the splitter using a TNC male-to-male adaptor. Data pertaining to channel tracking status were collected from the OEM3 receiver. After approximately ten minutes, the splitter was quickly removed from the configuration so that the OEM3 receiver was connected directly to the GPS antenna. Data collection was not interrupted during this period. After approximately ten minutes, the apparatus was returned to its original configuration. Data collection was not interrupted during this period. Data were collected for yet another ten minute period.

Results

The carrier to noise ratio pertaining to three different satellites measured by the primary GPS receiver is shown in Figures II.2, II.3, and II.4. The carrier to noise ratio was not affected by the inclusion of a GPS antenna signal splitter. From the time marked 'A' to the time marked 'B', the splitter was used to provide the signal to both receivers. From the time marked 'B' to the time marked 'C', the signal was provided directly to the

primary receiver. From the time marked 'C' to the time marked 'D', the splitter was again used to provide the signal to both receivers. Note that the carrier to noise ratio fluctuated somewhat throughout the entire period of data collection for each satellite, but that there was no appreciable difference between the period where the signal was provided directly to a single receiver and the period where the signal power was divided between two receivers.

Interpretation and Discussion

The inclusion of a signal splitter results in a theoretical signal attenuation of three decibels. The results show that this attenuation is not manifested in the measurement of the carrier to noise ratio. It was concluded that the noise present in the signal was equally attenuated, and the carrier to noise ratio was unaffected. The carrier to noise ratio pertaining to individual satellites governs the signal rejection decision in a GPS receiver. As long as the total signal attenuation between the antenna and the receiver does not exceed the manufacturer's specification, the use of a signal splitter will not adversely affect receiver performance.

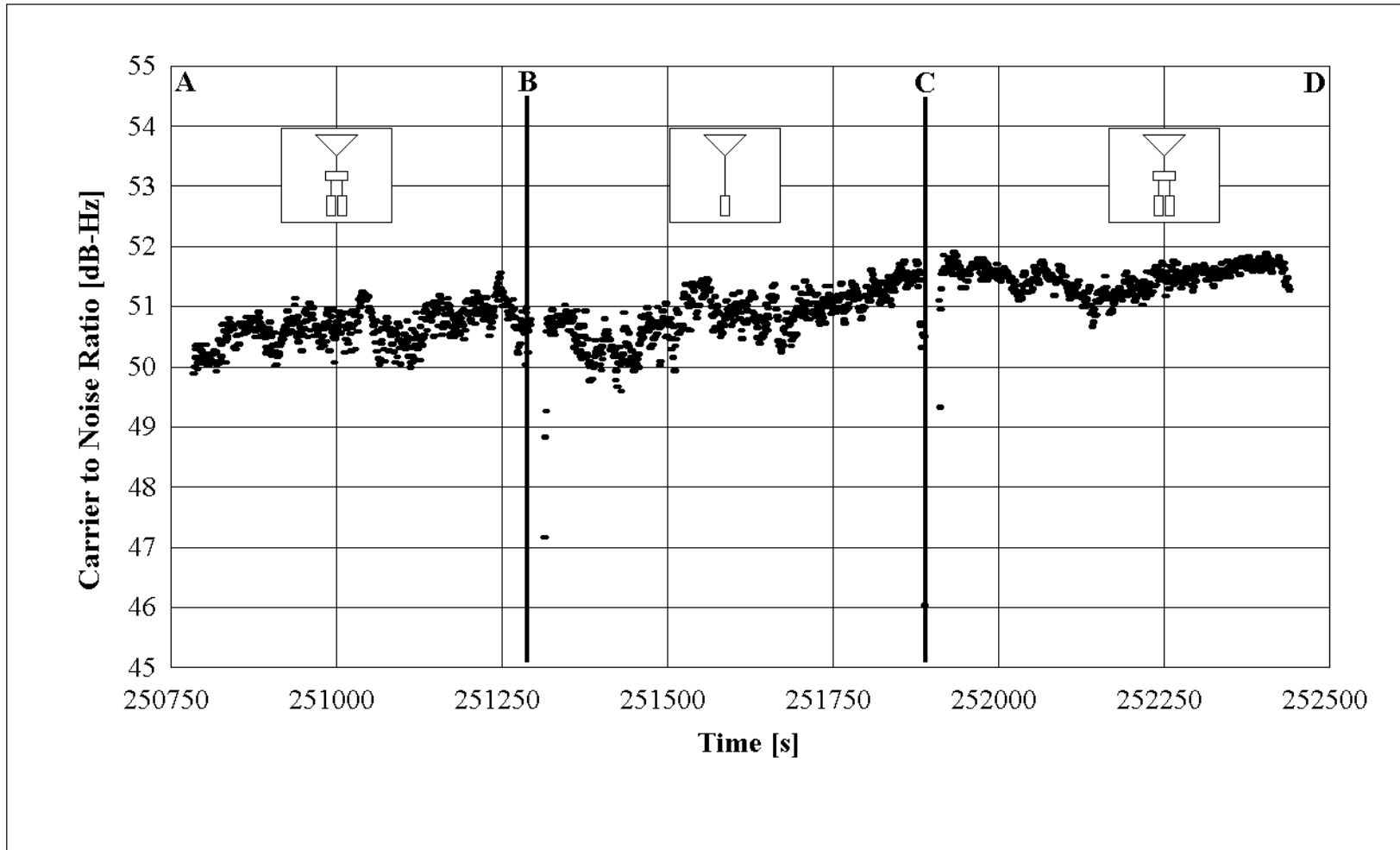


Figure II.2 The carrier to noise ratio for satellite PRN 23 was unaffected by the presence of a signal splitter

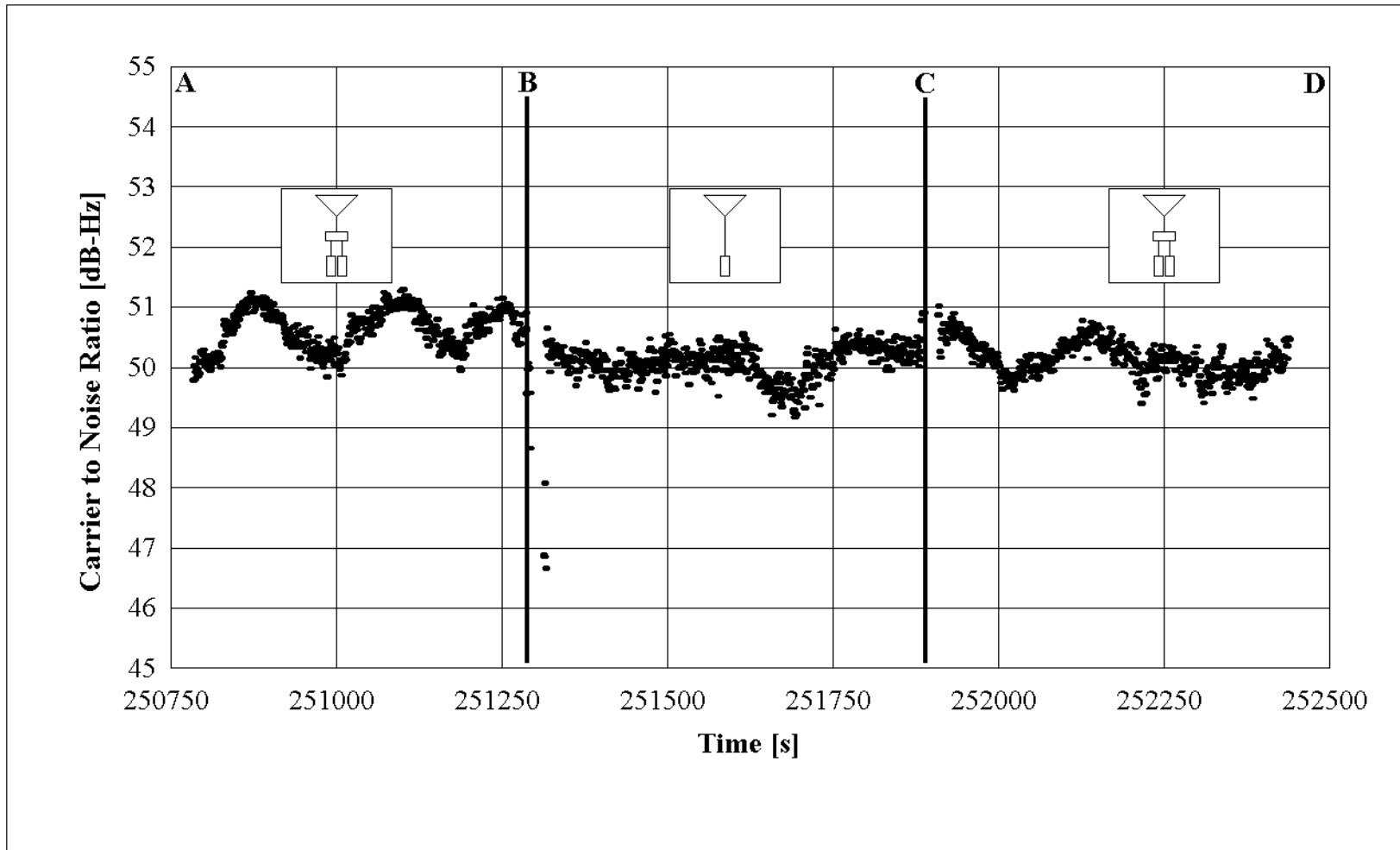


Figure II.3 The carrier to noise ratio for satellite PRN 17 was unaffected by the presence of a signal splitter

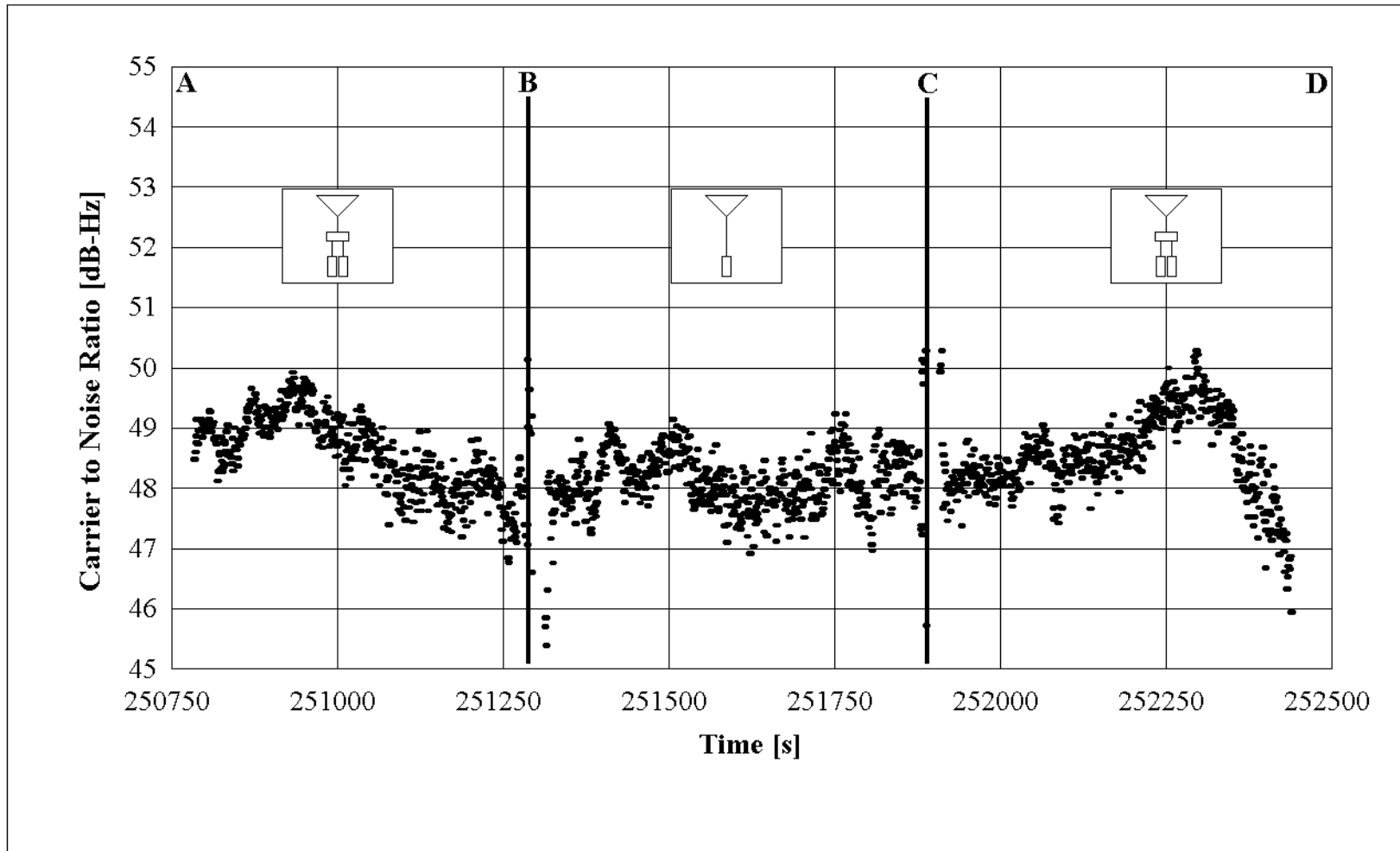
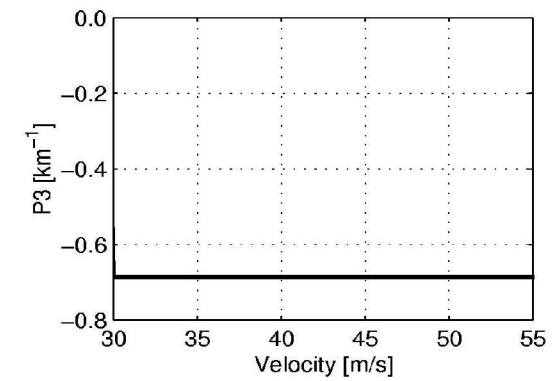
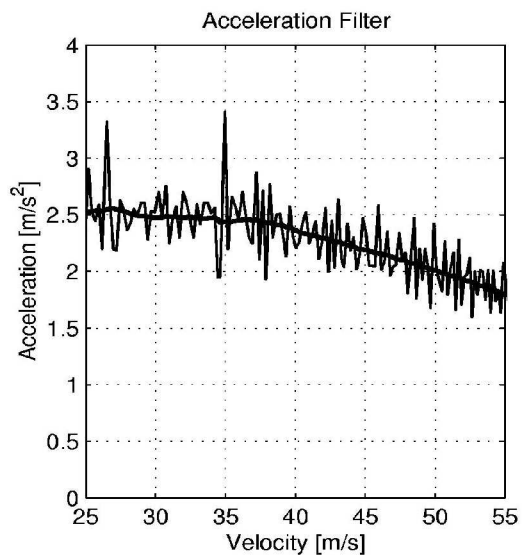
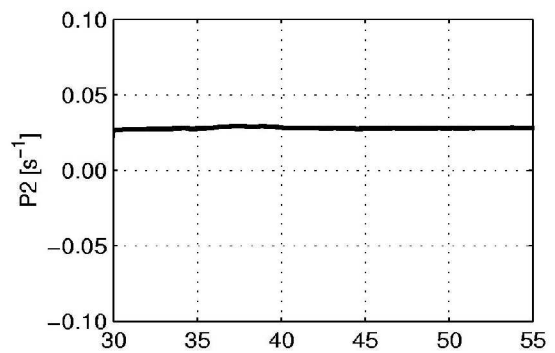
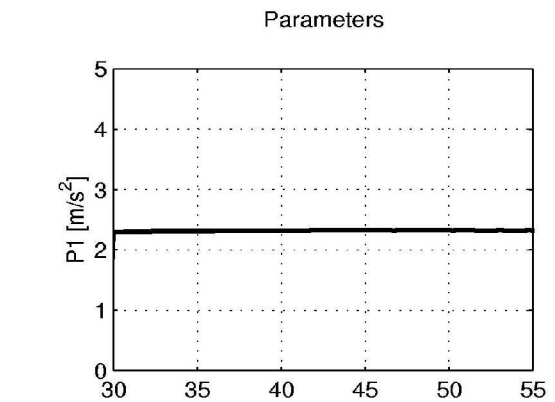
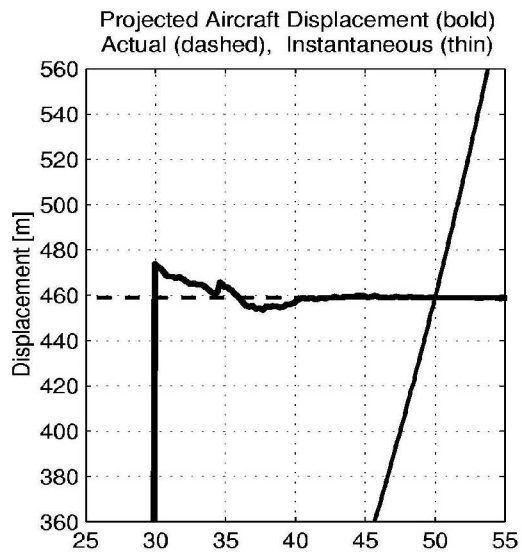


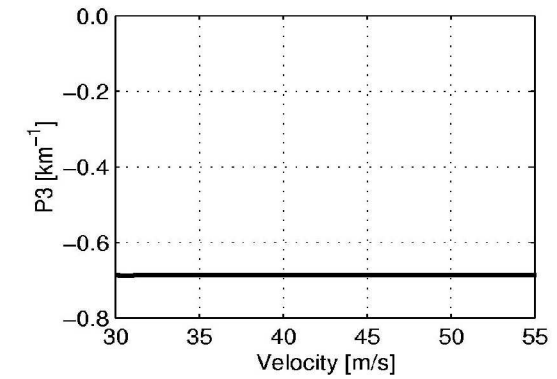
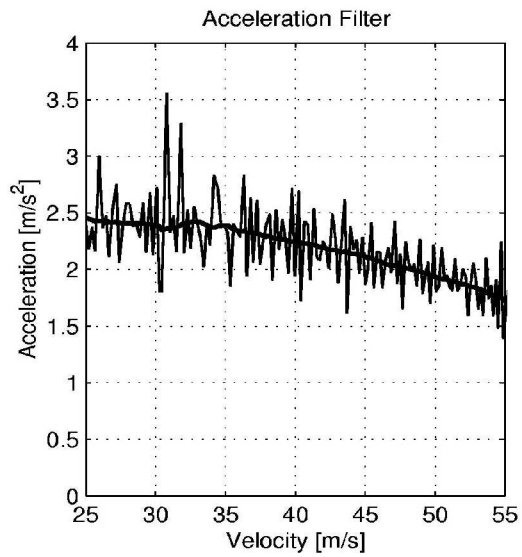
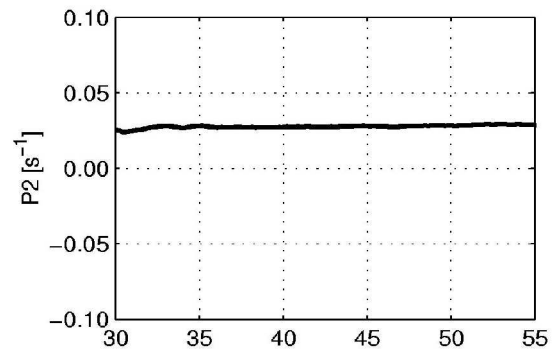
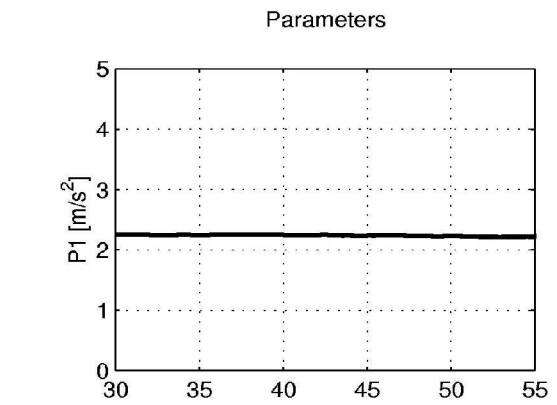
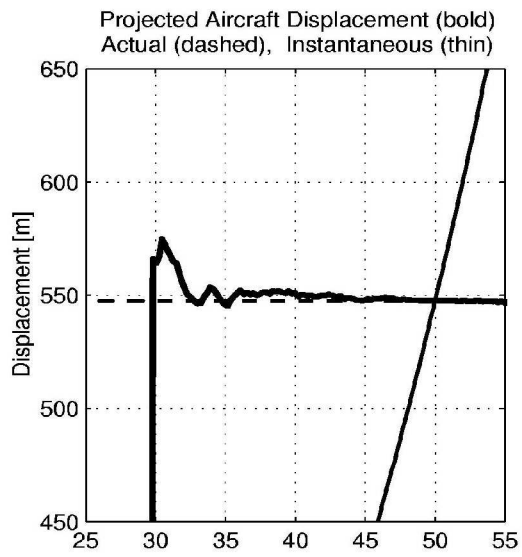
Figure II.4 The carrier to noise ratio for satellite PRN 26 was unaffected by the presence of a signal splitter

Appendix IV - Takeoffs from Runway 15, Saskatoon Airport

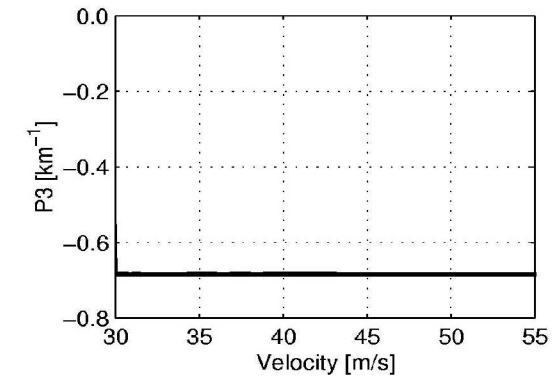
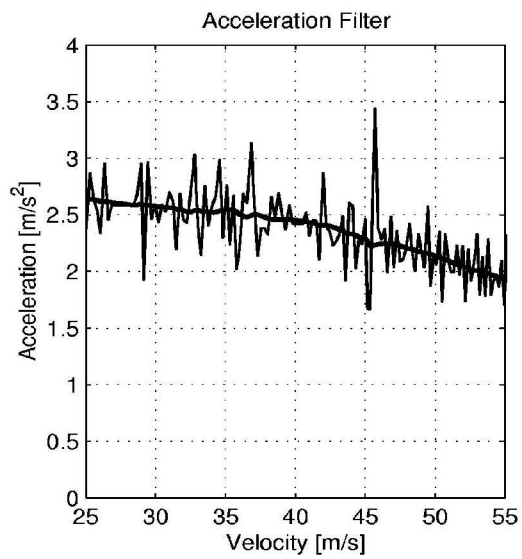
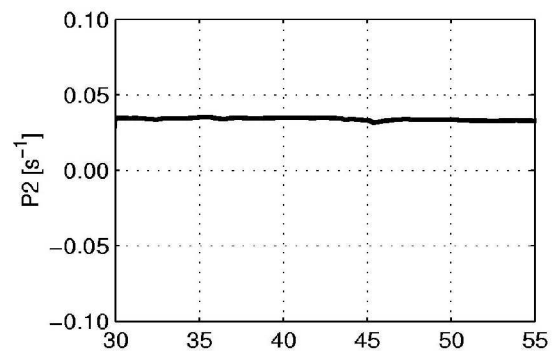
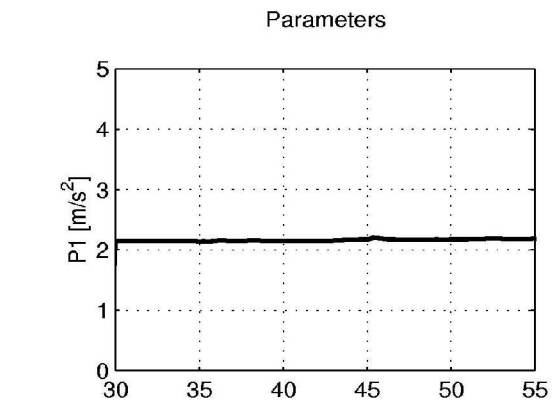
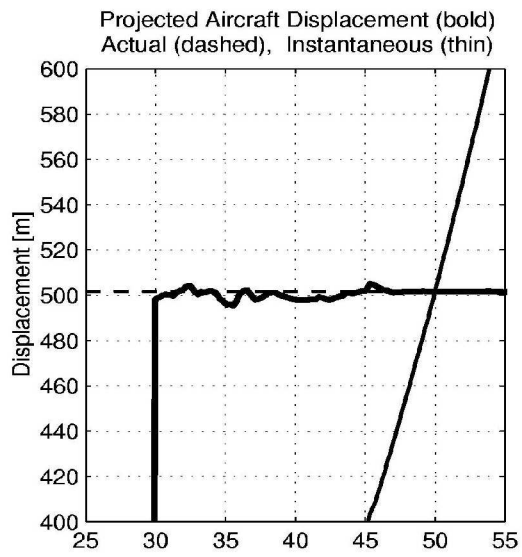
This appendix contains data pertaining to a subset of takeoffs that were recorded using the Global Positioning Data Recorder. All takeoffs within this subset took place from the same runway at Saskatoon Airport, with the same direction of departure. When comparing individual takeoffs, note that the model developed in section 4.2 specifies that each of the parameters are influenced by factors that are constant for each takeoff, such as control settings, runway slope, wind speed, and aircraft mass. Consequently, the value of each parameter should be expected to change from one takeoff to the next, but should be relatively constant for a given takeoff. A change in the value of a parameter during a takeoff could indicate a change in a control setting by the pilot, a sudden change in wind direction or speed, or a change in runway slope as the aircraft displaces.



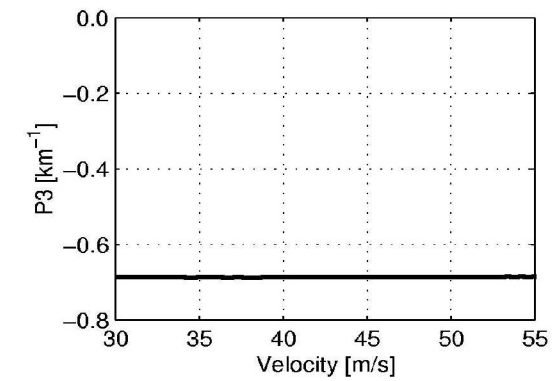
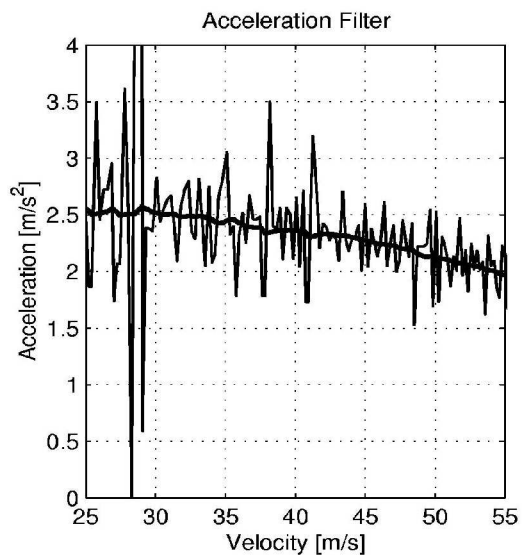
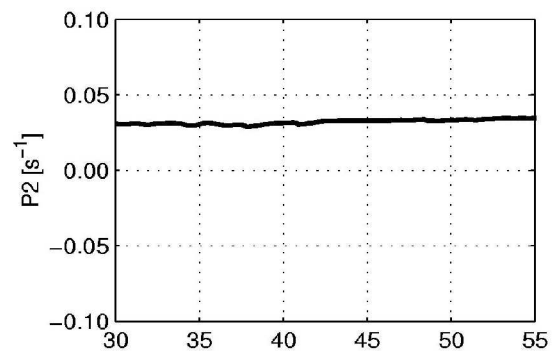
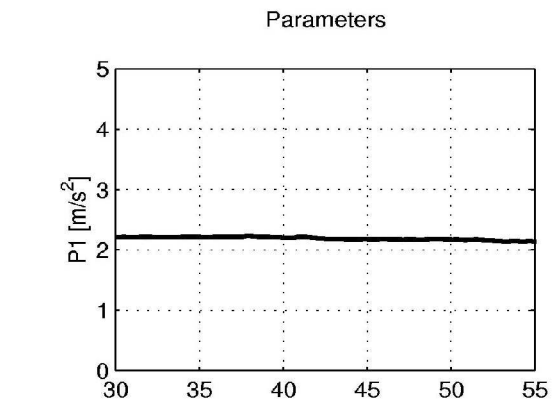
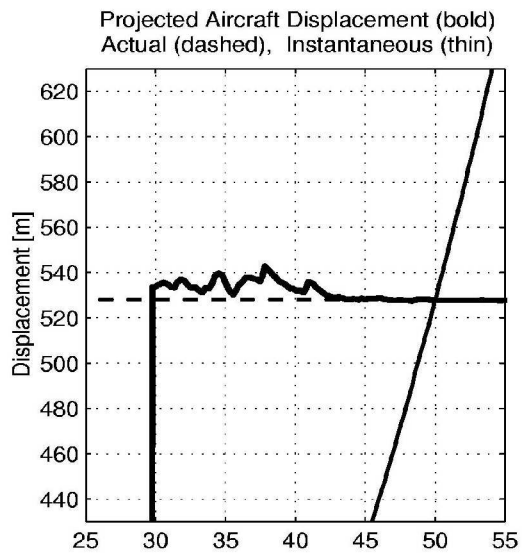
Filename: /yxe15/j06g0818.bik, Airport Identifier: cyxe, Runway: 15 Date: 06 Oct 2000 at 0708 CST



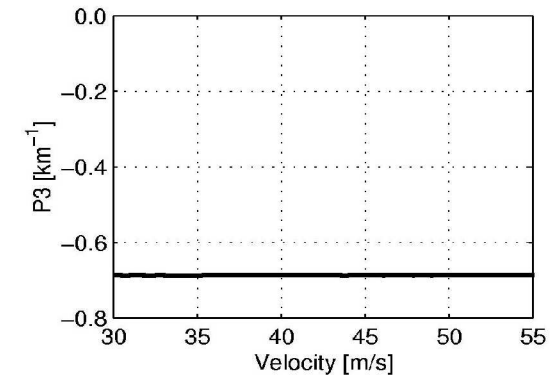
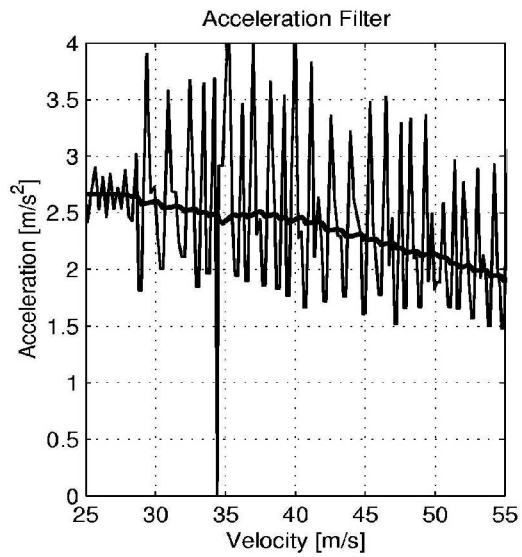
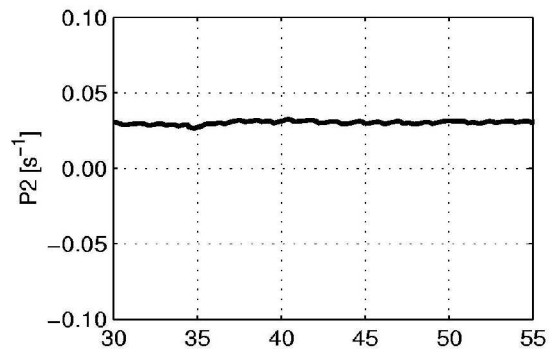
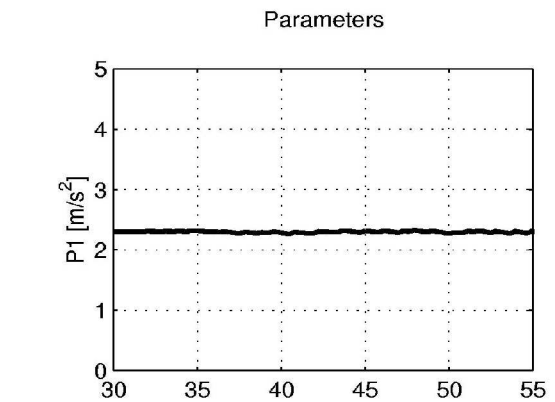
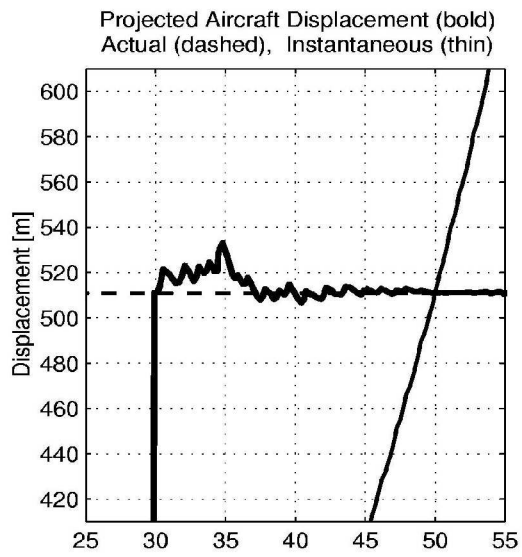
Filename: /yxe15/j18g1112.bik, Airport Identifier: cyxe, Runway: 15 Date: 18 Oct 2000 at 0711 CST



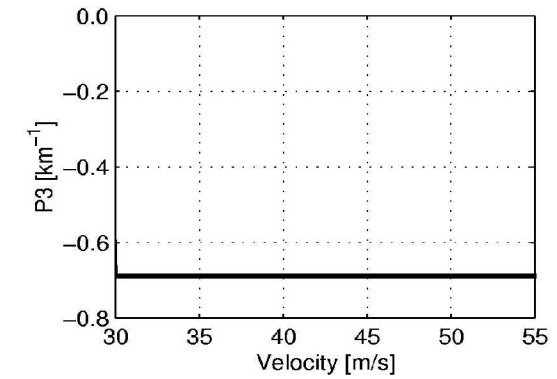
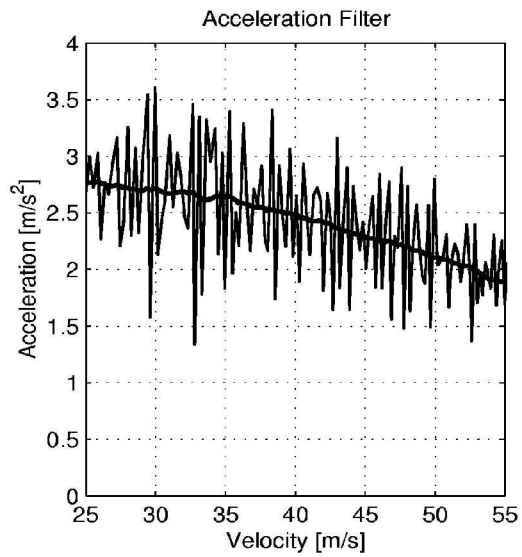
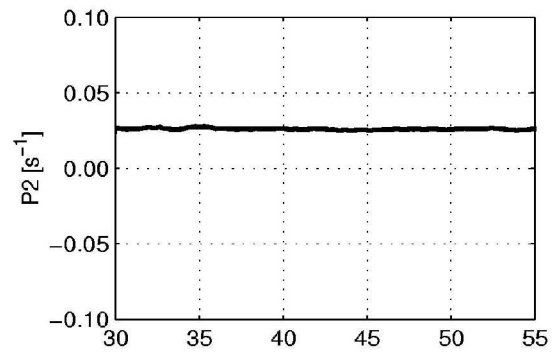
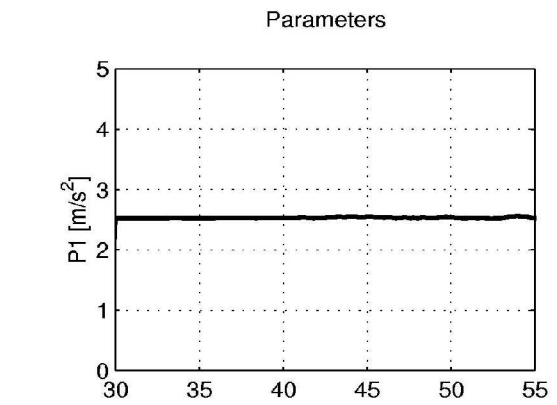
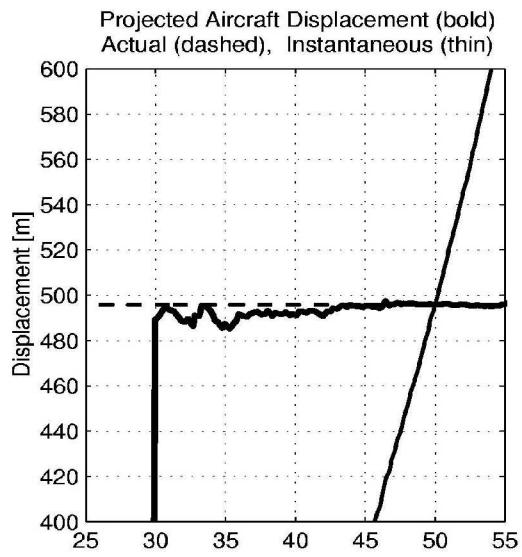
Filename: /yxe15/j24g1203.bik, Airport Identifier: cyxe, Runway: 15 Date: 24 Oct 2000 at 0712 CST



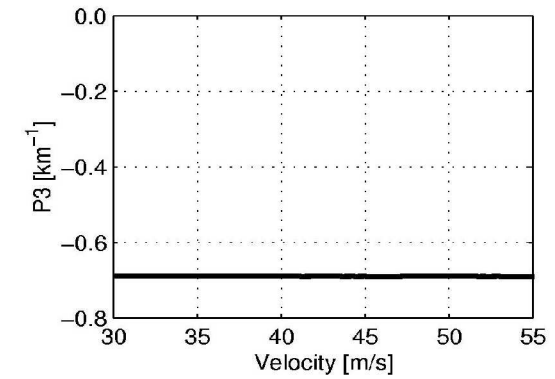
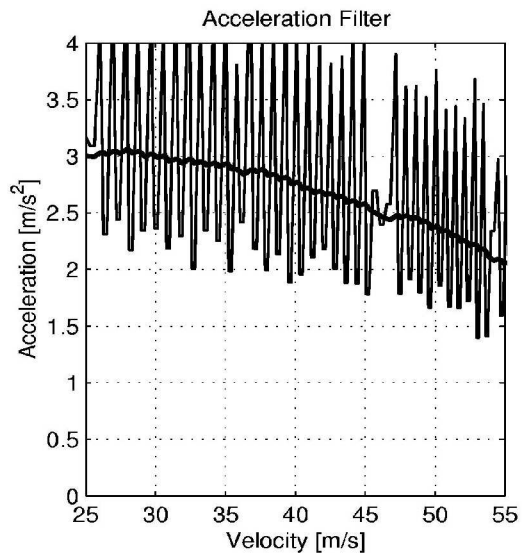
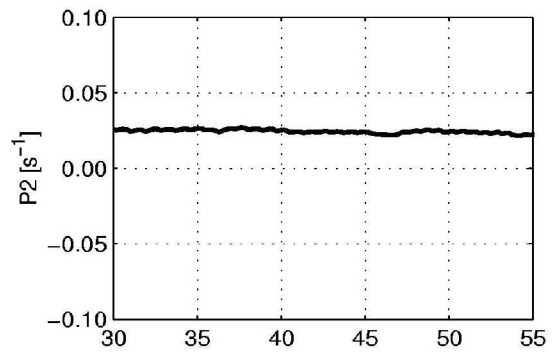
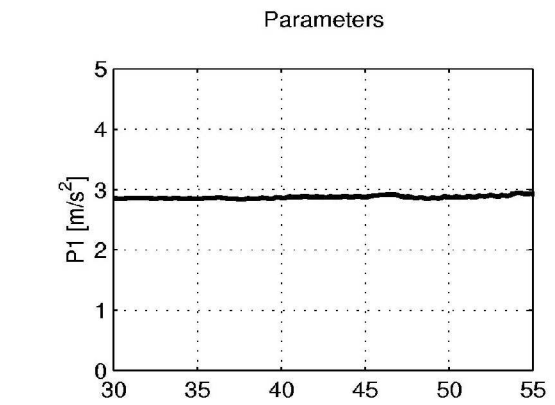
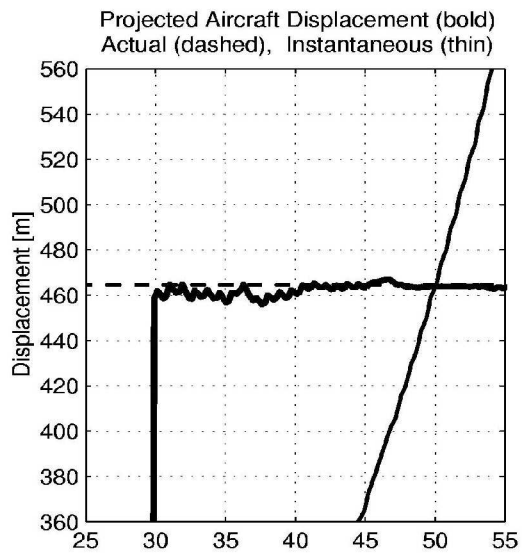
Filename: /yxe15/k01q1124.bik, Airport Identifier: cyxe, Runway: 15 Date: 01 Nov 2000 at 1711 CST



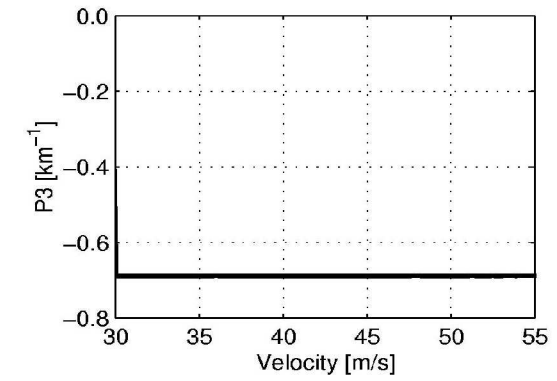
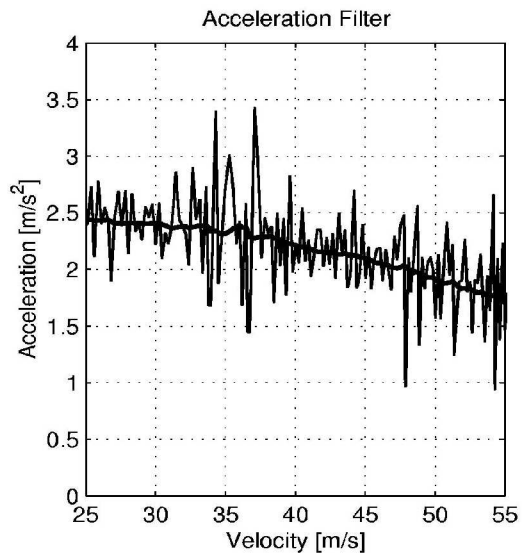
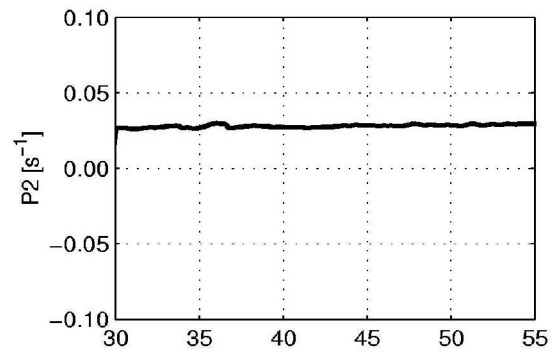
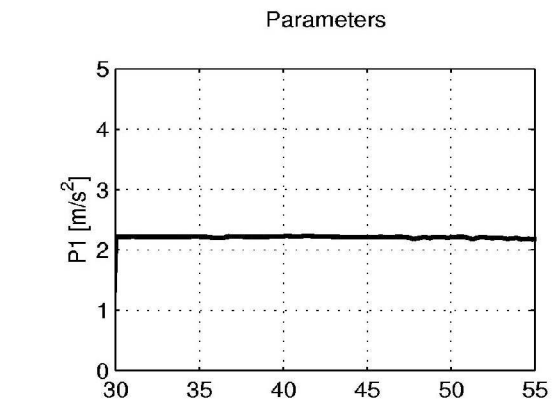
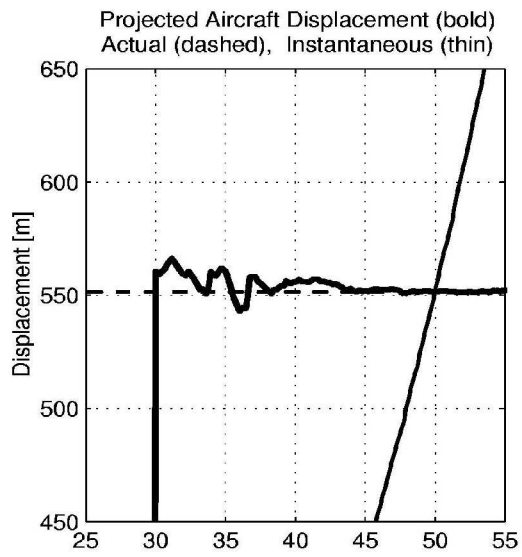
Filename: /yxe15/k03g0805.bik, Airport Identifier: cyxe, Runway: 15 Date: 03 Nov 2000 at 0708 CST



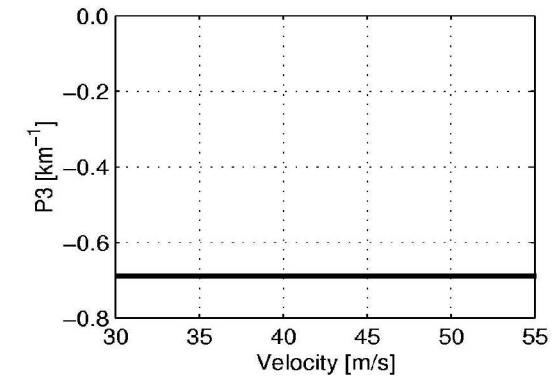
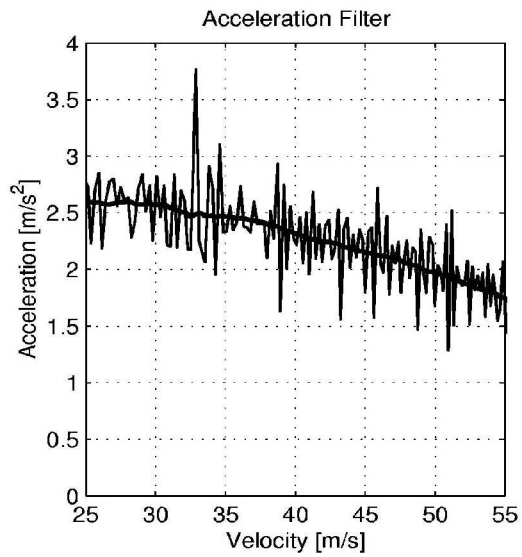
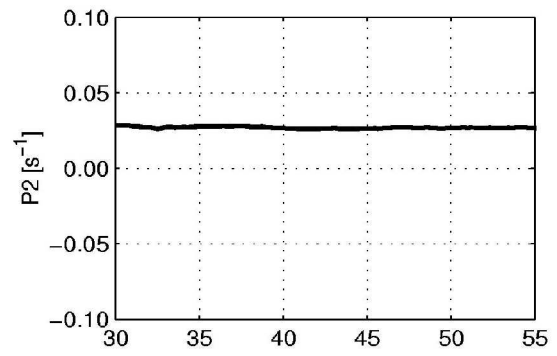
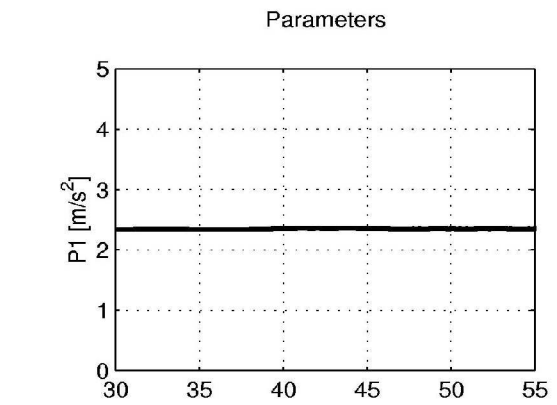
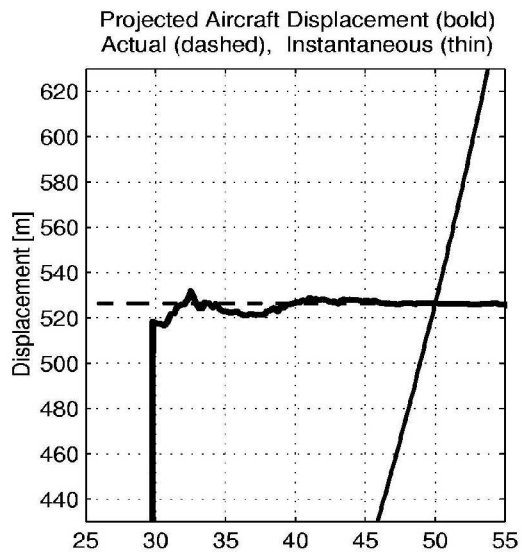
Filename: /yxe15/k27g0755.bik, Airport Identifier: cyxe, Runway: 15 Date: 27 Nov 2000 at 0707 CST



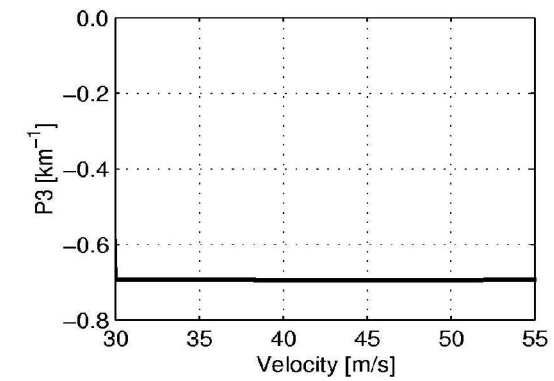
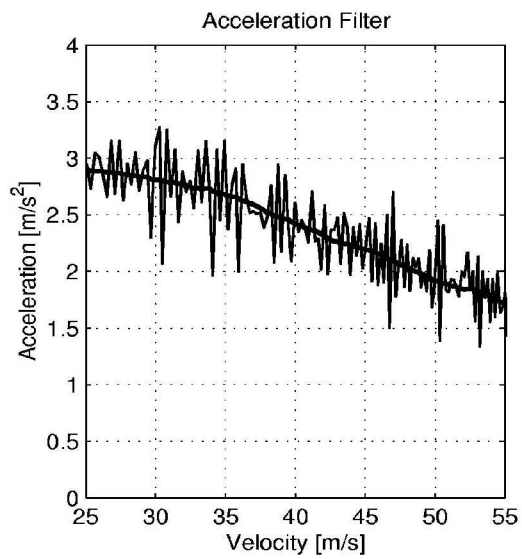
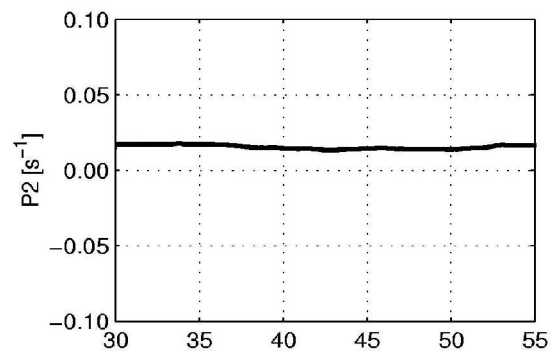
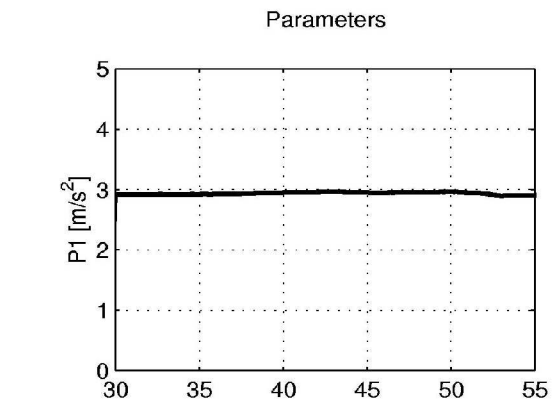
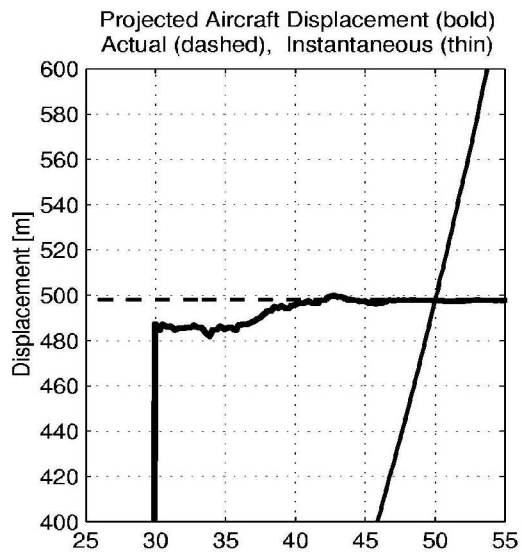
Filename: /yxe15/k28l2056.bik, Airport Identifier: cyxe, Runway: 15 Date: 28 Nov 2000 at 1220 CST



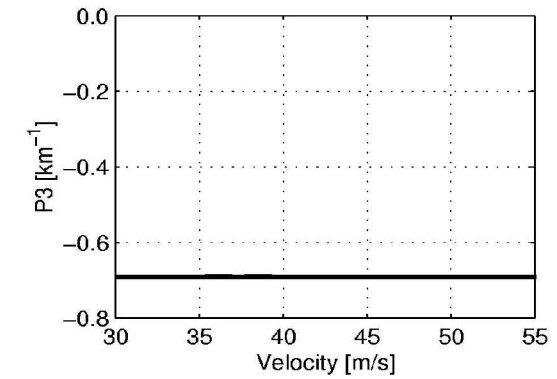
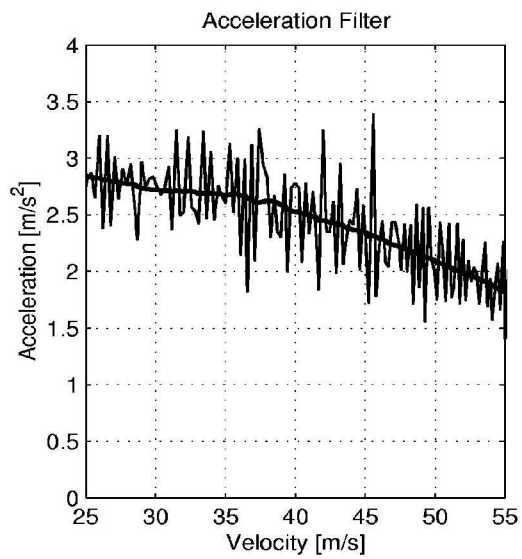
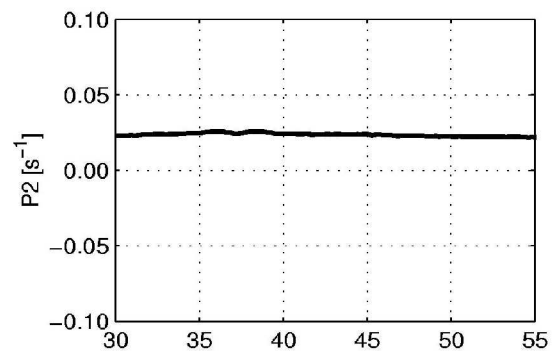
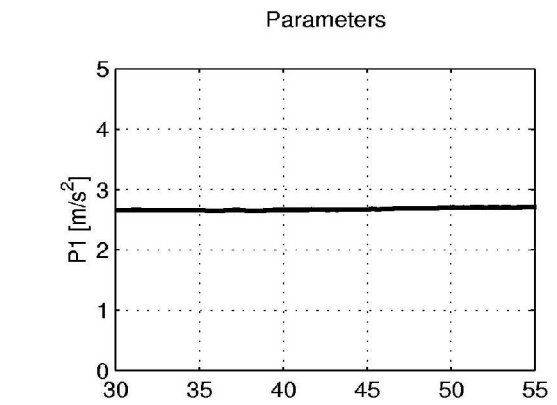
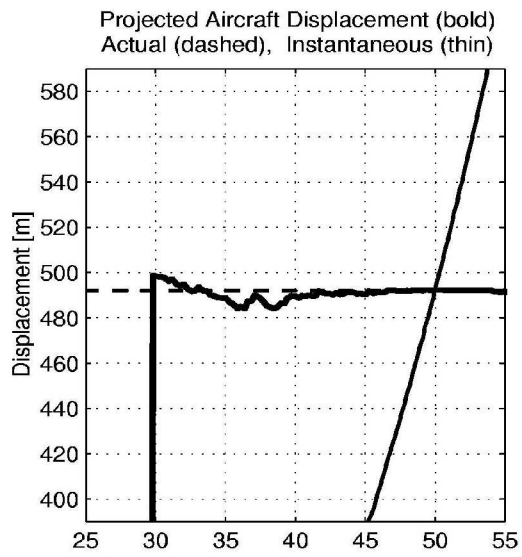
Filename: /yxe15/k29g1041.bik, Airport Identifier: cyxe, Runway: 15 Date: 29 Nov 2000 at 0710 CST



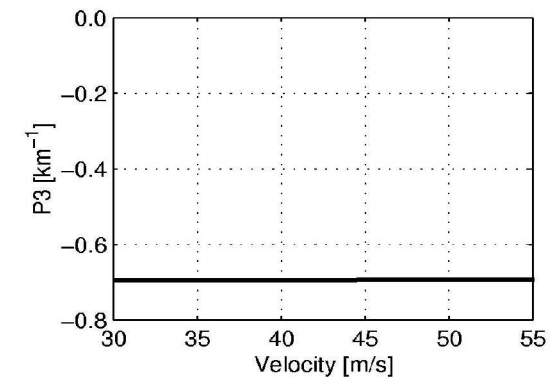
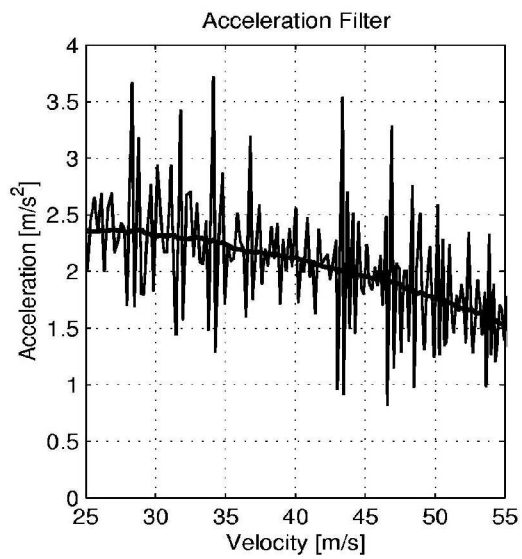
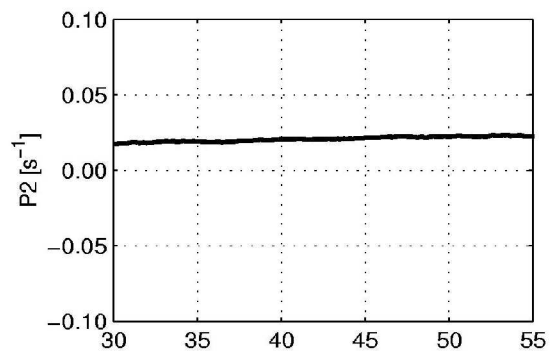
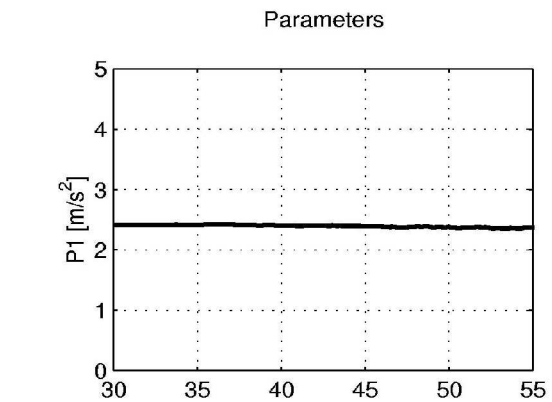
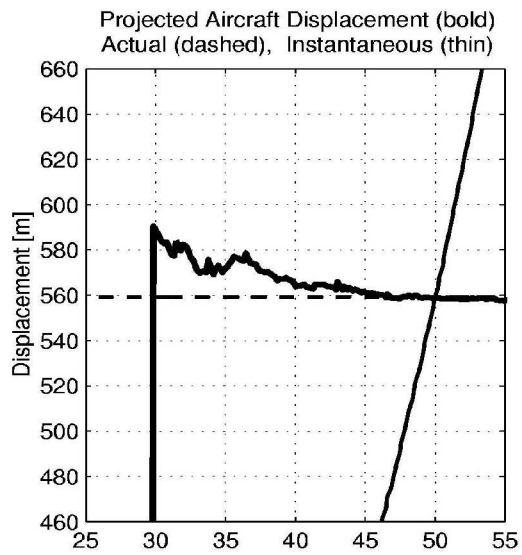
Filename: /yxe15/k30g0537.bik, Airport Identifier: cyxe, Runway: 15 Date: 30 Nov 2000 at 0705 CST



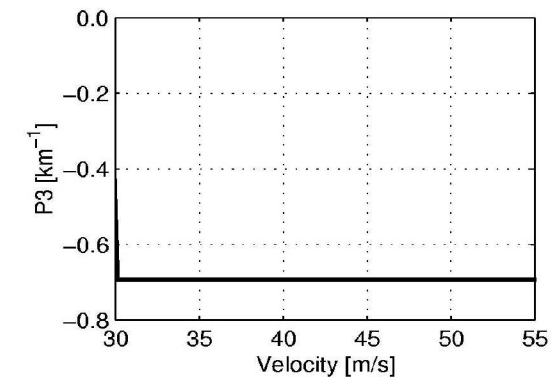
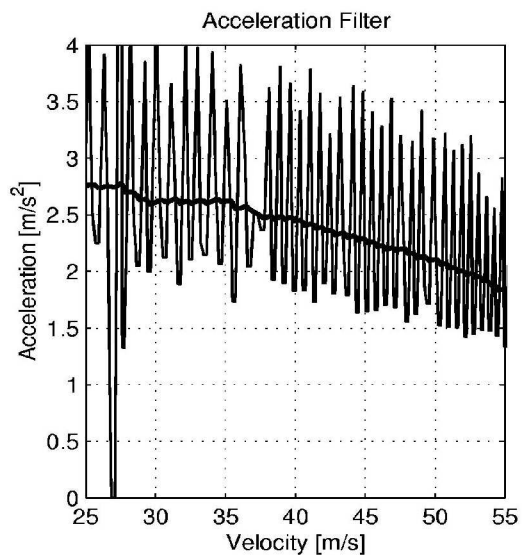
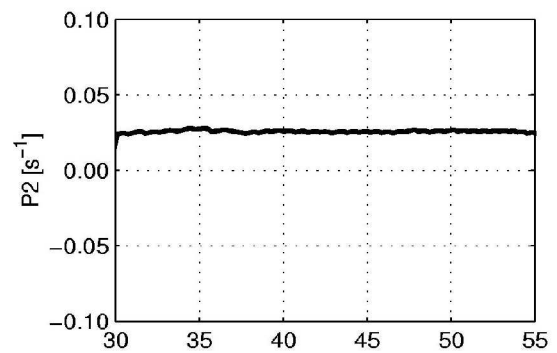
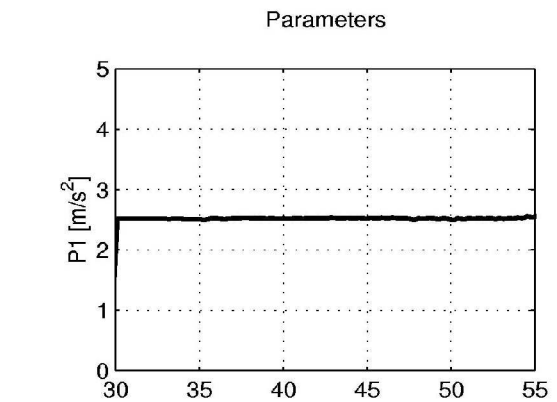
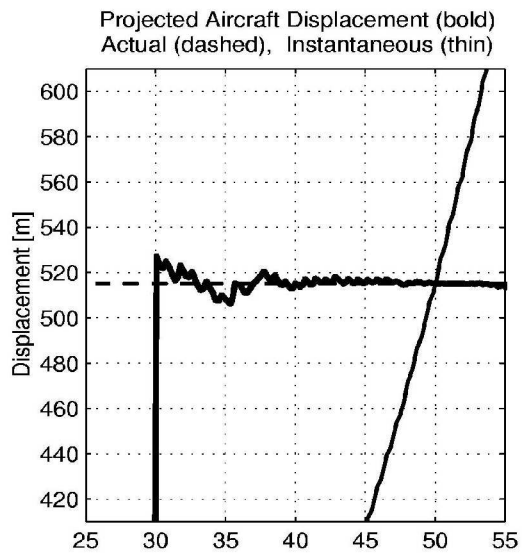
Filename: /yxe15/01s2108.bik, Airport Identifier: cyxe, Runway: 15 Date: 01 Dec 2000 at 1921 CST



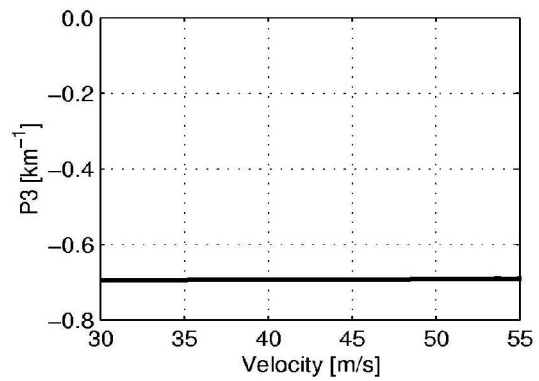
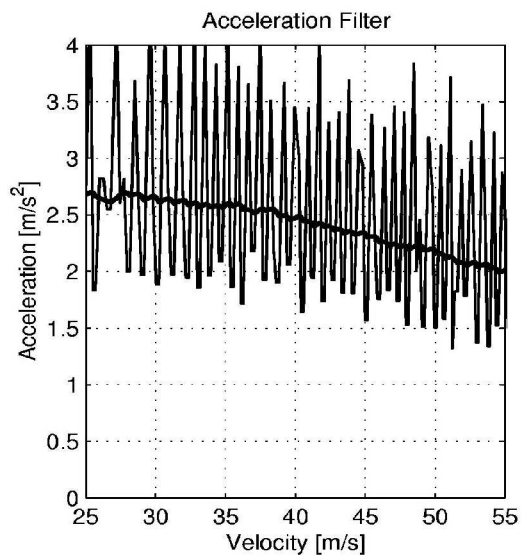
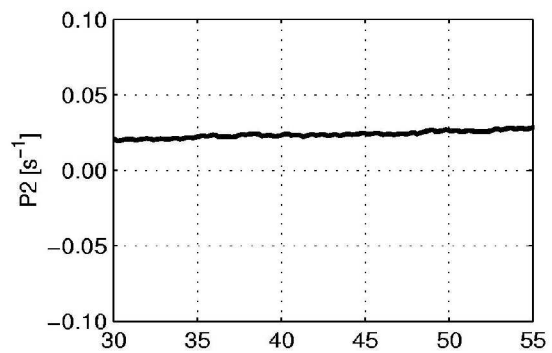
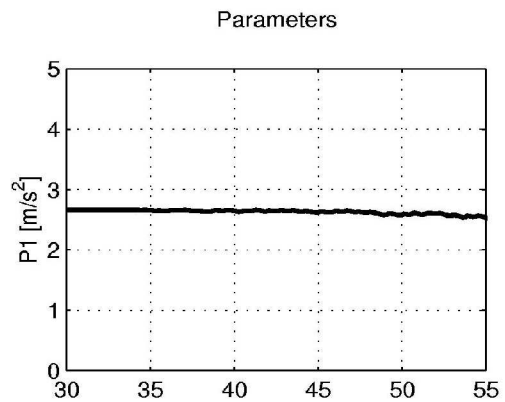
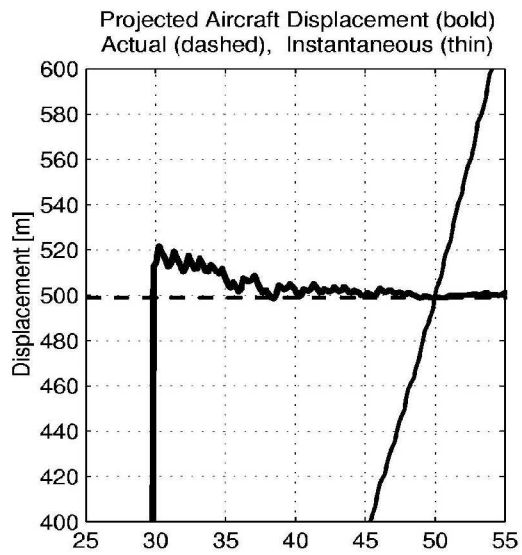
Filename: /yxe15/104p3209.bik, Airport Identifier: cyxe, Runway: 15 Date: 04 Dec 2000 at 1632 CST



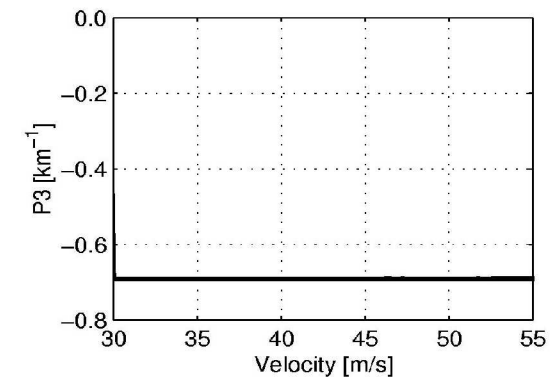
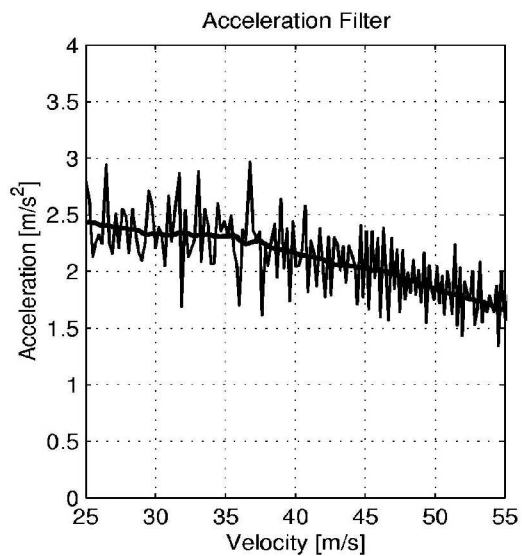
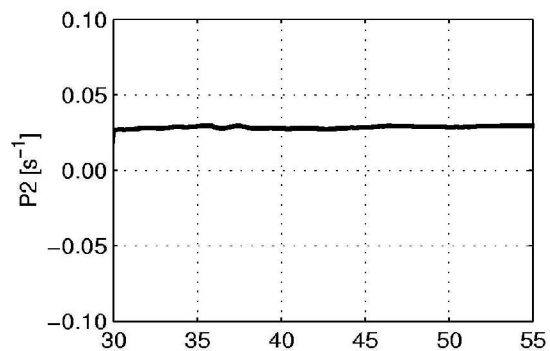
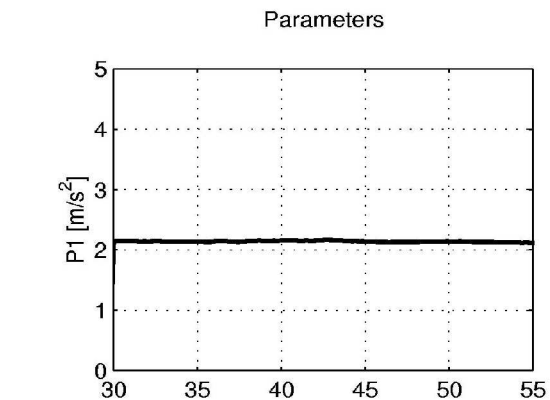
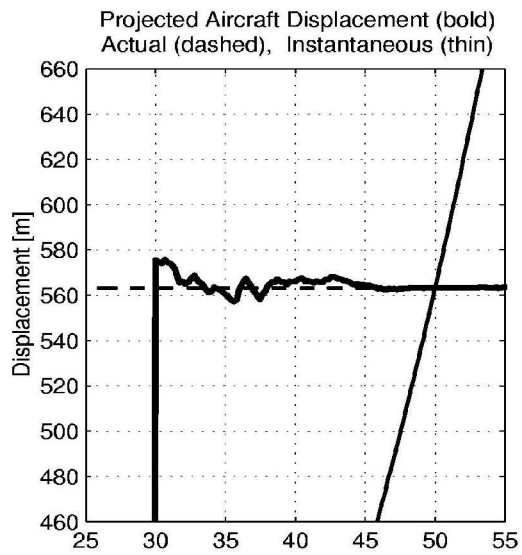
Filename: /yx15/106g5518.bik, Airport Identifier: cyxe, Runway: 15 Date: 06 Dec 2000 at 0755 CST



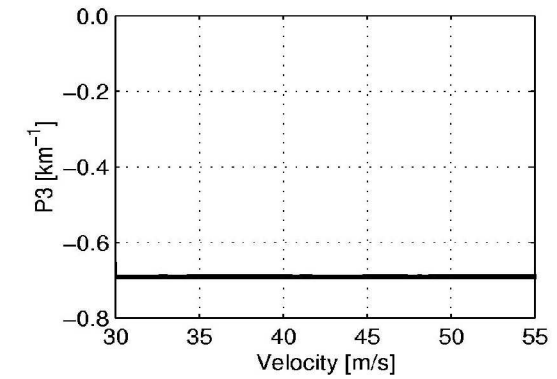
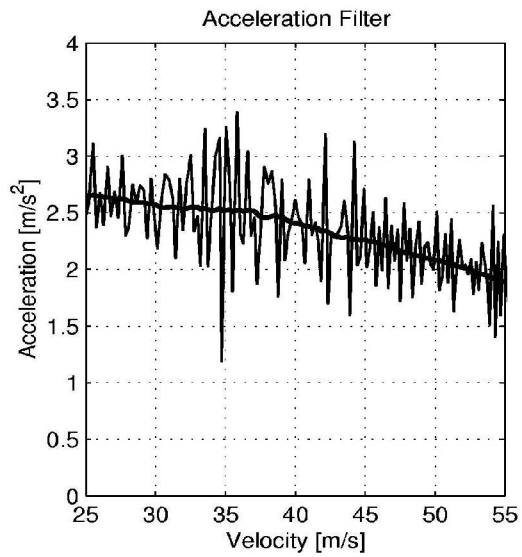
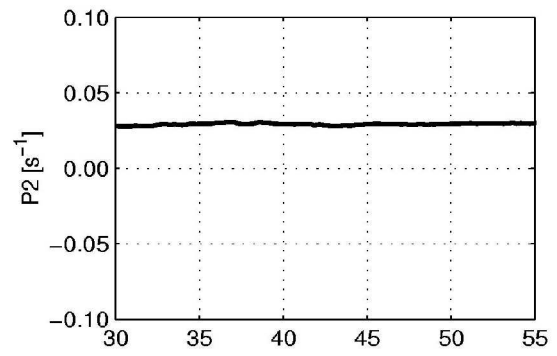
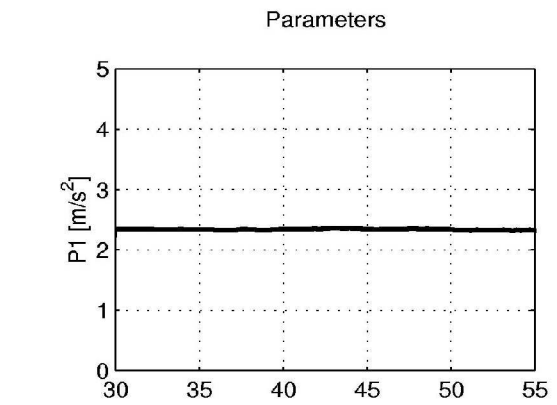
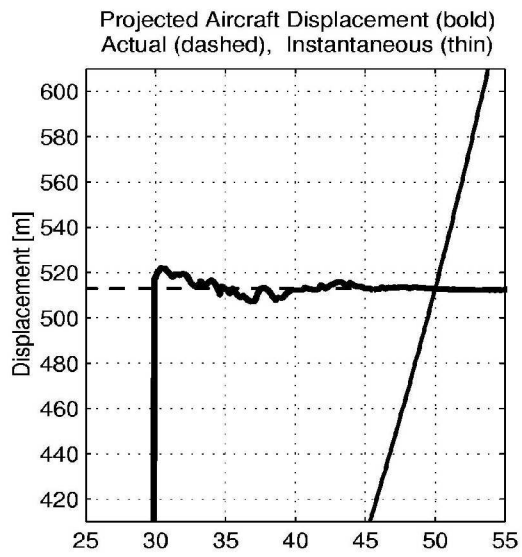
Filename: /yxe15/106j1052.bik, Airport Identifier: cyxe, Runway: 15 Date: 06 Dec 2000 at 1010 CST



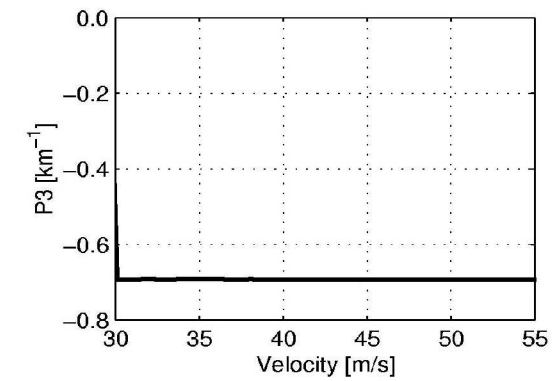
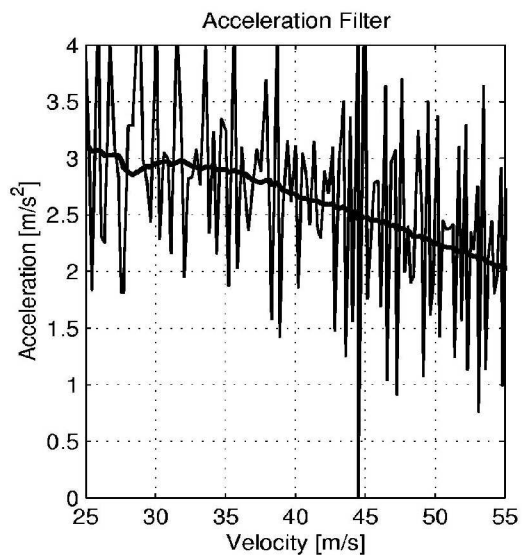
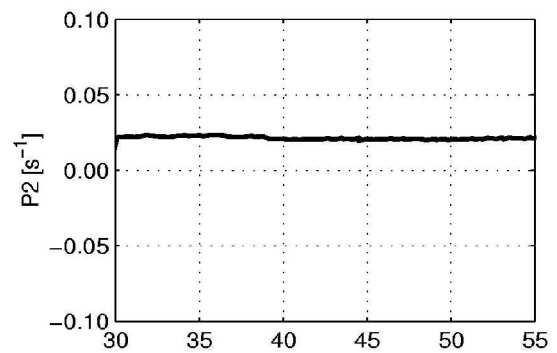
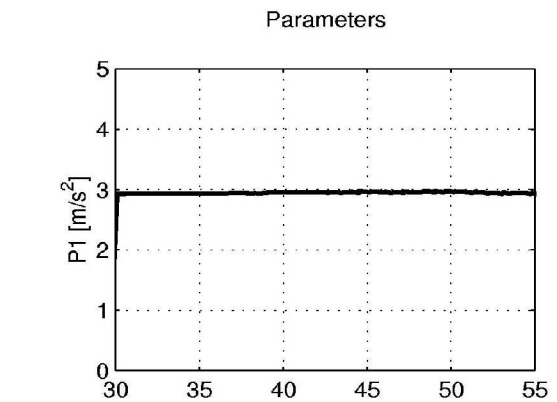
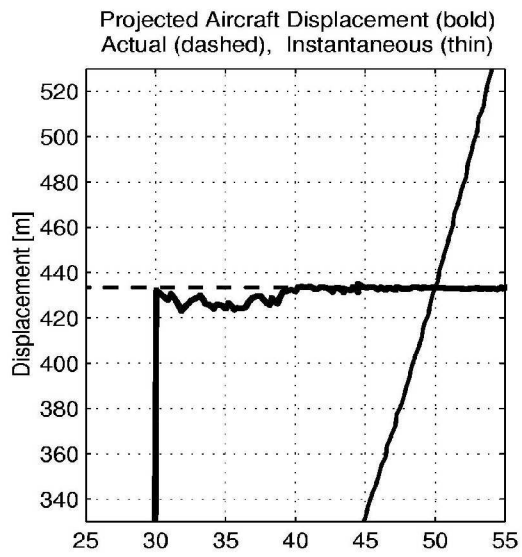
Filename: /yx15/07/11240.bik, Airport Identifier: cyxe, Runway: 15 Date: 07 Dec 2000 at 1212 CST



Filename: /yxe15/107q4525.bik, Airport Identifier: cyxe, Runway: 15 Date: 07 Dec 2000 at 1745 CST



Filename: /yx15/107t1217.bik, Airport Identifier: cyxe, Runway: 15 Date: 07 Dec 2000 at 2012 CST



Filename: /yx15/11110313.bik, Airport Identifier: cyxe, Runway: 15 Date: 11 Dec 2000 at 1203 CST

COMMERCIAL USE LICENSE AGREEMENT

PLEASE READ CAREFULLY: This Commercial Use License Agreement (the "Agreement") is an agreement between You (either an individual or a single entity) and the Boeing Management Company ("Boeing"). It governs Your rights and obligations for photographs, images, graphics and other informational materials (collectively, "Images") licensed and delivered to You by Boeing in the format requested by You or downloaded by You from the Boeing licensing site located at (the "Site"). Your rights and obligations regarding the Images selected and purchased by You are subject to terms of the options selected by You during the ordering process (the "Order"). The terms of the Order are hereby incorporated by reference into this Agreement. You must agree to the terms of this Agreement to use the Images downloaded by You from this Site or delivered to You by Boeing pursuant to Your Order.

BY CLICKING ON THE "I ACCEPT" BUTTON BELOW OR DOWNLOADING OR TAKING DELIVERY OF THE IMAGES, YOU ACKNOWLEDGE THAT YOU HAVE READ THIS AGREEMENT AND AGREE TO BE BOUND BY ITS TERMS AND CONDITIONS. IF YOU DO NOT AGREE TO THE TERMS OF THIS AGREEMENT, DO NOT CLICK THE "I ACCEPT" BUTTON, DOWNLOAD OR OTHERWISE ACCEPT DELIVERY OF THE IMAGES. IF, AFTER YOU ACCEPT THIS AGREEMENT, YOU NO LONGER AGREE TO THE TERMS AND CONDITIONS AND WISH TO TERMINATE THIS AGREEMENT, YOU MUST PROMPTLY DELETE THE LICENSED IMAGE(S) FROM YOUR COMPUTER AND DESTROY ANY COPIES THEREOF, WHETHER IN PRINTED OR ELECTRONIC FORM.

1. License Grant. Subject to the terms of the Agreement and Your payment of any applicable royalties and taxes, Boeing grants to You a limited, non-exclusive, non-transferable, non-sublicensable license to use a copy of the Image(s), whether in electronic or other form, selected by and licensed to You from the Site for commercial use in accordance with the terms of this Agreement and the Order only. The license granted is personal to You and not to any other person or entity.
2. Use Limitations. Unless expressly authorized by the Order and then only to the extent permitted by the Order, You must adhere to the following limitations and restrictions regarding Your use of the Image(s):
 - a. No Sublicense. You may not transfer, sublicense, rent, lease, network, distribute, or grant Your rights in the Image(s) to any other person or entity except with the express, prior written consent of Boeing.
 - b. Permitted Copies. During the term of this Agreement, You may make commercial use only in accordance with the terms of this Agreement of each copy of an Image licensed under this Agreement. Every copy of an Image must be separately downloaded through the Site. For example, if, pursuant to Your Order, You are licensed to use and download an Image on Your commercial web site and wish to use an additional copy in Your annual report, You must license both copies in separate transactions. You may make a limited number of physical copies from the electronic copy of the Image(s) only for Your internal purposes in accordance with the terms of this Agreement. Any reproduction or distribution of copies for external purposes must be specifically authorized by Your Order.
 - c. Unauthorized Copies. Except as provided by this Agreement, You may not (1) copy, display or distribute the Image(s) to others; (2) publish, display or post any Images on any computer network or broadcast or publications media; or (3) systematically download, copy or place or use the Image(s) in or as part of a clipart or stock photography collection or compilation of any sort.
 - d. No Modifications. You may not alter, modify or prepare derivative works of the Image(s). Without limiting the foregoing, You may not use or otherwise incorporate the Image(s) in another work, regardless of format or medium, unless authorized by Your Order.
 - e. Commercial Use. Except as explicitly authorized under the terms of this Agreement and Your Order, You may not use the Image(s) to develop any product for distribution, sell any product produced through use of the Image(s), or otherwise make any commercial use whatsoever of the Image(s), including, without limitation, using the Image(s) on a commercial web site.
 - f. Notices; Attribution. You may not remove or alter any copyright and other proprietary notices contained in the Image(s). You agree to add the following legal notice wherever the Image(s) is/are used, including all printed versions: "™ & © Boeing. Used under license".
 - g. Integrity. You may not use the Image(s) in any manner or context that reflects unfavorably or adversely on Boeing, or that is distasteful or objectionable to Boeing, or that otherwise casts Boeing in a poor light. Without limiting the foregoing, You may not use the Image(s) on any web site or with any product or service associated with alcohol, tobacco, firearms, drugs, nudity, pornography or obscene materials.
3. Proprietary Rights.
 - a. Reservation of Rights. The Image(s) are licensed, not sold, to You. Except for the limited license granted to You, Boeing reserves all right, title and interest to the Image(s), including ownership of the Image(s) and all copyrights, trademark, or other intellectual property rights in the Image(s). Without limiting the foregoing, Boeing expressly reverses all moral rights in the Image(s), including the right of attribution and integrity expressed in this Agreement.
 - b. Copyright. All Images are ALL RIGHTS RESERVED Copyright © Boeing Management Company. The Image(s) are protected under U.S. and international copyright laws.
 - c. Trademarks. Boeing, McDonnell Douglas, McDonnell Aircraft, Douglas Aircraft, North American Aviation, their distinctive airplane liveries and product markings, and the products and services described in this website are trademarks, service marks or registered trademarks owned by Boeing, and may not be copied, imitated or used, in whole or in part, other than in accordance with the terms of this Agreement without the express, prior written permission of Boeing. You agree that You will not display, disparage, dilute, or taint Boeing's trademarks and service marks or use any confusingly similar marks or use our marks in such a way that would misrepresent the ownership of such marks. Any permitted use of our service marks or trademarks by You shall inure to the benefit of Boeing.
 - d. No Sponsorship. Nothing in this Agreement shall be interpreted as Boeing's sponsorship, affiliation or endorsement of any product or service for which the Image(s) are used pursuant to Your Order. You may not suggest or imply any sponsorship, affiliation or endorsement in the sale, promotion, or use of Your goods or services.
4. Royalties. As a condition of the license grant above, You agree to pay all applicable royalties and taxes associated with the Image(s) selected by You in accordance with the terms of the Order. Any failure of You to make timely payment shall result in the immediate termination of this Agreement.
5. Term and Termination.
 - a. Term. The license granted in this Agreement is effective upon acceptance by You of the terms and conditions set forth in the Agreement. The Agreement shall continue until terminated.
 - b. Termination. The Agreement will terminate immediately without notice by Boeing if you fail to comply with the terms and conditions of this Agreement. Upon termination of this Agreement, You shall immediately discontinue all use of the Image(s), and destroy the original and all copies, print or electronic, of such Image(s). Further, Boeing has the unqualified right to terminate this Agreement if, at any time during the term of this Agreement (i) You breach the terms or conditions of this Agreement; or (ii) any unfavorable publicity or claim should arise or be made in relation to any particular use of the Image(s) which use reflects adversely or unfavorably on Boeing or its trademarks, copyrights or other intellectual property. Termination of this Agreement under this section shall be without prejudice to any rights that Boeing may otherwise have against You and shall not preclude the exercise by Boeing of any other right or remedy that it may have by law against You. The following provisions shall survive the termination of this Agreement: 2, 3, and 5(b) through 9.
6. Disclaimer. ANY AND ALL IMAGES ARE PROVIDED "AS IS" WITHOUT WARRANTY OF ANY KIND. BOEING HEREBY DISCLAIMS ALL EXPRESS OR IMPLIED WARRANTIES REGARDING THE IMAGES OR ANY OTHER MATERIALS ACCESSIBLE FROM THE SITE, INCLUDING, BUT NOT LIMITED TO, IMPLIED WARRANTIES OR CONDITIONS OF MERCHANTABILITY OR FITNESS FOR A PARTICULAR PURPOSE, IMPLIED WARRANTY OR CONDITION ARISING FROM COURSE OF PERFORMANCE, COURSE OF DEALING, OR USAGE OF TRADE, AND ANY IMPLIED WARRANTY OF NONINFRINGEMENT. BOEING DOES NOT REPRESENT OR WARRANT THAT THE IMAGES OR OTHER MATERIALS OBTAINED FROM THE SITE ARE ACCURATE, COMPLETE, RELIABLE, CURRENT, OR ERROR FREE. ANY WRITTEN OR ORAL INFORMATION OR ADVICE GIVEN BY BOEING, ITS EMPLOYEES, AGENTS AND/OR REPRESENTATIVES SHALL NOT IN ANY WAY BE CONSTRUED AS GRANTING OR CREATING A WARRANTY.
7. Limitation of Liability. BOEING SHALL NOT BE LIABLE UNDER ANY THEORY FOR ANY DAMAGES SUFFERED BY YOU, ANY OTHER USER OF THE IMAGE(S), OR ANY THIRD PARTY. UNDER NO CIRCUMSTANCES SHALL BOEING BE LIABLE TO YOU OR ANY OTHER PERSON FOR ANY DIRECT, INDIRECT, SPECIAL, INCIDENTAL, OR CONSEQUENTIAL DAMAGES OF ANY KIND OR OTHER LIABILITY, WHETHER IN AN ACTION OF CONTRACT, TORT OR OTHERWISE, ARISING FROM, OUT OF, OR IN CONNECTION WITH THE USE OR INABILITY TO USE THE IMAGE(S) OR OTHER DEALINGS IN CONNECTION WITH THE IMAGE(S), EVEN IF BOEING WAS INFORMED OF THE POSSIBILITY OF SUCH DAMAGES, OR FOR ANY THIRD-PARTY CLAIMS. THIS DISCLAIMER OF LIABILITY APPLIES TO ANY DAMAGES OR INJURY CAUSED BY ANY FAILURE OF PERFORMANCE, ERROR, OMISSION, INTERRUPTION, DELETION, DEFECT, DELAY IN OPERATION OR TRANSMISSION, COMPUTER VIRUS, COMMUNICATION LINE FAILURE, THEFT OR DESTRUCTION OR UNAUTHORIZED ACCESS TO, ALTERATION OF, OR USE OF THE IMAGE(S) WHETHER FOR BREACH OF CONTRACT, TORT, OR NEGLIGENCE, OR UNDER ANY OTHER CAUSE OF ACTION. BOEING'S ENTIRE LIABILITY AND YOUR EXCLUSIVE REMEDY WITH RESPECT TO THE USE OF THE SITE OR IMAGE(S) SHALL BE LIMITED TO THE REPLACEMENT OF ANY IMAGE FOUND TO BE DEFECTIVE OR RETURN OF THE ROYALTIES PAID BY YOU. YOUR SOLE AND EXCLUSIVE REMEDY FOR ANY OTHER DISPUTE WITH BOEING IS THE TERMINATION OF THIS AGREEMENT.
8. Indemnification. You agree to hold harmless, indemnify, and defend Boeing, its officers, employees, directors, agents, and any users from and against any loss, damage, liability, claim of loss, lawsuit, cause of action, or other claim asserted against them or any of them arising out of, or in any way connected with, Your use of the Image(s) in violation of this Agreement.
9. General Provisions.
 - a. Export Controls. You agree that the Image(s) will not be shipped, transferred, or exported into any country or used in any manner prohibited by the United States Export Administration Act or any other export laws, restrictions, or regulations. You will be solely responsible for Your compliance with all applicable United States and foreign laws and regulations and international treaties with respect to the export, import or use of the Image(s). By entering into this Agreement, You represent and warrant that (1) no U.S. federal agency has suspended, revoked, or denied You export privileges (a "Prohibited Person"), (2) You are not located in or under the control of a national or resident of any country subject to a U.S. embargo or trade restrictions applicable to the Image(s), including Iraq, (a "Prohibited Country"), and (3) You will not export or re-export the Image(s) to any Prohibited Country, or to any Prohibited Person as specified by U.S. law.
 - b. Requests for Expanded License. This Agreement and Your Order set forth Your entire right to use the Image(s) posted on the Site. Any other use, such as the duplication or distribution of Image(s) beyond the limitations expressed in this Agreement or Your Order, requires the prior written consent of or a further license from Boeing, which may be granted or denied in its sole discretion.
 - c. Governing Law; Entire Agreement. This Agreement: (1) will be governed by the law of the State of Washington, exclusive of Washington's choice of law rules; (2) constitutes the entire Agreement, and supersedes any and all other Agreements, understandings, and communications between the parties related to Images; and (3) may only be amended or otherwise modified by a written instrument executed by an authorized representative of Boeing. All parties hereto consent to the jurisdiction and venue of the federal and state courts of the State of Washington, located in King County, Washington, for any action arising under this Agreement.



Honeywell International Inc.
Business and General Aviation
One Technology Center
23500 West 105th
Olathe, KS 66061
(913) 782-0400

Shane D Pinder
University of
Saskatchewan

Honeywell grants permission to the entity named above or representative thereof, to reproduce, in whole or in part, the KLN 89/89B Installation manual (006-10522-0003) used for internal purposes only.

This copyright release is given with the following stipulations:

1. Reproduced documentation is considered uncontrolled.
2. Honeywell will not be held responsible for the currency of the content of the excerpts or the currency of the documentation from which the excerpts were taken.
3. Honeywell will not be held responsible for documentation containing excerpts from the above mentioned publications.

If you have questions about these stipulations please contact me.

Jeffrey K. Darby
Technical Publications
Honeywell International Inc.
Business and General Aviation
Phone & Fax: (913) 712-2398
E-mail: Jeff.Darby@honeywell.com

Shane Pinder

From: Debora Klaus [Debora.Klaus@novatel.ca]
Sent: Thursday, April 11, 2002 2:35 PM
To: 'Shane Pinder'
Subject: RE: Reproduction of Copyrighted Electronic Documents

Dear Shane,

We acknowledge receipt of your email requesting authorization to reproduce NovAtel documents. We would ask that you acknowledge NovAtel's copy rights by numbering any insertions referencing the documents; and either footnoting at the point of insertion or in a bibliography at the back of the thesis and using the copyright symbol as such:

(c) NovAtel Inc.

I trust that answers your request.

Sincerely,

Debora Klaus
Legal Assistant
NovAtel Inc.
Tel. (403) 295-4566
Email Debora.Klaus@novatel.ca

-----Original Message-----

From: Shane Pinder [mailto:ShaneP@Navsys.com]
Sent: Tuesday, April 09, 2002 10:11 AM
To: 'debora.klaus@novatel.ca'
Subject: Reproduction of Copyrighted Electronic Documents

Debora,

I am a Ph.D. student at the University of Saskatchewan. My thesis involved the use of a NovAtel GPS receiver as the core device in a prototype aircraft instrument.

I would like to include electronic (.pdf) copies of four documents in a CD-ROM appendix to my thesis manuscript. These include:

1. OM-20000032 Rev 2, 15 June 1999, the Specification Sheet for the Model 531 Antenna
2. OM-20000007 Rev 2.0, 01 May 1995, the OEM Series GPSCard Installation and Operating Manual
3. OM-20000004 Rev 3.0, 28 November 1994, the GPSCard PowerPak User Manual
4. OM-20000008 Rev 3, 02 February 1999, the GPSCard Command Descriptions Manual for Software Version 3.36

I will include any acknowledgement you wish in the preface to my thesis manuscript. Please indicate whether you require more information to authorize the reproduction of these electronic documents.

Best regards,

Shane Pinder
(719)481-4877 x138
53 Bandit Creek Drive
Monument, CO 80132

PERMISSION TO REPRODUCE MAPS AND CHARTS

Date Thursday, April 4, 2002

Attn : Shane Pinder
University of Saskatchewan

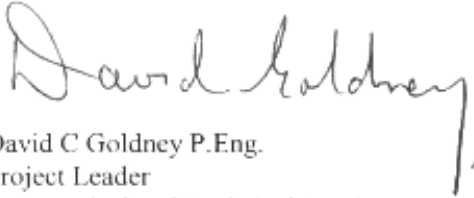
Geomatics Canada (GC) of Natural Resources Canada (NRCan) authorizes Shane Pinder to reproduce map and charts for the reasons attached herein and subject to the following conditions:

- 1) that this authorization does not restrict NRCan in any way from authorizing other parties to use the same information in the same kind of products or in different products;
- 2) that the maps and charts reproduced are solely for use with:
Takeoff Performance Monitoring in Far-northern Regions: An Application of the Global Positioning System, Ph.D. Thesis, Author: Shane Pinder;
- 3) that the maps and charts reproduced shall not be reproduced for resale purposes;
- 4) that this authorization applies solely to the *Wollaston Lake* plate from the Canada Flight Supplement;
- 5) that this authorization may be changed including but not limited to change in NRCan policy, and/or non compliance with conditions in this letter;
- 6) that the following copyright authorization must appear in *Takeoff Performance Monitoring in Far-northern Regions: An Application of the Global Positioning System, Ph.D. Thesis, Author: Shane Pinder* in an acknowledgements section:

Aeronautical charts are based on information taken from Canada Flight Supplement .
© 2002 Her Majesty the Queen in Right of Canada with permission of Natural Resources Canada.
- 7) that Shane Pinder will maintain adequate records in case of audit to confirm compliance with the conditions herein;
- 8) that no royalty fee will be payable by Shane Pinder to GC;
- 9) The Data is provided on an "as is" basis and Canada makes no guarantees, representations or warranties respecting the Data, either expressed or implied, arising by law or otherwise, including but not limited to, effectiveness, completeness, accuracy or fitness for a particular purpose;
- 10) Canada shall not be liable in respect of any claim, demand or action, irrespective of the nature of the cause of the claim, demand or action alleging any loss, injury or damages, direct or indirect, which may result from the End-User's use or possession of the Data or in any way relating to this Agreement. Canada shall not be liable in any way for loss of profits or contracts, or any other consequential loss of any kind resulting from the End-User's use or possession of the Data or in any way attributable to this Agreement;
- 11) The End-User shall indemnify and save harmless Canada and its Ministers from and against any claim, demand or action, irrespective of the nature of the cause of the claim, demand or action, alleging loss, costs, expenses, damages or injuries (including injuries resulting in death) arising out of the End-User's use or possession of the Data or in any way relating to this Agreement.

This authorization will come into effect upon receipt of a copy of this letter signed with an acceptance by Shane Pinder.

Yours truly,



David C Goldney P.Eng.
Project Leader
Aeronautical and Technical Services
Natural Resources Canada
615 Booth Street, room 178
Ottawa, Ontario
K1A 0E9

Email: dgoldney@nrcan.gc.ca
Tel.: (613) 992-4594
Fax: (613) 943-8959

THE CONDITIONS STATED HEREIN ARE ACCEPTED:

Date: 04 APR 2002 Per: 
Shane Pinder